The Thesis Committee for Anthony Louis Dondrea III
Certifies that this is the approved version of the following thesis:

UNDERCUT AND GROUTED ANCHORS AS POST-INSTALLED SHEAR REINFORCEMENT

APPROVED BY
SUPERVISING COMMITTEE:

Supervisor:

Oguzhan Bayrak

Trevor Hrynyk

UNDERCUT AND GROUTED ANCHORS AS POST-INSTALLED SHEAR REINFORCEMENT

by

Anthony Louis Dondrea III, B.S. Arch.E.

Thesis

Presented to the Faculty of the Graduate School of

The University of Texas at Austin

in Partial Fulfillment

of the Requirements

for the Degree of

Master of Science in Engineering

The University of Texas at Austin

December 2014

Dedication

To my wife, Kelsey. Thank you for your endless support and patience.

Acknowledgements

This research project was made possible by the enormous support of our sponsors, for which I am grateful. Equally important was the project supervisor, Dr. Oguzhan Bayrak who was instrumental in giving me a role in this project. His professional and technical guidance is much appreciated. Special thanks also go to Dean Deschenes for his great oversight, insight, and approachability.

One of the most satisfying aspects of working in the Ferguson lab is getting to see your design work come to life and your problem-solving tested on the lab floor. Of course, that involves a good deal of physical labor and perhaps even more practical expertise. That is to say, this project would have been absolutely impossible without the hard work, dedication, and patience of the lab's technicians: Dennis Fillip, David Braley, and Blake Stasney. Each and every one of them provided invaluable advice, support, and unforgettable conversation. To all of the Ferguson students, both graduate and undergraduate (too many to list here), I thank you for your willingness to lend a hand without hesitation. More so, thank you for an enjoyable and memorable experience at Ferguson.

Finally, my family deserves great thanks for their support. To my parents, for providing me the great opportunity to attend the University of Texas and their unwavering encouragement. To my wife, Kelsey, for her support, patience, and love.

ABSTRACT

UNDERCUT AND GROUTED ANCHORS AS POST-INSTALLED SHEAR REINFORCEMENT

Anthony Louis Dondrea III, M.S.E.

The University of Texas at Austin, 2014

Supervisor: Oguzhan Bayrak

The need for conservation in engineering has become apparent in the past several decades as a result of resource depletion, aging infrastructures, and diminishing real estate. In addition, many structures see increased loads due to building re-purposing; others simply do not meet the demands of modern code provisions. As a result, techniques to retrofit existing buildings are becoming increasingly important.

This thesis investigates the use of post-installed undercut and grouted (rods grouted in place) anchors for strengthening reinforced concrete beams in shear. These techniques are especially useful when access to members requiring retrofit is limited. Experimental results are compared to the ACI-DAfStb shear database[19,20] and to American Structural Design Code provisions. The results indicate that high strength anchors can effectively strengthen beams and achieve equivalent or greater deformation and load capacity as traditionally reinforced elements. However, precautions should be

taken to avoid alternate anchor failure modes; a designer should validate that anchor yield can be achieved, or account for the possibility that post-installed anchors will not yield.

Table of Contents

List of Tables

List of Figures

CHAPTER 1

Introduction

In recent decades, the philosophy of conservation has become increasingly important to civil engineers. This is largely a product of diminishing resources, limited real estate, and aging infrastructures. The result has been a surge in projects whose aim is to re-purpose existing structures or rehabilitate deficient ones. As such, strengthening techniques for reinforced concrete members have been the focus of a significant amount of research. Of particular concern is the shear strength of existing reinforced concrete structures, as even today, despite decades of research effort, shear behavior is not fully understood.

ACI Committee 364[1] identified five common methods for shear strengthening of individual reinforced concrete members. Methods proposed by ACI Committee 364 (Fig. 1–1) include: (i) addition of external steel reinforcement; (ii) enlargement of the concrete section; (iii) addition of internal steel or FRP reinforcement; (iv) externally adhered FRP plates or strips; (v) near-surface-mounted reinforcement (NSM). Of those, considerable research utilizing FRP near-surface-mounted and jacketing techniques has been performed. Recently Kunz et al.[2], in addition to other researchers[3,4,5,6,7,8], have evaluated the effectiveness of post-installed, epoxy-bonded steel bars as shear reinforcement—and shown them to be effective for improving shear behavior. Often, post-installed bars are oriented at a 45 degree angle relative to the member axis, increasing epoxy bond length and providing greater shear resistance. While post-installed bars chemically bonded by epoxy have received increasing amounts of research attention, significantly less effort has been devoted to studying options which rely on mechanical anchorage or are bonded by grout.

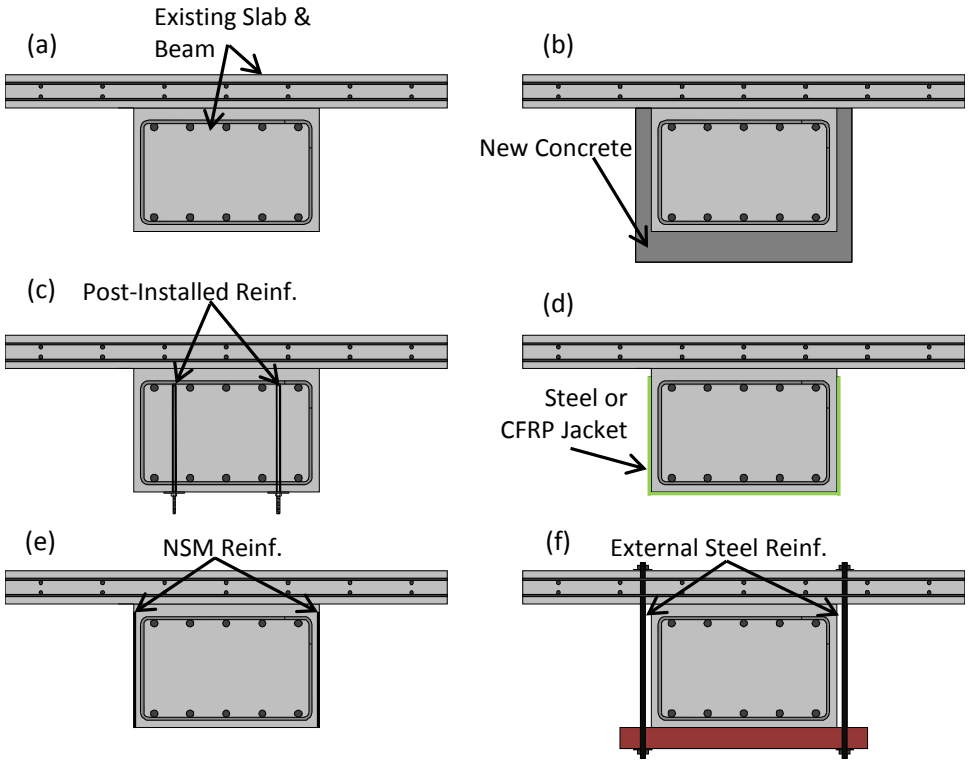

Fig. 1–1: Strengthening existing RC elements in shear. a) unreinforced section; b) section enlargement by additional concrete and reinforcement; c) post-installed, bonded or un-bonded reinforcement-steel or FRP; d) external jacketing with CFRP or steel; e) near-surface mounted steel or CFRP rods or bars; (f) addition of external reinforcement.

The objective of this study was to investigate the effectiveness of undercut and grouted anchors as post-installed shear reinforcement, expanding the retrofit knowledgebase beyond epoxy-bonded solutions. Both techniques involve drilling holes in locations where shear reinforcement is desired, and then either setting and tensioning undercut anchors (Fig. 1–2 (b)) or grouting steel threaded rods into place (Fig. 1–2 (c)). These techniques require access to only one side of a concrete member—often making them more practical than many of the techniques suggested by ACI Committee 364 and especially appealing in scenarios where space is limited. The methods' effectiveness was confirmed by an experimental program conducted at the University of Texas at Austin.

Both techniques showed considerable gains in shear strength and deformation capacity prior to failure when compared to members without transverse reinforcement. Employed retrofits were also proven to produce behavior comparable to elements with an equivalent amount of cast-in-place transverse reinforcement.

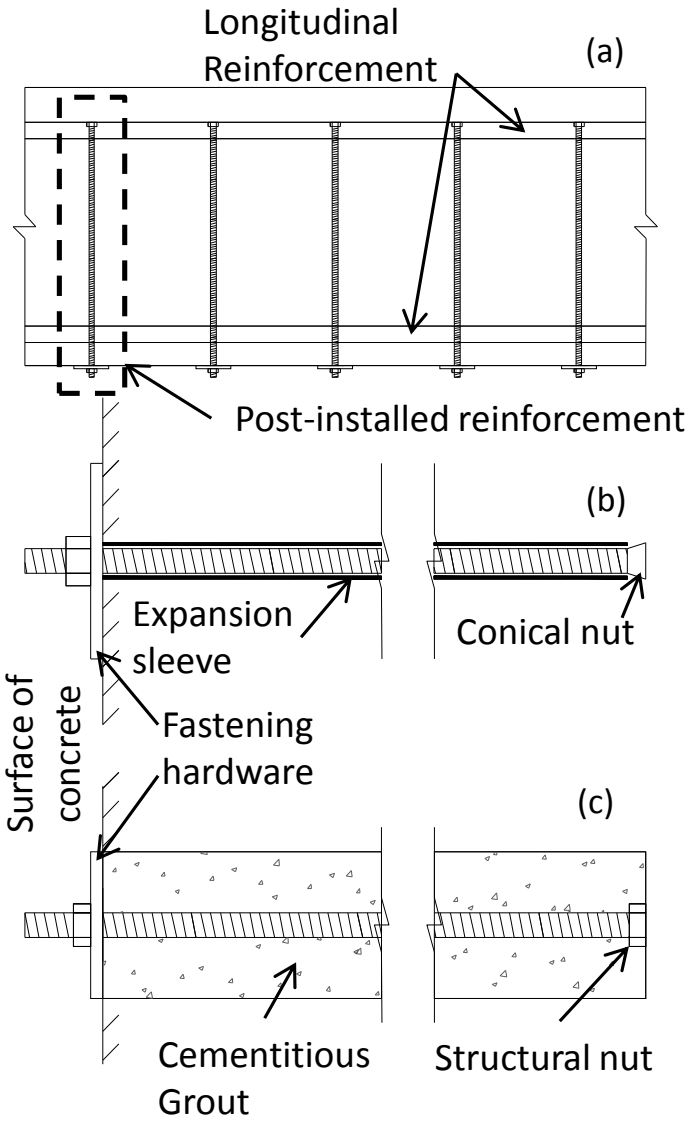

Fig. 1–2: Retrofit techniques under investigation. a) schematic layout of post-installed reinforcement in a specimen without transverse reinforcement; b) undercut anchor components; c) grouted anchor components.

Results of the experimental study were compared to calculations performed according to current code formulations in the United States, particularly the ACI 318-11[9] equations 11-3 and 11-5, as well as the AASHTO LRFD shear design provisions[10]. Despite inherent behavioral differences between traditional cast-in-place reinforcement and post-installed reinforcing bars, the use of code design equations resulted in reasonable estimations of experimental capacities.

CHAPTER 2

Background

2.1 POST-INSTALLED ANCHORS

The retrofit (shear strengthening) techniques investigated within this thesis utilized mechanical undercut anchors or threaded steel rods grouted into position as post-installed shear reinforcement. Throughout this thesis, mechanical undercut anchors will be referred to as "undercut anchors" (abbreviated as UA) and steel rods grouted into place will be referred to as "grouted anchors" (abbreviated as GA).An undercut anchor consists of a high strength threaded rod, a conical nut, and a two-piece expansion sleeve (Fig. 1–2 (b) & Fig. B–4). A grouted anchor is comprised only of high strength threaded rod with a structural nut fastened to the embedded end of the rod (Fig. 1–2 (c) Fig. B–5). Both shear retrofit methods are capable of strengthening concrete members without transverse reinforcement to a level that equals or exceeds a section with an equivalent amount of cast-in-place reinforcement. However, these post-installed anchors may fail in alternate modes not typically considered in shear design provisions.

The tensile and shear strengths of several kinds of post-installed anchors have been extensively studied by several researchers who provided excellent summaries of post-installed anchor behavior and failure modes[11,12]. Post-installed anchors are typically used to suspend piping, electrical conduit, or other equipment. As such, they are likely to be subjected to pure axial or shear forces depending on their installation orientation. Research efforts investigating the tensile strength of anchors, forming the basis of ACI 318-11 Appendix D, were utilized in designing and evaluating post-installed anchors' contributions to sections shear strength. Additionally, previous research was used to determine the hole diameter required for grouted anchors[16].

Undercut anchors typically fail in three ways: 1) yield and fracture of the undercut anchor; 2) concrete splitting between anchor locations; 3) formation of a concrete breakout cone, whose failure surface is assumed to extend at a 35 degree angle from the anchor centerline until it intersects with another anchor failure surface or the surface of the concrete. These failure modes are illustrated in Fig. 2–1 (a), (b), and (c), respectively. Typically the concrete capacity design model (which considers the above failure modes) developed by Fuchs et. al.[13] (the basis of current ACI 349[14] and ACI 318 Appendix D design provisions), is used to predict the ultimate tensile strength of undercut, cast-in-place, and friction anchors. Headed grouted anchors have three potential failure modes: 1) yield and fracture of the rod; 2) bond failure at the grout/concrete interface; 3) formation of a concrete breakout cone. Grouted anchor strengths may also be predicted by ACI 349, with the additional consideration of slip between the grout and concrete at their interface. The potential failure modes mentioned above are shown in Fig. 2–1 (a), (d), and (e), respectively.

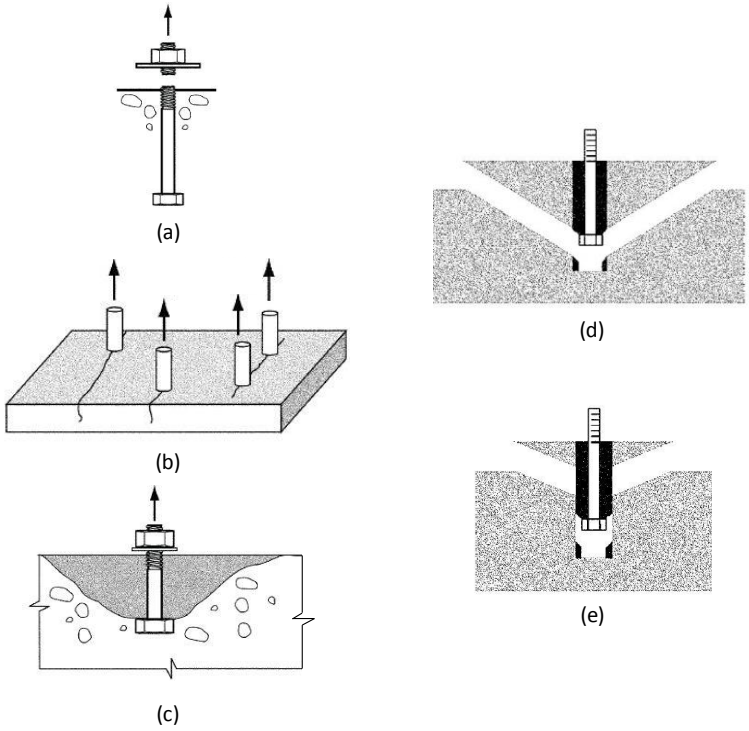

Fig. 2–1: Potential failure modes for post-installed anchors. a) yield or fracture of anchor; b) concrete splitting between anchor locations; c) concrete break out cone formation (undercut anchors); d) concrete break out cone formation (grouted anchors); e) bond failure at the grout/concrete interface.[9,12]

2.2 UNDERCUT AND GROUTED RETROFIT METHODS

The retrofit methods of interest are depicted in Fig. 1–2. The undercut and grouted anchor retrofits, both utilizing 0.50 in (12.7 mm) high strength rods as post-installed shear reinforcement, were installed in holes of 0.75 inch (19.0 mm) and 3.0 inch (76.2 mm) diameters respectively. All holes were diamond cored perpendicular to the longitudinal axis of specimens and sufficiently deep that the anchors engaged the compression side of the member (holes cored from the tension side of the member). Therefore each anchor was effectively embedded between the tension face of the concrete and the level of the compression reinforcement. After drilling, holes were cleaned according to established best practices[15] (in agreement with techniques recommended by

the undercut anchor and grout manufacturers) to facilitate proper installation of undercut anchors and ensure adequate bond between the grout to concrete interface for grouted anchors.

Undercut anchors were installed following the procedure provided by their designer and manufacturer. The entire anchor—consisting of threaded rod, conical nut, and expansion sleeve—was placed into the cored hole, "set" using a tool which forces the expansion sleeve into the undercut pocket, and then tensioned to approximately 80% of the anchor's yield strength. Grouted anchors were installed by centering the steel rod with poly carbonate "face plates" fabricated expressly for this project. Grout was then injected through a fitting until the hole was filled. Appendix D.4 includes a detailed description of the installation procedures for both shear retrofit methods.

It is important to note some key differences between the undercut and grouted anchor retrofit techniques (Fig. 2–2). Undercut anchors are mechanically anchored at only two points—the tension face of the member and the undercut location. Undercut anchors are not bonded along their length. Furthermore, the undercut sleeve is likely to allow a small amount of slip at the initiation of diagonal cracking once the anchors are engaged in resisting shear stresses[11].

In contrast, grouted anchors are capable of developing stress along their entire length. Grout bond strength was estimated based on test data collected and analyzed by Cook, Burtz, and Ansley[16]. Those estimates were confirmed, and the bond at the grout/concrete interface was deemed adequate, by a pair of informal tests conducted at Ferguson Laboratory. Notably, prior test results indicate that the grouted anchor system is not prone to slip at the initiation of diagonal cracking[11]. (Appendix B.4)

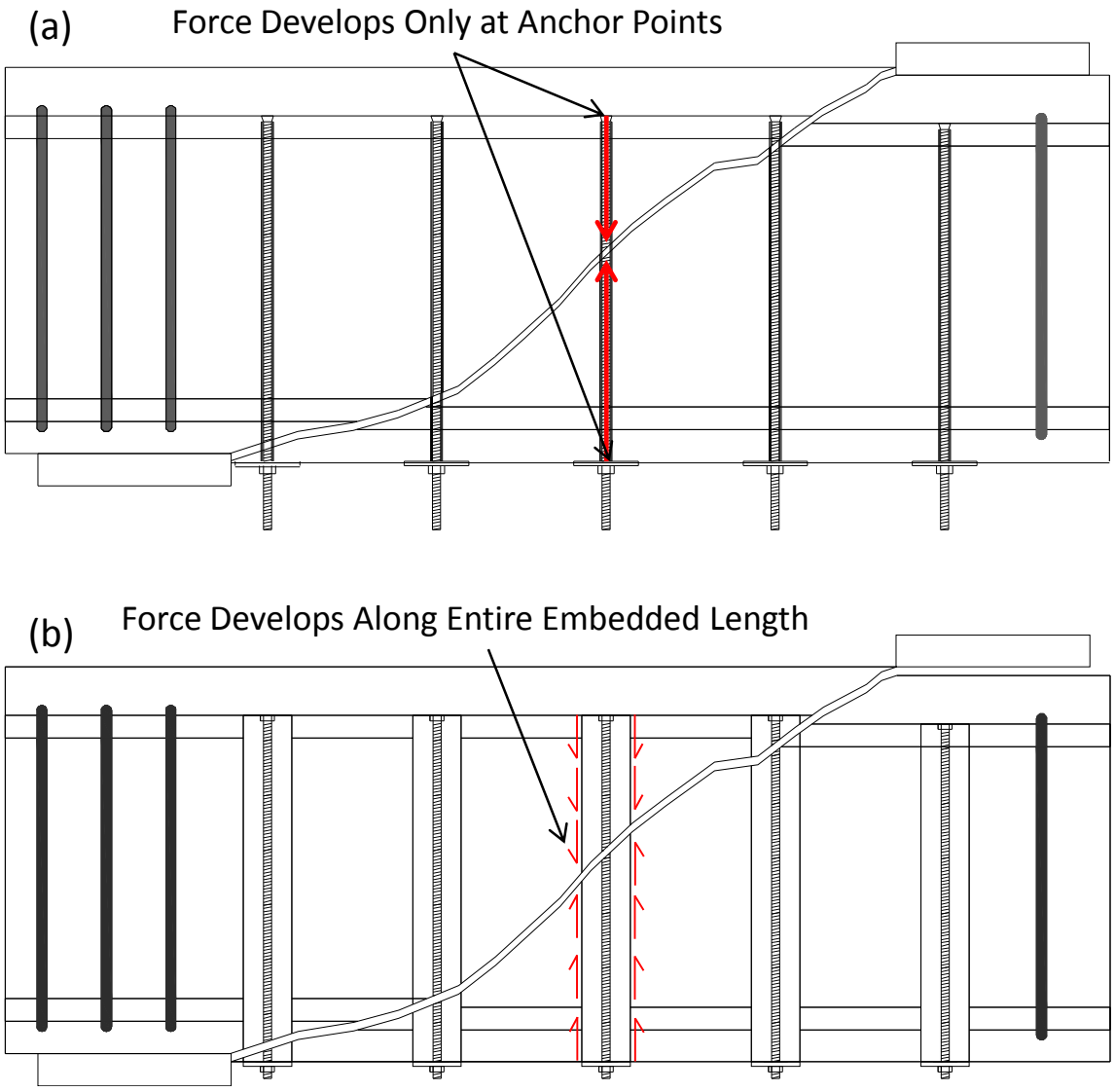

Fig. 2–2: Force development for post-installed reinforcement methods. (a) undercut anchors; (b) grouted anchors.

CHAPTER 3

Experimental Program

3.1 OVERVIEW

A set of three beams was fabricated (labeled SR1, SR2, and SR3 according the order in which they were cast) for the purposes of evaluating the shear strengthening techniques outlined in the above section. Each beam included shear test regions at either end, resulting in six total shear tests. Tests included one unreinforced control span (data from two additional spans from a companion testing program were also used), one control span reinforced with ACI 318-11 minimum transverse reinforcement (ACI 318-11 Eqn. 11-13), two spans retrofitted with undercut anchors, and two spans retrofitted with grouted anchors. An overview of the experimental program, including specimen nomenclature, dimensions, and relevant test parameters, is provided in Fig. 3–1.

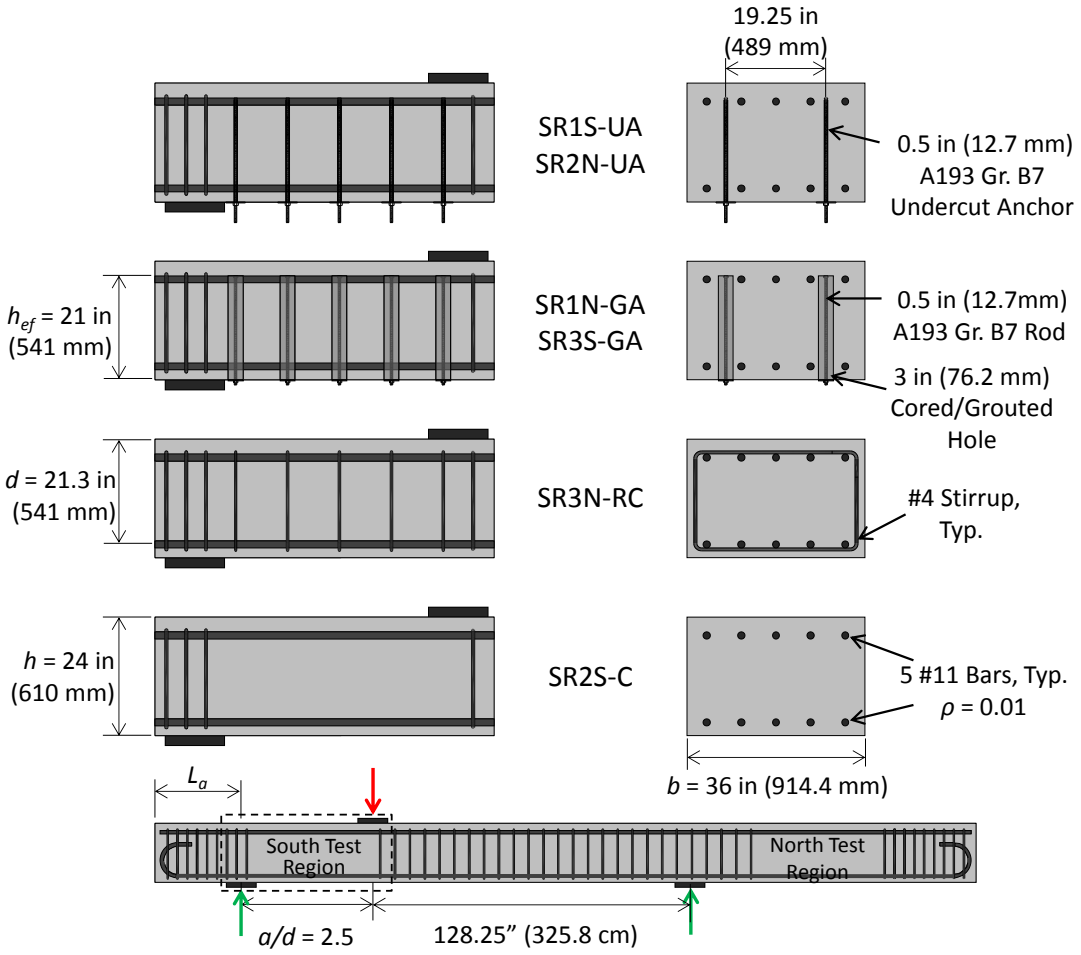

Fig. 3–1: Overview of test program, specimen variables, and specimen nomenclature.

3.2 SPECIMENS & TEST SETUP

Specimen dimensions, longitudinal reinforcement ratio, and shear span-to-depth ratio were kept constant for all tests; only transverse reinforcement—consisting of traditional reinforcement, undercut anchors, and grouted anchors—was varied. Each specimen was 36 in. (919 mm) wide (b) by 24 in. (610 mm) tall (h) by 332 in. (8.43 m) long. Each shear test region had an effective depth (d) of 21.3 in. (541 mm) and overall length of 53.3 in. (1353 mm) as measured between the centerlines of the support and the nearest applied load. The resulting shear span-to-depth ratio (a/d) was 2.5. The flexural

tension reinforcement ratio was kept constant at 1%, a moderate percentage of flexural reinforcement for beams.

No.4 deformed reinforcing bars were used in the shear test region reinforced with ACI 318 minimum transverse steel. The high strength rod used in four of the six shear tests was 0.5 in. (12.7 mm) diameter with an effective area of 0.142 in^2 (91. 6 mm^2). Spacing of all transverse reinforcement within the test regions was 10.5 in. (267 mm).

While the span-to-depth ratio was kept constant between tests, the length of specimen overhanging the support varied between tests to accommodate the retrofit hardware (Fig. 3–2). Note that during shear testing, the span not being tested overhung the far support and did not experience any shear stresses except those caused by the self-weight of the beam. Finally, the back span of each specimen (Fig. 3–1) was heavily reinforced with No.5 stirrups to ensure that a failure occurred only within the test region.

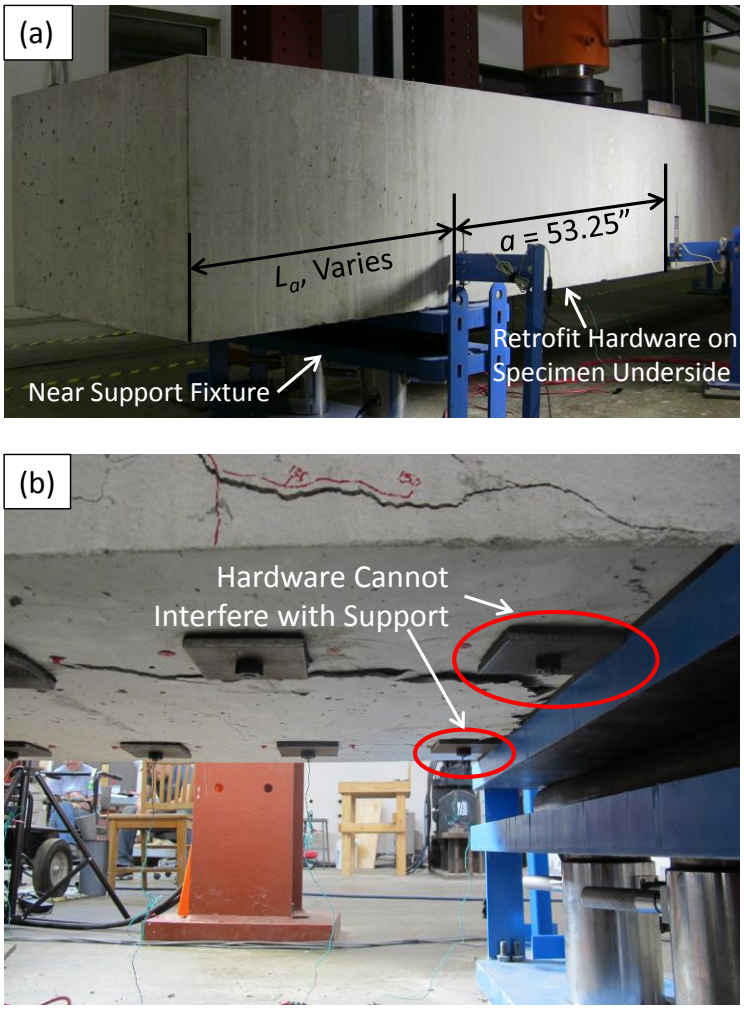

Fig. 3–2: Photographs of shear test setup. (a) specimen prepared for testing; (b) support overhang varies to prevent clashing between anchor hardware and the support.

3.3 RETROFIT DESIGN OBJECTIVES

The minimum transverse reinforcement prescribed by ACI 318 Section 11.4 was a particularly important benchmark for this series of tests. It should be noted that existing structures that do not contain transverse reinforcement have their design strength limited to $1\sqrt{f_c'}$. Adding transverse reinforcement automatically increases design strength by a factor of at least 2 (by allowing the use of $2\sqrt{f_c'}$ for the concrete contribution). Additionally, the standard allowed the shear behavior of elements reinforced with

traditional transverse reinforcement and elements reinforced with post-installed bars to be compared directly, using a code-determined baseline. More specifically, it was possible to determine if code-prescribed spacing limitations were appropriate for post-installed retrofits, assess the repeatability of retrofit tests and what factors may impact retrofit effectiveness, and compare the load-deflection behavior of retrofit and cast-in-place options.

A No. 4 rebar was chosen for the reinforced control specimen as the smallest possible bar which would meet or exceed the ACI minimum area requirements for transverse reinforcement when placed at *d/2* (10.5 in.). Similarly, a spacing of *d*/2 was chosen for the retrofit options, and then an anchor of appropriate diameter—such that rod and rebar yield forces were similar—was chosen. Note that at yield, an anchor can develop 24% more force than a #4 bar. However, it must be strained 75% more to realize that benefit. Perhaps more importantly, when a No. 4 bar yields, it will develop 12 kips (53.4 kN) of force; the equivalent anchor must strain 40% more to develop the same amount of force. Because shear failures tend to be brittle, shear cracks may not open wide enough for anchors to reach full yield or even develop as much force as mild reinforcement.

3.4 MATERIALS

Normal strength, ready-mix concrete was utilized for all beams, having a maximum aggregate size of 1 in. crushed limestone (25.4 mm) and with measured cylinder strengths ranging from 3.1 ksi (21.4 MPa) to 4.5 ksi (31.0 MPa) at the time of testing. All flexural reinforcement had a measured yield strength of 69.3 ksi (478 MPa). The measured yield strength of cast-in-place No. 4 transverse reinforcement was 61.3 ksi (423 MPA), with 118.3 ksi (816 MPa) and 130.3 ksi (898 MPa) yield strengths for

undercut anchors and grouted anchors respectively. A cementitious, non-shrink grout with extended working time and expected 3-day strength of 5000 psi (34.5 MPa) or greater was utilized in grouted anchor retrofits. Material properties are summarized in Table 3–1 for the reader's convenience.

Table 3–1: Summary of material properties.

Span ID	Transverse Reinforcement	f_c' - 28 Day	f_c'- Test	f_g' - Test	$f_{y,L}$	$f_{y,v}$ **or** $f_{y,ua}$ **or** $f_{y,ga}$
		psi	psi	psi	ksi	ksi
LD1S-C	None	3714	3658	N/A	69.3	N/A
LD1N-C	None	3714	3658	N/A	69.3	N/A
SR2S-C	None	4595	4360	N/A	69.3	N/A
SR3N-RC	ACI Minimum, CIP	3734	3311	N/A	69.3	61.3
SR1S-UA	Undercut Anchors	3699	3165	N/A	69.3	118.3
SR2N-UA	Undercut Anchors	4595	4498	N/A	69.3	118.3
SR1N-GA	Grouted Anchors	3699	3304	8576	69.3	130.3
SR3S-GA	Grouted Anchors	3734	3190	9960	69.3	130.3

3.5 MEASUREMENTS AND INSTRUMENTATION

The load-deflection response of each shear test region was measured with a data acquisition system and several sensors. A pair of linear potentiometers at each support and the point of applied load continuously recorded displacements. A "tripod" configuration of load cells was used to continuously record load, with two load cells at the support nearest the applied load and one load cell at the far support. Additionally, crack patterns were marked at discrete load steps during each test, and the largest diagonal crack width was measured whenever possible and safe.

Several strain measurements were also taken during shear tests. Cast-in-place transverse reinforcement, post-installed anchors, and longitudinal reinforcement were gauged for each test. Strain data and installation procedures are not discussed here, but are documented in Appendix E.4.

3.6 SHEAR TESTING

Shear spans were loaded monotonically in load steps equivalent to approximately 10% of the failure load calculated using the ACI 318-11 provisions for shear strength. The specimen's condition was photographed at the end of every load step. Once roughly 80% of the beam's nominal shear capacity had been reached, load was continuously applied until failure of the beam. All tested shear spans failed in shear and tests were stopped once the applied load fell to 70% or less of the peak load—recorded as V_u—reached over the course of the test.

For post-analysis, both the specimen's ultimate experimental load (V_u) and an estimate of the concrete's contribution to shear strength (V_c) were recorded. For evaluation purposes, it was critical to have a consistent definition of the concrete contribution (V_c) to a member's shear strength. Therefore, ACI Committee 326's definition[17] (i.e. ACI 318-11's current definition) of the concrete contribution to shear strength was adopted. Both documents take V_c to be the load applied up to first diagonal cracking. As such, a reasonable estimate (based on observation) of load at first diagonal cracking was recorded during testing and used as the experimental V_c term in post-analysis. In addition, the *experimental* steel contribution to shear capacity was calculated as the ultimate load on the test span minus the applied load at first diagonal cracking (experimental V_c). Finally, many values will be presented as "normalized shear stress", defined by Equation 1.

$$\boldsymbol{Normalized\ Shear = \frac{Shear\ Force}{\sqrt{f'_c} * b_w * d}} \qquad \textbf{Equation 1}$$

Where:

b_w = width of the web effective in resisting shear

d = effective member depth taken as the distance between the extreme compression fiber and the centroid of longitudinal tension steel

f'_c = average concrete compressive strength determined by cylinder testing

CHAPTER 4

Experimental Results &Analysis

4.1 EXPERIMENTAL OBSERVATIONS

The load-deflection response for each shear test region is summarized in Fig. 4–2. Maximum deflection at the point of the applied load was adjusted for rigid body motion of the entire specimen, i.e. movement at the supports (Fig. 4–1). From the data, it is clear that all specimens with transverse reinforcement carried much greater shear forces than unreinforced specimens, and that both retrofit options performed as well as, if not better than, the traditionally reinforced specimen (i.e. a specimen containing transverse reinforcement compliant with ACI 318-11 minimum requirements). Note that if the assumption that transverse reinforcement yields holds true, the steel contribution to shear strength of post-installed bars was expected to be 24% greater than that of cast-in-place bars.

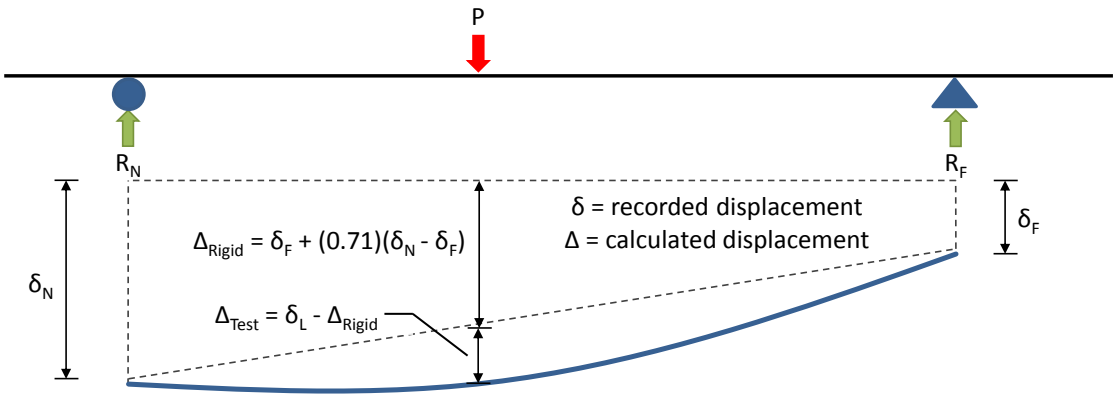

Fig. 4–1: Schematic (not to scale) for calculation of true deflection under the applied load, accounting for rigid body motion between the supports.

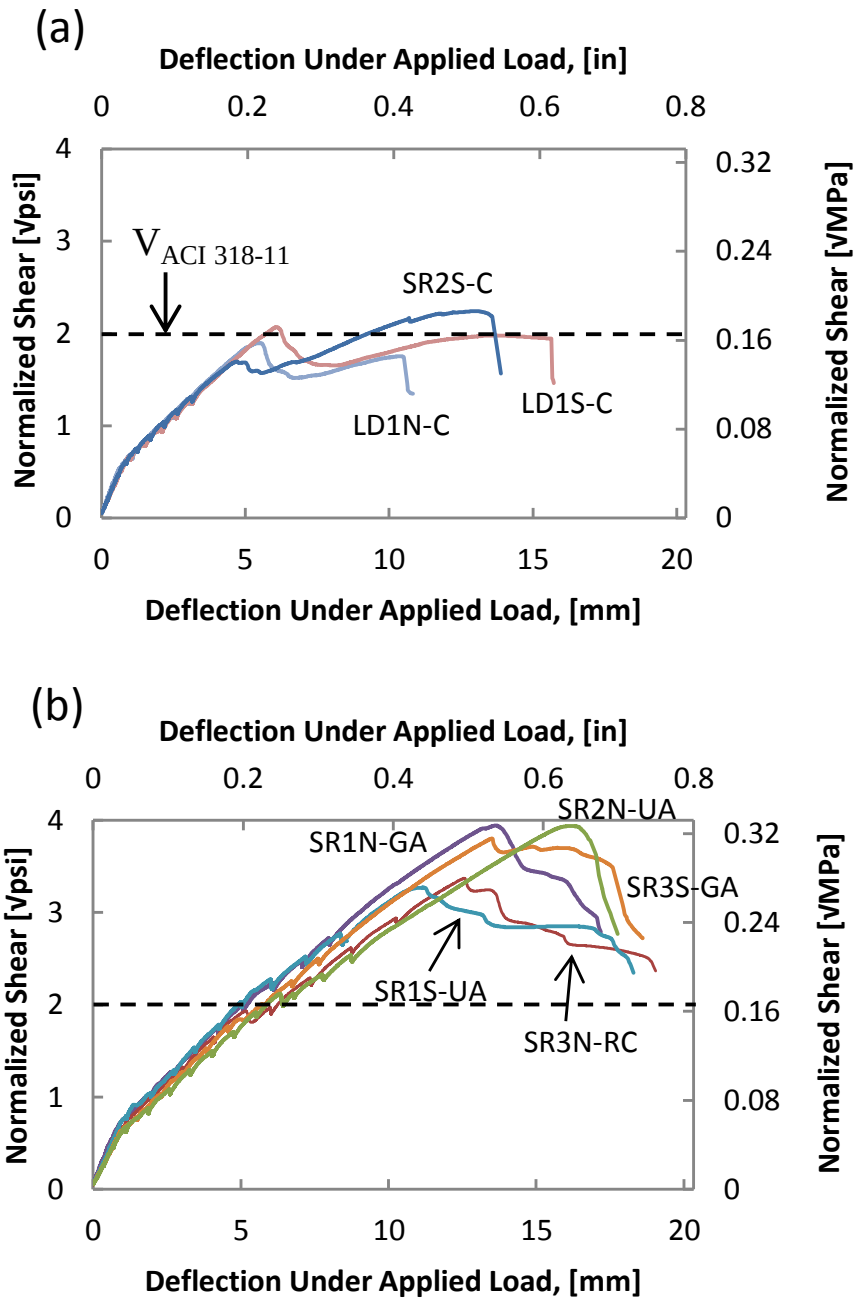

Fig. 4–2: Load-Deflection plot for all specimens included in the experimental program; (a) unreinforced control tests; (b) transversely reinforced specimens.

The location and orientation of the critical shear crack for each specimen is shown in the series of photographs included in Fig. 4–3. It is interesting to note that sections

retrofit with undercut anchors appeared to develop a single, very large critical shear crack (Fig. 4–3(e) & (f)). The crack continued to widen until force transfer was no longer possible and the test span failed. However, both grouted anchor specimens (Fig. 4–3(b) & (c)) initially developed a single diagonal crack, followed by several smaller cracks, before failure of the span. "Fanning" in the distribution of the cracks—development of many small, closely spaced cracks—is indicative of load redistribution, attributable to the continuous bond between transverse reinforcement and concrete.

Such behavior is to be expected. Unreinforced specimens developed a single diagonal crack and failed shortly after without any reinforcement to maintain equilibrium. Prior to diagonal cracking, sections with undercut anchors behaved identically. After cracking, tensile forces provided by straining the anchors prevented the diagonal crack from opening rapidly, and the section could sustain additional load. On the other hand, test spans that contained post-installed grouted anchors were expected to act similarly to specimens that contained cast-in-place shear reinforcement (i.e. stirrups), considering the continuous bond between transverse reinforcing bars and the concrete. Specimens reinforced with cast-in-place bars and grouted post-installed bars both failed after several smaller shear cracks developed, indicative of force redistribution[18].

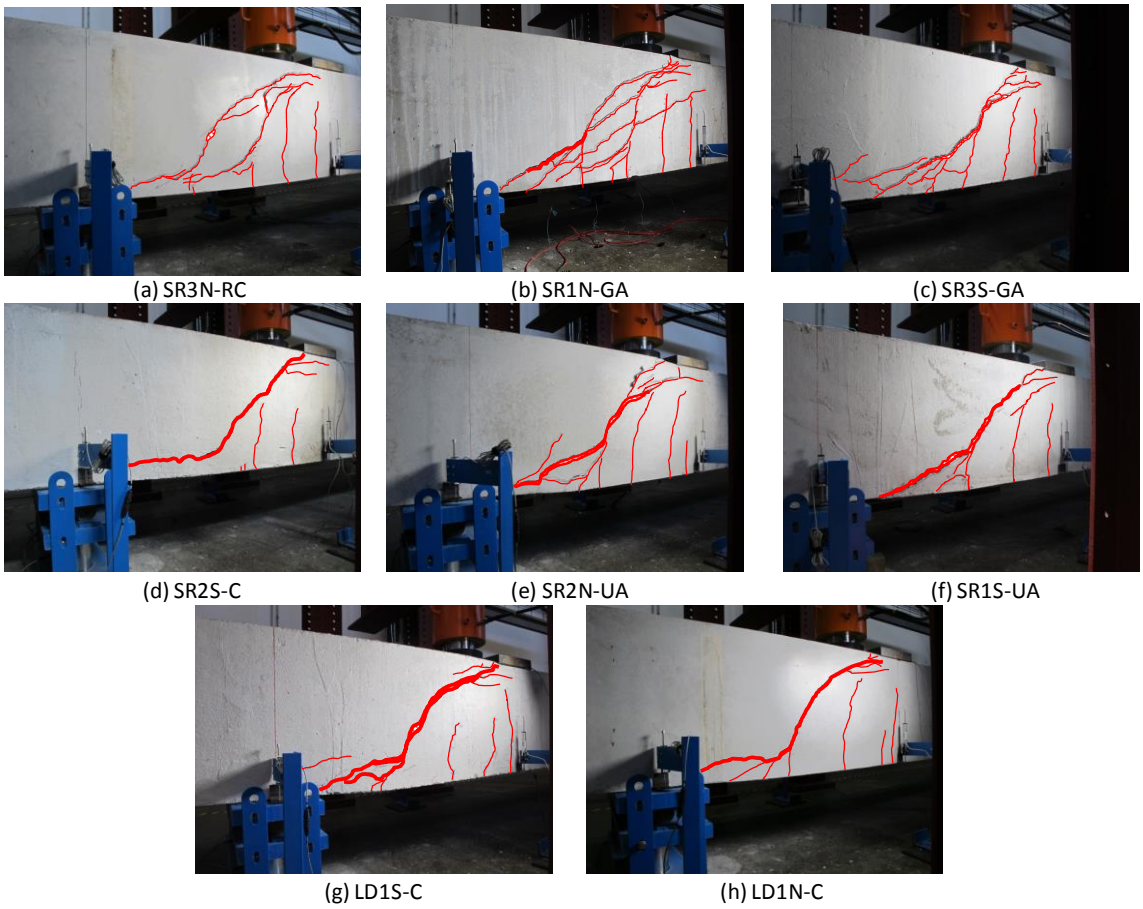

Fig. 4–3: Diagonal cracking pattern at failure for all test spans.

The results presented in Table 4–1 indicate that the shear capacities calculated according to typical code provisions agreed well with the experimental shear capacities of retrofit specimens. However, strain data from the undercut anchors, as well as observations during and after shear testing, strongly suggests that local stresses and reinforcement anchorage conditions influence the overall behavior of the retrofit. Highly stressed undercut anchors—especially those with anchor points close to the critical diagonal crack—appeared to "punch" through the concrete, implying a concrete breakout cone may have formed inside the beam (evidence of this phenomenon is presented in Fig. 4–4). Grouted anchors did not experience any "punching", but cover plates are visibly

bent on anchors where stresses were highest. This behavior may imply that slip was occurring at the grout/concrete interface, and the plates bent as the anchors were pulled toward the critical crack (refer to Fig. 4–4).

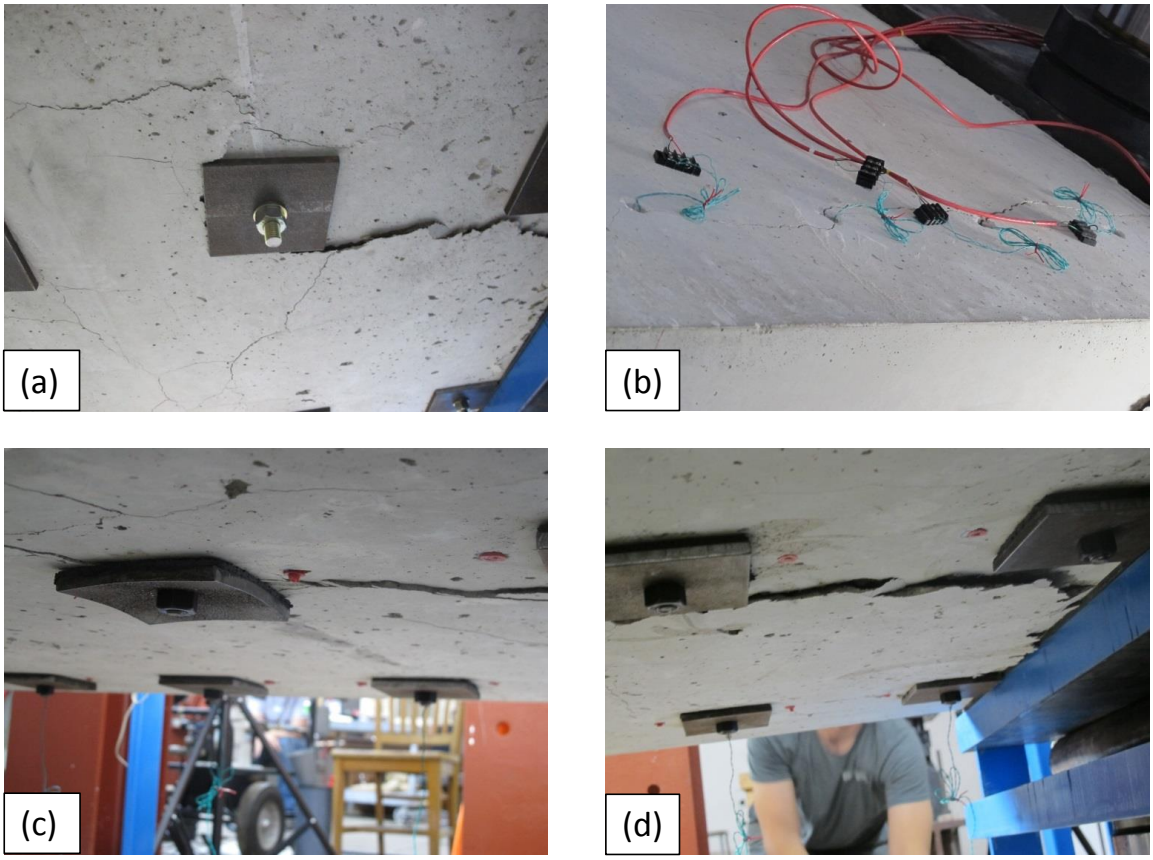

Fig. 4–4: Localized failures of anchor reinforcement. (a) undercut anchor plate "punching through" tension face of beam; (b) splitting between undercut anchor locations; (c) washer plate yielding; (d) structural core concrete failing between regions confined by post-installed anchors.

The above discussion implies that critical shear crack location can significantly impact the effectiveness of post-installed reinforcement (while having minimal impact on cast-in-place bars). Provided that the critical crack crosses a cast-in-place bar, that bar can practically always develop its full yield force since the bar is anchored by longitudinal reinforcement. However, post-installed bars do not have the benefit of being

anchored by longitudinal reinforcement. As such, the potential capacity of post-installed bars is controlled by the distance between the diagonal crack and the anchorage location, or potential anchorage length, of the bar. For undercut and grouted anchors, the crack location determines the size and capacity of a potential concrete break out cone. Crack location additionally affects the length over which the force at the crack must be developed by the concrete/grout bond (for grouted anchors). For a given post-installed bar, capacity decreases as the diagonal crack approaches the anchor location for that bar (Fig. 4–5).

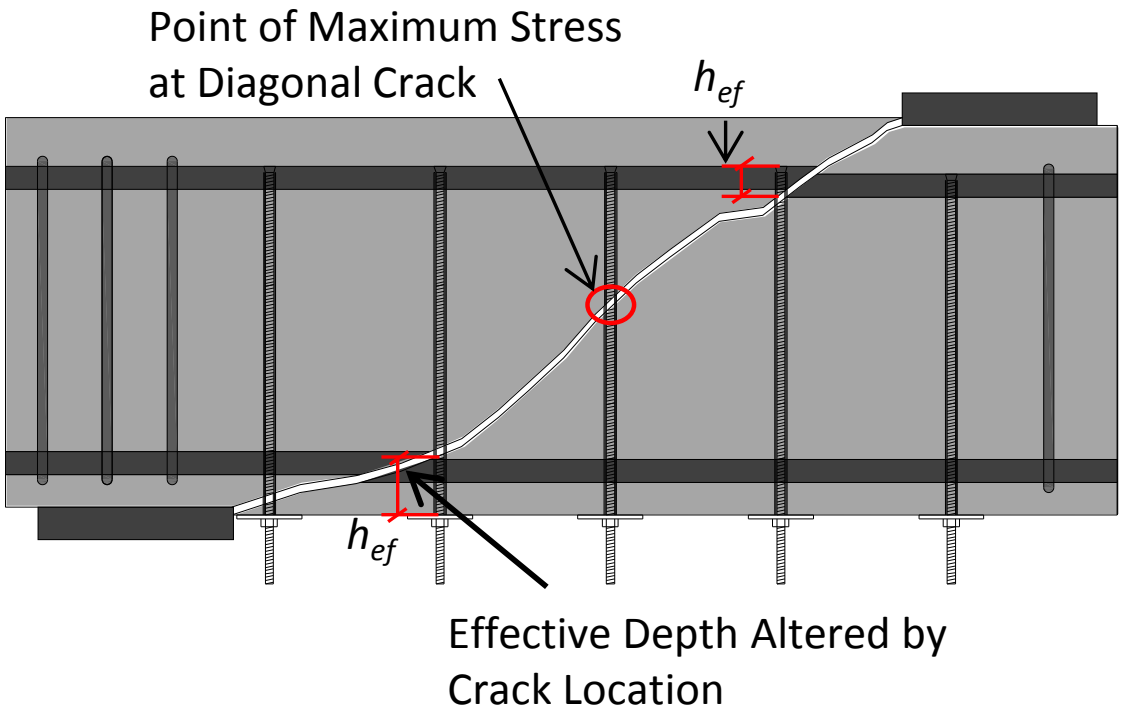

Fig. 4–5: Impact of diagonal crack location on effective embedment depths of post-installed reinforcement.

Table 4–1: Summary of experimental results & comparison to code provisions. Note: critical shear section assumed 26.625 in. from center of applied load.

	Span I.D.	V_{test}	V_{simple}	V_{test}/V_{simple}	$V_{general}$	$V_{test}/V_{general}$	V_{AASHTO}	V_{test}/V_{AASHTO}
		lb (kN)	lb (kN)	-	lb (kN)	-	lb (kN)	-
Concrete Contribution, V_c	SR2S-C	85905 (382.3)	101240 (450.5)	0.85	112350 (500.0)	0.76	110659 (492.4)	0.78
	LD1N-C	87899 (391.1)	92733 (412.7)	0.95	104314 (464.2)	0.84	104209 (463.7)	0.84
	LD1S-C	95983 (427.1)	92733 (412.7)	1.04	104314 (464.2)	0.92	104209 (463.7)	0.92
	SR3N-RC	85161 (379.0)	88225 (392.6)	0.97	99839 (444.3)	0.85	83139 (370.0)	1.02
	SR1S-UA	93013 (413.9)	86258 (383.8)	1.08	97927 (435.8)	0.95	76853 (342.0)	1.21
	SR2N-UA	109048 (485.3)	102830 (457.6)	1.06	113637 (505.7)	0.96	88450 (393.6)	1.23
	SR1N-GA	93392 (415.6)	88131 (392.2)	1.06	99688 (443.6)	0.94	76528 (340.5)	1.22
	SR3S-GA	79850 (355.3)	86598 (385.4)	0.92	98234 (437.1)	0.81	75440 (335.7)	1.06
	Span I.D.	V_{test}	V_{simple}	V_{test}/V_{simple}	$V_{general}$	$V_{test}/V_{general}$	V_{AASHTO}	V_{test}/V_{AASHTO}
		lb (kN)	lb (kN)	-	lb (kN)	-	lb (kN)	-
Steel Contribtuion, V_s	SR3N-RC	63531 (282.7)	49729 (221.3)	1.28	49729 (221.3)	1.28	65246 (290.3)	0.97
	SR1S-UA	48060 (213.9)	68012 (302.7)	0.71	68012 (302.7)	0.71	87314 (388.5)	0.55
	SR2N-UA	93415 (415.7)	68012 (302.7)	1.37	68012 (302.7)	1.37	86083 (383.1)	1.09
	SR1N-GA	80393 (357.7)	74911 (333.4)	1.07	74911 (333.4)	1.07	95182 (423.6)	0.84
	SR3S-GA	84803 (377.4)	74911 (333.4)	1.13	74911 (333.4)	1.13	95307 (424.1)	0.89
	Span I.D.	V_{test}	V_{simple}	V_{test}/V_{simple}	$V_{general}$	$V_{test}/V_{general}$	V_{AASHTO}	V_{test}/V_{AASHTO}
		lb (kN)	lb (kN)	-	lb (kN)	-	lb (kN)	-
Total Shear Strength, V_n	SR2S-C	85905 (382.3)	101240 (450.5)	0.85	112350 (500.0)	0.76	110659 (492.4)	0.78
	LD1N-C	87899 (391.1)	92733 (412.7)	0.95	104314 (464.2)	0.84	104209 (463.7)	0.84
	LD1S-C	95983 (427.1)	92733 (412.7)	1.04	104314 (464.2)	0.92	104209 (463.7)	0.92
	SR3N-RC	148692 (661.7)	137954 (613.9)	1.08	149568 (665.6)	0.99	148384 (660.3)	1.00
	SR1S-UA	141073 (627.8)	154269 (686.5)	0.91	165939 (738.4)	0.85	164167 (730.5)	0.86
	SR2N-UA	202463 (901.0)	170842 (760.2)	1.19	181649 (808.3)	1.11	174534 (776.7)	1.16
	SR1N-GA	173785 (773.3)	163042 (725.5)	1.07	174599 (777.0)	1.00	171710 (764.1)	1.01
	SR3S-GA	164653 (732.7)	161508 (718.7)	1.02	173145 (770.5)	0.95	170748 (759.8)	0.96

4.2 ANALYSIS & EVALUATION OF CODE PROVISIONS

The experimental results of this study were evaluated against the current provisions of the ACI 318-11 Building Code and the AASHTO LRFD shear provisions using known values for material properties. The provisions were chosen as the most likely formulations to be used by practicing engineers in the United States when designing a retrofit system. Commonly used design specifications elsewhere, specifically CSA A23.3 and EuroCode 2 should produce estimates comparable to AASHTO LRFD, as all three specifications are based on similar simplifications to the modified compression field theory (MCFT).

This section aims to outline important parameters which affect shear resistance in reinforced concrete elements. Additionally, each set of provisions used to estimate shear strength in this study is reviewed briefly. Finally, experimental results are compared to code predictions and to the ACI-DAfStb shear database[19,20].

4.3 PARAMETERS AFFECTING SECTIONAL SHEAR STRENGTH

Research concerning shear behavior and mechanisms has been intensely pursued over the past several decades. Yet, the complexity of reinforced concrete members' shear response—owing to a large number of influential variables—continues to make accurate and consistent shear strength predictions difficult. However, recent research efforts have identified several key section properties which can significantly impact shear capacity of members *without transverse reinforcement*. Those parameters are discussed briefly here and are covered extensively in a report produced by ACI Committee 445[21].

Generally, the shear span to depth ratio (*a/d)* and longitudinal reinforcement ratio (ρ) tend to have the greatest effect on relative shear strength, i.e. shear strength normalized by concrete compressive strength, $\sqrt{f'_c}$[22]. However, implicit to those two

parameters is a host of properties that are not typically accounted for individually. Kani[23], along was among the first to take interest in the so called "size effect", which was later thoroughly researched by Bazant[24,25,26] along with Collins & Mitchell[27]. Kani observed that relative shear resistance tends to decrease with increasing member depth, while Bazant noted that the ratio of member depth to maximum aggregate size may be a more appropriate metric for size effects than absolute member depth. Other researchers have demonstrated that the size effect is less a function of overall section depth, and is instead related to a member's ability to restrict crack widths[28,29]. Such research is consistent with the current thought that "aggregate interlock" and "dowel action" provide much of the shear resistance for members without shear reinforcement.

Geometry and loading also impact reinforced concrete members' ability to resist shear. Research has indicated that the shear transfer mechanism for reinforced concrete changes as the shear span lengthens; beams with a/d less than about 2.0 can typically resist higher shear stresses prior to failure. Additionally, shear forces do not typically act independently on a reinforced concrete element. Moments and axial forces can have significant impacts on shear carrying capacity. For example, large moments induce greater tension in flexural reinforcement, weakening the tension ties in truss models and reducing a member's ability to control cracks in MCFT-based models; furthermore, axial compression delays cracking (beneficial to shear capacity), while tension weakens the section by pulling crack faces apart[18].

Clearly, it is quite difficult to synthesize all of the components which affect an element's shear strength into a practical model. As such, very simple models, which may only consider one or two important parameters, tend to be overly conservative, but designer-friendly. More complex models incorporate a greater number of components, trading computational convenience for more realistic estimates. Notably, factors that

increase the shear strength of members without shear reinforcement by limiting crack widths (smaller member depth, more flexural reinforcement, etc.) are significantly less influential for members that do contain shear reinforcement. Although scatter in shear test data tends to be large, the trends discussed above are evident in the data collected within the ACI-DAfStb databases (Fig. 4–6).

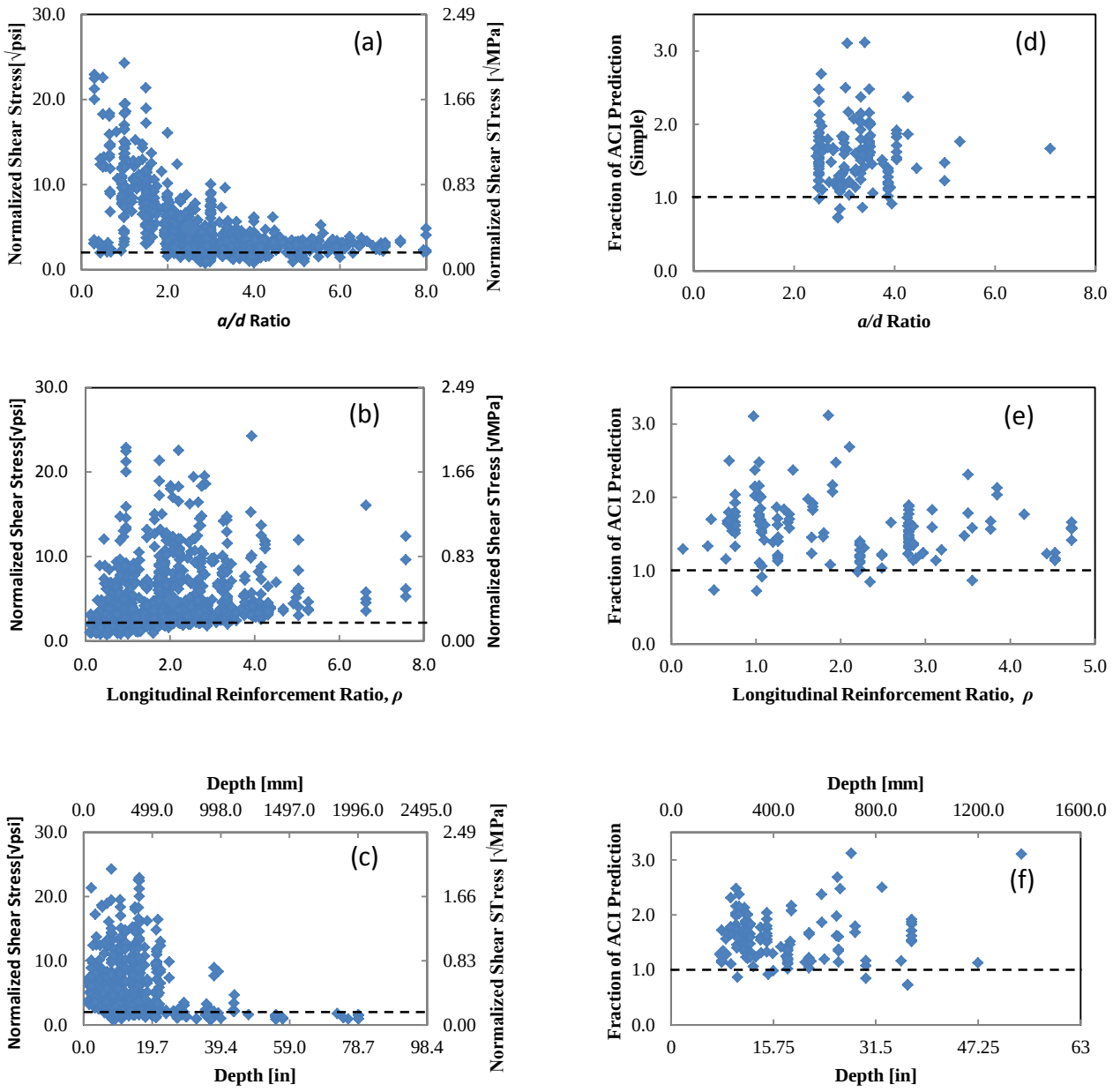

Fig. 4–6: Trends in shear behavior revealed by the ACI-DAfStb database. (a), (b), (c) presents data from unreinforced specimens. (d), (e), (f) presents data from transversely reinforced specimens.

4.4 ANCHOR CONTRIBUTION TO SHEAR STRENGTH

As noted previously, the force which develops in post-installed anchors is dependent upon where the critical diagonal crack forms. If the anchor strain and the crack location are known at the time of failure, the strength of a breakout cone or force developed by friction at the concrete-grout interface can be theoretically back-calculated; however, a designer will not have access to such information. Furthermore, ACI 318-11 and AASHTO LRFD impose respective limits of 60 ksi (413.7 MPa) and 75 ksi (517.1 MPa) for the yield stress of transverse bars. Such provisions essentially impose a "safe" strain limit on transverse reinforcement—or an allowable crack width—before sectional failure. Members failing in shear may not allow higher strength steel (as used in this research) to strain to its yield point prior to failure.

In summary, high levels of uncertainty in crack location and post-installed anchor strains make it particularly difficult to accurately estimate anchor contribution to member shear strength. However, for the purposes of this research, member shear capacities were calculated assuming yield of both cast-in-place and post-installed transverse reinforcement. Alternate calculations using the nominal material strengths and strengths limited by code provisions are provided in Appendix F.

4.5 ACI 318, SIMPLE EQUATION

The ACI 318-11 Building Code provides several expressions for the concrete contribution, V_c, to element shear strength. The ACI 318 model is "semi-empirical" and strength estimates are made by summing independently calculated "steel contributions" and "concrete contributions". A fixed 45 degree truss analogy allows direct calculation of a "steel contribution", V_s, (assuming that reinforcement is both vertical and yields prior to section failure) while ACI equation 11-3 is an empirical expression for the "concrete

contribution" (reproduced here as Equation 2). Equation 3 presents the generalized steel contribution term, used in more complex formulations; Equation 4 results from the simplifying assumptions mentioned above[9,21].

$$V_c = 2\sqrt{f'_c} * b_w * d \qquad \textit{Equation 2}$$

$$V_s = \frac{A_s * f_y * d * (\cot\theta + \cot\alpha) * \sin\alpha}{s} \qquad \textit{Equation 3}$$

$$V_s = \frac{A_s * f_y * d}{s} \qquad \textit{Equation 4}$$

Where:

A_s = total area of longitudinal tension steel

f_y = yield strength of steel (value used in calculations may vary, see Appendix F.2)

s = spacing of transverse reinforcement along member length

α = angle of transverse reinforcement relative to longitudinal axis of member

θ = Angle between member axis and concrete compressive strut (relative angle between member and critical shear crack)

The primary benefit of the above equations (specifically Equation 2 and Equation 4) is their simplicity, making implementation for designers very straightforward. Unfortunately, they do not account for factors that are widely known to significantly affect sectional strength for members without shear reinforcement.

4.6 ACI 318, GENERAL EQUATION

The "general" ACI equation for concrete shear capacity (ACI 318-11 equation 11-5) is reproduced as Equation 5, below. The analysis model is the same as in the previous section; the general equation simply adjusts V_c based on longitudinal reinforcement ratio and moment-shear interaction.

$$\boldsymbol{V_c = \left(1.9\sqrt{f'_c} + 2500\rho_w \frac{V_u d}{M_u}\right) b_w} \qquad \textbf{\textit{Equation 5}}$$

Where:

M_u = moment at a location corresponding to the critical shear section

V_u = sectional shear force at the critical section at failure

ρ_w = longitudinal reinforcement ratio, taken as: $A_s/(b_w*d)$

The general equation tends to decrease conservatism by making a more accurate prediction of the estimated concrete contribution to shear strength. Note that while this equation can be used for transversely reinforced elements, its express purpose is the prediction of shear capacity for members without shear reinforcement. As noted previously, the relative influence of longitudinal reinforcement on shear capacity is reduced by the addition of shear reinforcement. However, the shear-moment interaction remains important since large moments will still induce high strains in the flexural steel, permitting larger shear cracks and weakening sectional shear resistance.

4.7 AASHTO LRFD SHEAR DESIGN PROVISIONS

The AASHTO LRFD manual includes shear provisions for reinforced concrete members based on the modified compression field theory (MCFT). MCFT was originally developed by Vecchio and Collins at the University of Toronto as a rational, mechanical model to explain the behavior of reinforced concrete subjected to shear forces[30]. The

method enforces general equilibrium and compatibility using average stresses/strains and also considers local behavior at crack locations. MCFT is lauded for its accuracy, but the full theory (often used in finite element software) is burdensome for hand calculations. Vecchio, Collins, and Bentz simplified the method specifically for designing reinforced concrete elements; the simplified procedure forms the basis of current AASHTO LRFD shear provisions[31].

Some components of the equations provided in the AASHTO specification were not needed for this series of tests and the simplified set of equations (Equation 6 through Equation 10 and Equation 3) is presented below.

$$V_c = 0.0316\beta\sqrt{f'_c}\,b_v d_v \qquad \textit{Equation 6}$$

$$\beta = \frac{4.8}{(1 + 750\varepsilon_s)}\,\frac{51}{(39 + s_{xe})} \qquad \textit{Equation 7}$$

$$\theta = 29 + 3500\varepsilon_s \qquad \textit{Equation 8}$$

$$\varepsilon_s = \frac{(\frac{|M_u|}{d_v} + |V_u|)}{E_s A_s} \qquad \textit{Equation 9}$$

$$s_{xe} = s_x \frac{1.38}{a_g + 0.63} \qquad \textit{Equation 10}$$

Where:

a_g = maximum nominal aggregate size

b_v = effective web width in resisting shear with the effective shear depth, d_v

E_s = Young's modulus for steel

s_x = constant taken as lesser of *dv* or maximum distance between layers of crack control reinforcement

s_{xe} = crack spacing parameter

β = factor adjusting cracked concrete's ability to transfer shear and tension

ε_s = average strain in longitudinal tensile reinforcement

The AASHTO equations incorporate the greatest number of parameters affecting reinforced concrete element shear capacity and require the greatest computational effort. While the AASHTO provisions are more demanding, they have the benefit of attaching physical meaning to the parameters involved. An engineer can clearly see how one parameter affects the system and generally has greater control over the design process.

4.8 RESULTS COMPARISON

Fig. 4–7 and Table 4–1 present a concise comparison between experimental results and code provision predictions. Recall that the concrete contribution, V_c, was estimated as the load to produce first visible diagonal cracking; the steel contribution, V_s, is a quantity back calculated by subtracting V_c from the peak test load, V_u. In addition, the critical section for shear was assumed to be the middle of the shear span (i.e. *a/2* = 26.625 in. from the center of the applied load). Finally, note that the scatter for this small series of tests is low, and the data is clustered around the line that represents a 1:1 ratio between experimental and analytical results (Fig. 4–7).

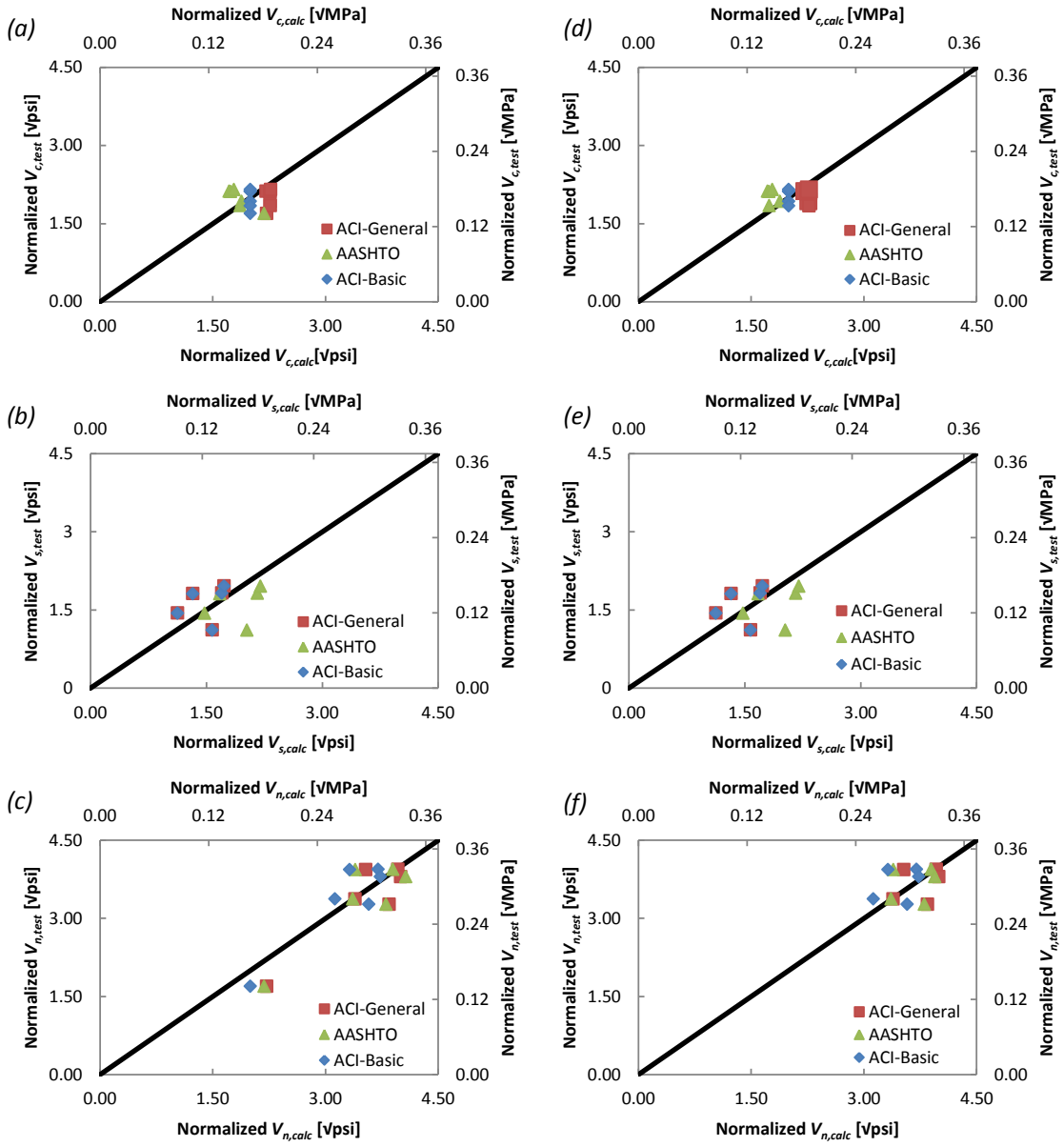

Fig. 4–7: Comparison of experimental results and code predictions. Points above the line represent conservative predictions; points below the line are unconservative. (a) concrete contribution—all tests; (b) steel contribution—all tests; (c) total shear strength—all tests; (d) concrete contribution—reinforced only; (e) steel contribution—reinforced only; (f) total shear strength—reinforced only.

The AASHTO LRFD equations tended to predict greater concrete contributions than experimentally observed in spans which were not transversely reinforced. In

addition, they consistently over-predicted the steel contribution to shear capacity in spans with shear reinforcement. Likely, this is a result of assuming that transverse steel will yield prior to failure. The high strength steel anchors require relatively large deformations to reach yield (observations during testing imply bars may not have yielded). For reasons discussed in previous sections, it may be particularly difficult to strain anchors enough to reach their yield point, resulting in an unconservative prediction of the steel contribution (note that using nominal values for yield stress provides more conservatism). Additionally, the critical shear crack angle is dependent upon the amount of transverse reinforcement. As such, high levels of transverse reinforcement will decrease the calculated concrete contribution, which, for these tests, resulted in overly conservative predictions of V_c in specimens reinforced by anchors.

Both ACI expressions ("simple" and "general") estimate V_s in the same way; predictions were typically conservative, since the expressions do not account for the angle of the shear crack. Interestingly, the simple ACI expression did a better job of predicting the concrete contribution, especially for unreinforced specimens.

Finally, observing the results of only the transversely reinforced specimens may offer better insights into each provision's ability to accurately predict shear strength. Comparisons between the experimental and analytical strengths for specimens with transverse reinforcement are shown in Fig. 4–7 (d), (e), and (f).

Additionally, experimental results were compared to the shear tests contained within the ACI-DAfStb databases for reinforced concrete elements both with and without shear reinforcement[19,20]. While comparisons to the databases did not necessarily provide new insights, they indicated that the experimental program conducted at the University of Texas agreed well with past studies. Specifically, retrofit test results aligned well with the trends established by transversely reinforced specimens (Fig. 4–6 (e), (f), (g)). That is to

say, despite behavioral differences in how cast-in-place and post-installed reinforcement transfer shear forces, the global response—at least for this set of tests—is largely unaffected.

The databases can be filtered (Appendix A) to obtain more direct comparisons to the experimental results. Those comparisons confirm the above observations that (i) the tests conducted under this experimental program agree well with tests performed in the past and (ii) both post-installed shear reinforcement and cast-in-place shear reinforcement diminish the impact that geometrical parameters such as *a/d* ratio, effective beam depth, and longitudinal reinforcement ratio have on the overall beam shear strength.

CHAPTER 5

Conclusions

This thesis investigated the use of post-installed grouted and undercut anchors as shear reinforcement for beam elements. The experimental program and subsequent comparisons between experimental results and code estimations permit the following conclusions to be drawn:

- Both undercut and grouted anchors, installed perpendicular to the axis of a beam element, are effective for shear strengthening. Both methods require only limited access to the member requiring retrofit.
- Experimental results from four tests of shear-strengthened beam specimens demonstrate that strength and deformation capacity can be increased significantly, and that behavior is similar to that of specimens containing cast-in-place transverse reinforcement.
- Careful consideration must be paid to alternate modes of anchor failure (i.e. failure prior to yielding). Concrete breakout cones, bond failure, and anchor failures may reduce overall section capacity. Higher concrete strength will make alternate failure modes less likely, and force anchors to yield.
- The common assumption that transverse reinforcement yields prior to section failure may not be appropriate when using high strength post-installed anchors. While higher strength concrete and excellent bond encourage post-installed bars to yield, the assumption may still be inaccurate. Note that strength predictions made with *nominal* material properties were conservative even if anchors did not yield. Further research should be performed with lower strength retrofit materials.

- Undercut anchors act as unbonded reinforcement, and they are much more sensitive to local failures than cast-in-place bars and grouted anchors. While undercut anchors are a fast and convenient solution, they should be implemented with due consideration given to alternate failure modes.

APPENDIX A

Shear Database Filtering

A.1 OVERVIEW

This appendix presents the results of filtering the ACI-DAfStb to obtain a subset of specimens that is more representative of the beams in this test program. For unreinforced specimens, the following filter ("Geometric") was applied:

- *a/d* ratio greater than 2.4
- longitudinal reinforcement ratio, ρ, between 0.75% and 1.25%
- Overall specimen depth between 17 inches and 25 inches
- *Note: this filter produces all rectangular beams*

Specimens which contained transverse reinforcement were filtered in two different ways. The first filter was identical to the one above. However, the filter produces a wide variety of beam geometries which may have an influence on shear capacity. Therefore, a second filter ("Rectangular") was also applied:

- Overall depth between 17 inches and 25 inches
- Beam geometry must be rectangular

As will be shown, comparisons to the database indicate that the tests performed agree well with data collected in the past. Clearly, the yield strength of transverse reinforcement will have a large impact on shear strength. Both ACI 318 and the AASHTO provisions place limits on transverse reinforcement yield strength. Therefore, plots included here will present calculated capacities based on actual material properties, and material properties limited by code provisions. Finally, information presented in the ACI-DAfStb database is compared only against ACI 318 (simple provisions) calculations and so comparisons will only be made on that basis.

A.2 TERMINOLOGY

The following graphs present information labeled as "Database", "UT Tests-Actual fy", and "UT Tests-Limited fy". For all Series, Vu is the maximum reported shear at specimen failure. Series labeled "UT Tests-Actual fy" are tested conducted under this program using actual material properties to determine the ultimate calculated shear capacity. Series labeled "UT Tests-Limited fy" are tests conducted under this program, but limiting transverse reinforcement yield strength to 60 ksi as required by ACI 318.

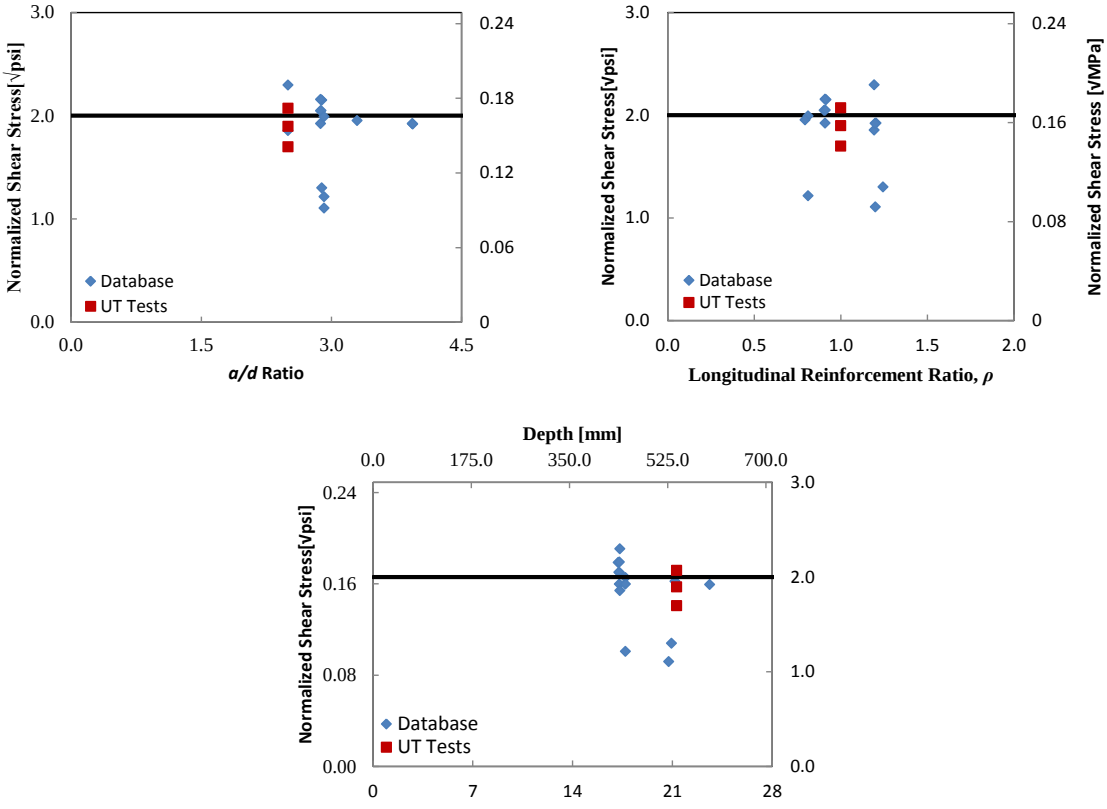

Fig. A-1: Comparison of control specimens to ACI-DAfStb for specimens without transverse reinforcement, using "Geometric" filter.

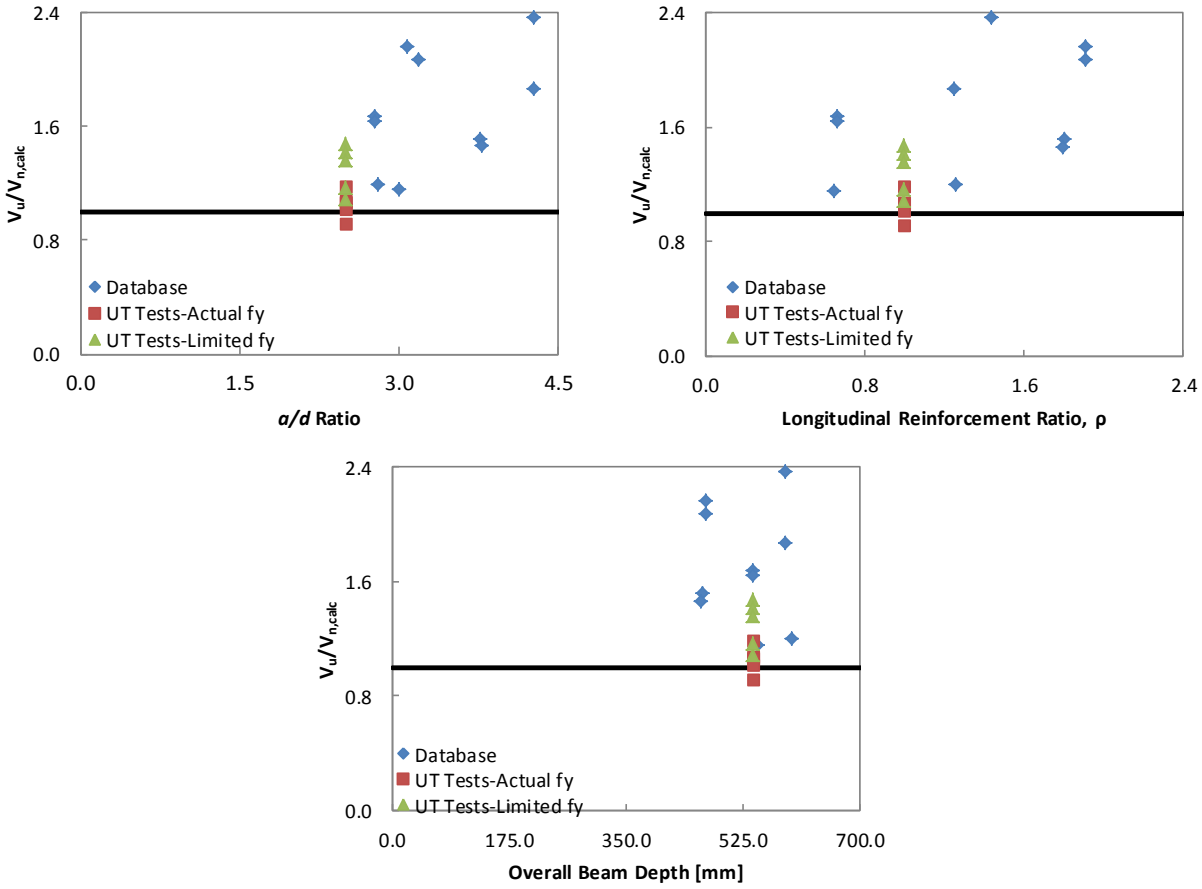

Fig. A-2: Comparison of transversely reinforced control and retrofit specimens to ACI-DAfStb database for transversely reinforced specimens, using "Geometric" filter.

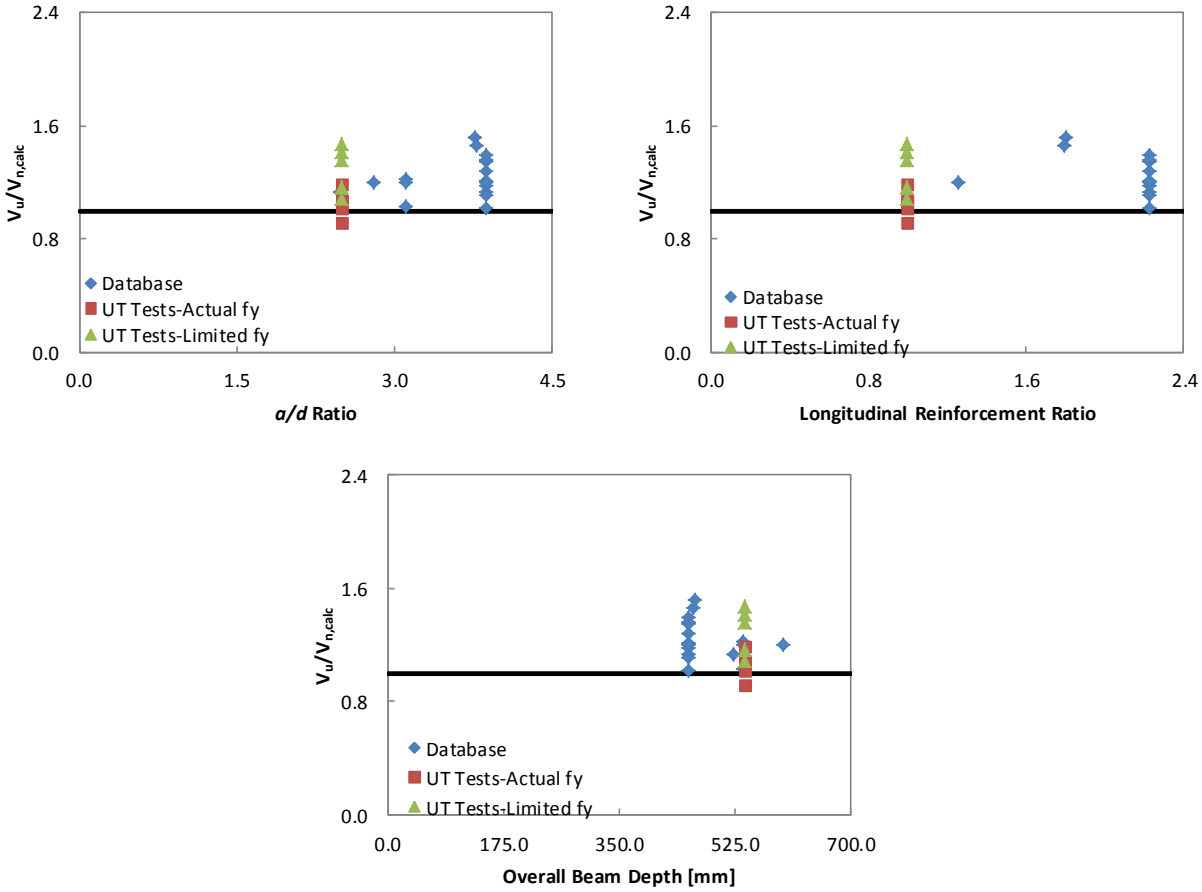

Fig. A-3: Comparison of transversely reinforced control and retrofit specimens to ACI-DAfStb database for transversely reinforced specimens, using "Rectangular" filter.

APPENDIX B

Specimen Design, Retrofit Design, and Test Setup

B.1 OVERVIEW

This appendix contains the complete drawing set for specimen construction and test setup layout. Sample photographs of cage fabrication and beam placement are provided. Additionally, the retrofit design process, along with informal testing conducted to aid that design, is presented.

B.2 SPECIMEN DESIGN

Overall specimen dimensions (height and width) were pre-determined by the project sponsor. As this project investigated the effectiveness of certain shear retrofit techniques, an appropriate amount of longitudinal reinforcement was selected to avoid flexural failure, yet still be within a practical construction limits (ρ = 1%). Hooks were provided on longitudinal tension steel, and the test region was located to preclude premature anchorage/flexural failure.

Test regions for the beam were 53.25 inches long, providing a shear span-to-depth ratio of 2.5. Only one span (of eight) was provided with cast-in-place #4 transverse reinforcing bars. Remaining spans were unreinforced to serve as either a control or retrofit (shear strengthened) span. The complete drawing set including elevation views, plan views, and sections views, is presented in Fig. B–1 and Fig. B–2.

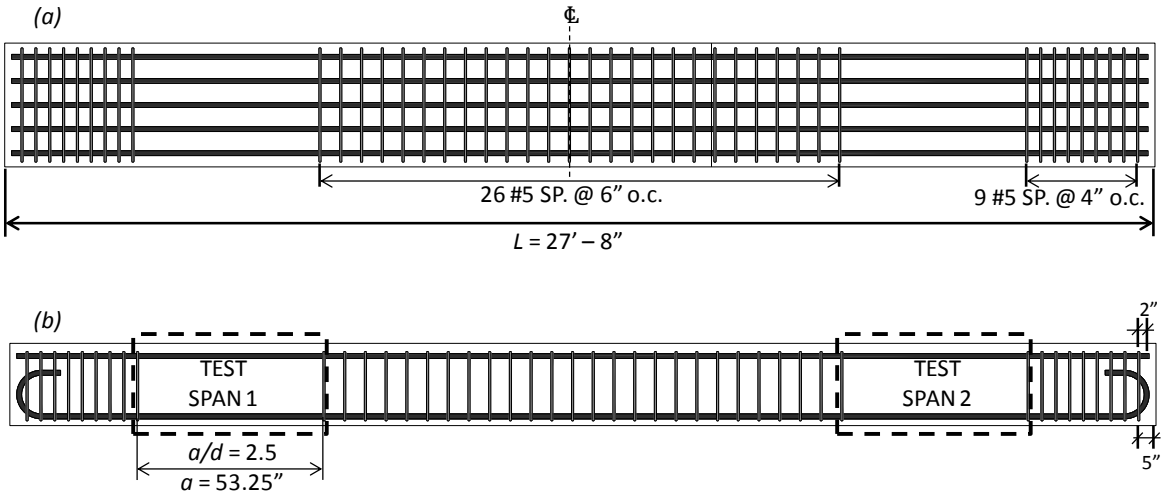

Fig. B–1: Overall specimen views. (a) Plan view; (b) Elevation view.

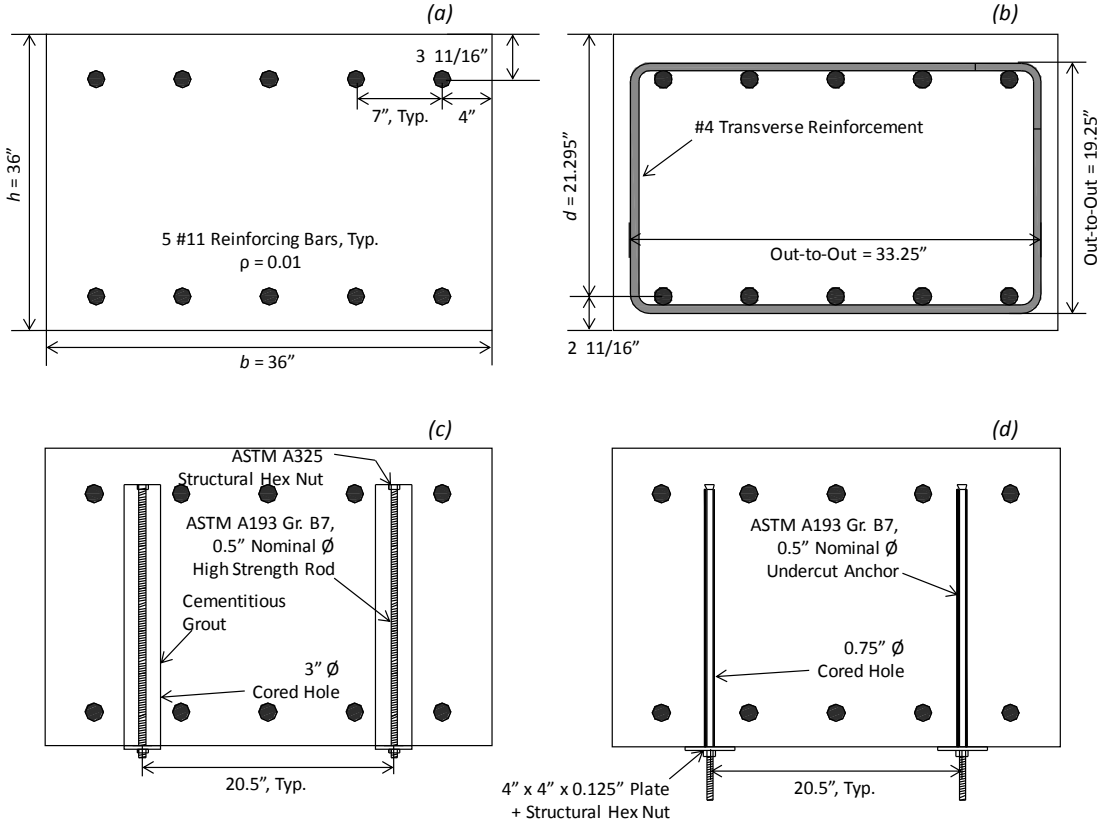

Fig. B–2: Test span section views. (a) unreinforced control; (b) cast-in-place reinforcement control; (c) grouted anchor retrofit; (d) undercut anchor retrofit

B.3 SPECIMEN FABRICATION

The 8 specimens within this program were constructed at the Ferguson Engineering Laboratory at the University of Texas at Austin. The construction process, documented in Fig. B–3, was as follows: 1) construct the cage with tension steel on top using saw horses; 2) prepare steel formwork and the casting area; 3) rotate the cage and place on steel formwork; 4) form specimen with ready-mix concrete and place cylinders for compression testing.

Fig. B–3: Specimen construction process. (a) completed reinforcing cage; (b) rotated cage set in formwork; (c) concrete placement; (d) completed specimen.

B.4 RETROFIT DESIGN

The ACI 318 minimum amount of transverse reinforcement was selected as an appropriate benchmark for this series of tests. As noted in the body of this report, all transverse reinforcement (both control and retrofit specimens) is spaced at 10.5 inches on center, using the smallest bar size that would accommodate the ACI 318 minimum. Standard 60 ksi rebar was used for the cast-in-place stirrups, while high strength B7 rod (105 ksi nominal yield strength) was used for the retrofit options. Notably, the high strength rod (with a smaller effective area) must reach a higher strain to achieve the same force as a reinforcing bar with same nominal diameter. Nevertheless, bar yield was assumed for high strength rod during the design process.

Anchors were embedded to a depth of 21 inches, roughly coinciding with the "top" of the compression steel. This ensured that post-installed reinforcement was well anchored in the compression zone and would not be affected by significant flexural cracking. Total anchor length was 22 inches and 24 inches for grouted and undercut anchors, respectively. Both anchor systems are pictured in Fig. B–4 and Fig. B–5.

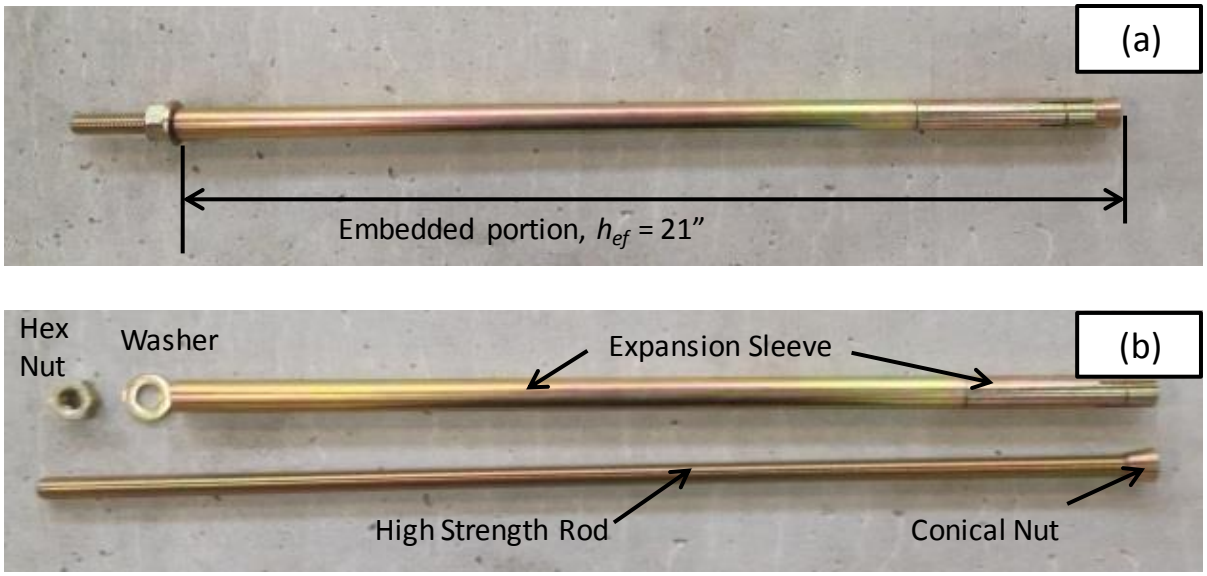

Fig. B–4: Undercut anchor system. (a) constructed anchor; (b) anchor components

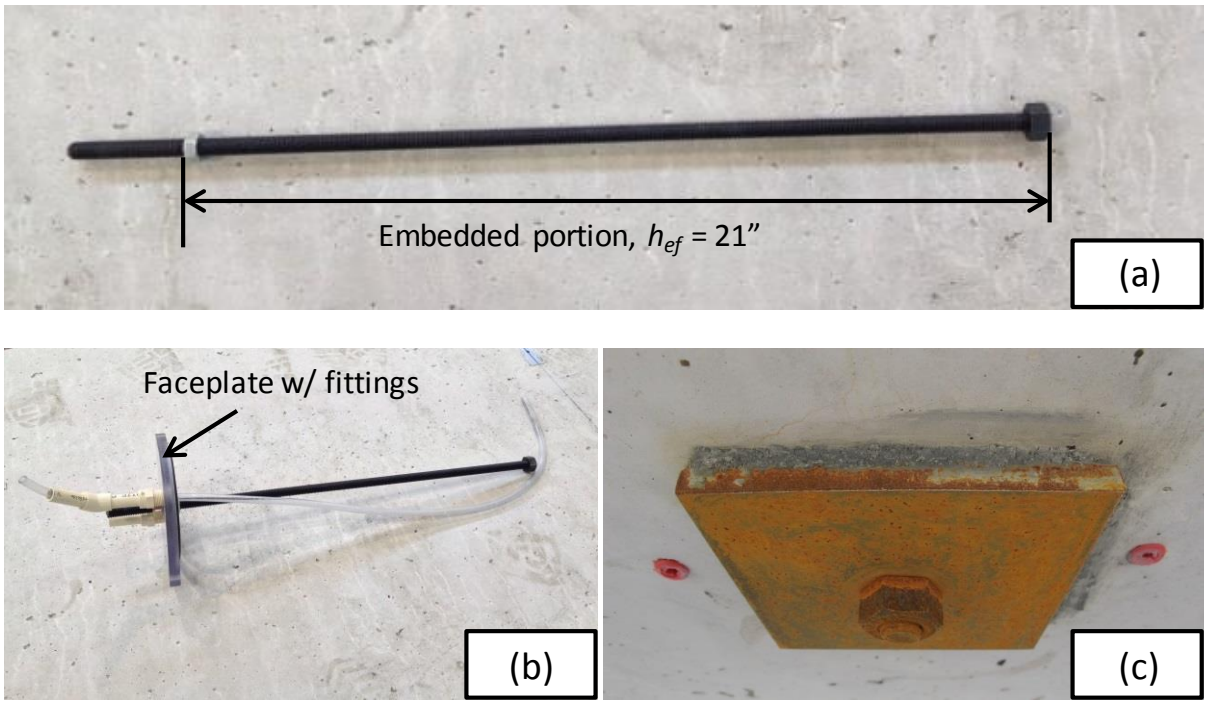

Fig. B–5: Grouted anchor system. (a) high strength rod with embedded structural nut; (b) assembly to be mounted on specimen prior to grouting (Fig. B–8); (c) installed system.

A number of failures—in addition to bar yield—are possible for post installed anchors, including concrete breakout cone for both undercut and grouted anchors, as well as a failure at the grout/concrete interface for grouted anchors. As noted in this report, the concrete breakout cone strength will be determined largely by critical shear crack location, which is difficult (if not impossible) to predict precisely. For this study, no adjustments were made to predicted anchor capacity based on the likely location of the critical shear crack. However, a "worst case" scenario in which the shear crack crosses an anchor at the centroid of longitudinal tension steel could be considered, a concrete breakout cone strength calculated, and shear resistance offered by the anchors adjusted accordingly.

Additionally, a series of informal "flow" and "pullout" tests were conducted in order to ensure that grouted anchor retrofits were feasible. The project sponsor was specifically interested in wall elements, and so grouted anchors had to be installed horizontally. Several grout consistencies and placement methods were experimented with to find a suitable technique for horizontal anchor installation (Fig. B–6 & Fig. B–7). The tests provided valuable information for ensuring that air voids were not left behind in the core holes after backfilling with grout. In this program, a set of polycarbonate "faceplates" was constructed and used as a platform for grout injection (Fig. B–8). Gravity feeding grout proved to be inconsistent even when a venting tube was provided. Achieving even distribution of grout proved too difficult when injecting thick grout without a faceplate.

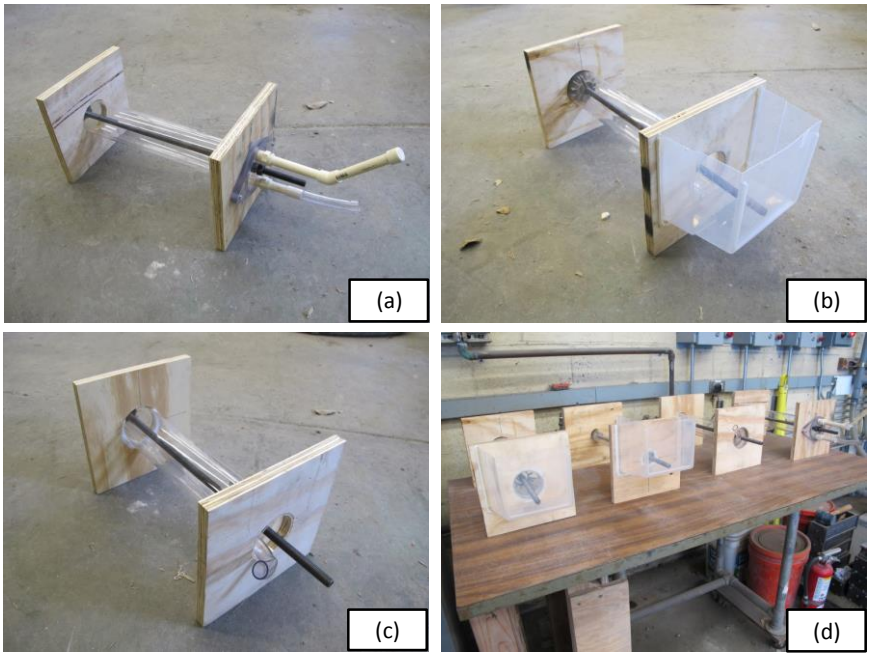

Fig. B–6: Various grout flow test setups. (a) faceplate option; (b) gravity fed option; (c) mortar placement option; (d) all setups.

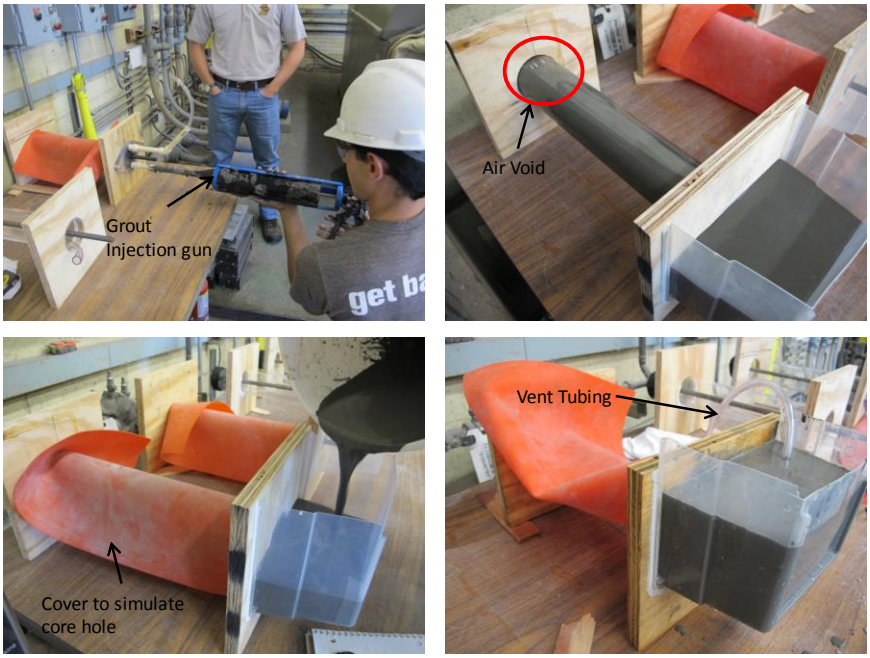

Fig. B–7: Trial runs for different grout delivery methods.

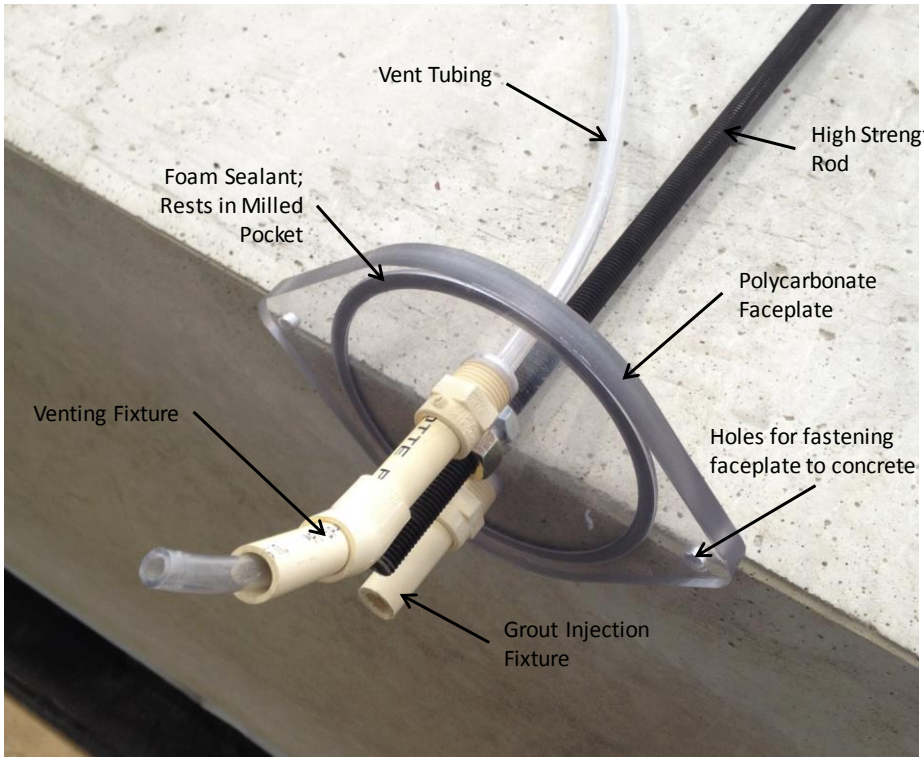

Fig. B–8: Faceplate platform with labeled components.

A pair of pullout tests with 3 inch anchor embedment and 3 inch hole diameter was conducted in 4.5 ksi concrete (greater than the expected strength of test program specimens). The tests were intended to demonstrate that bond at the grout/concrete interface was sufficient to prevent anchor failure at that location; the tests ended with the formation of a concrete break out cone (Fig. B–9). A summary of data collected is presented in Fig. B–10.

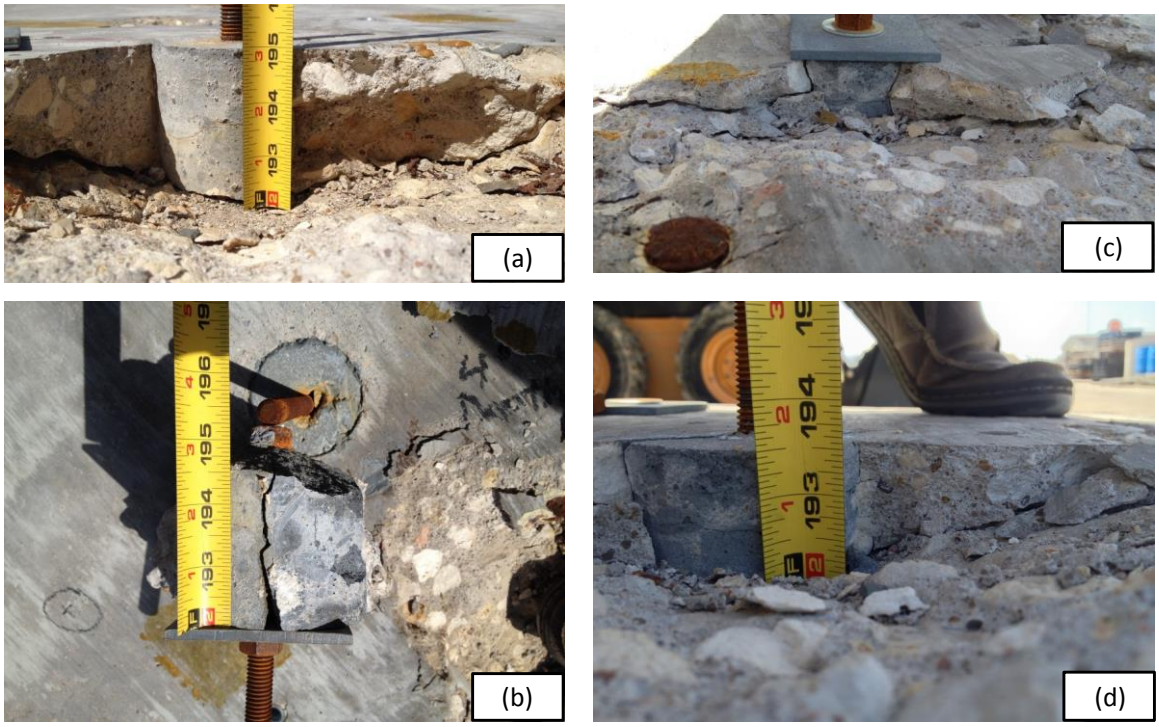

Fig. B–9: Pictures at anchor failure for informal pullout tests. (a) & (b): full concrete breakout cone; (c) & (d): shallow breakout cone.

Nominal Anchor Properties

f_y=	105.00	ksi
h_{ef}=	3.0	in
f'_c=	5000.00	psi
A_e=	0.142	in^2
k_c=	35.0	-
L_i=	7.0	in
d=	3.0	in

Test ID	Anchor Yield	Estimated Breakout Cone*	Maximum Load	Deflection at Failure	Grout/Concret Bond at Failure - τ_{min}**
	kip	kip	kip	in	psi
PO-1	14.91	12.86	14.06	0.06	497.25
PO-2	14.91	12.86	14.90	0.06	527.04

*Breakout cone strength calculated on CCD basis = $k_c*(f'_c)^{0.5}*h_{ef}^{1.5}$

**Minimum bond stress calculated = [Maximum Load]/(π*d*h_{ef})

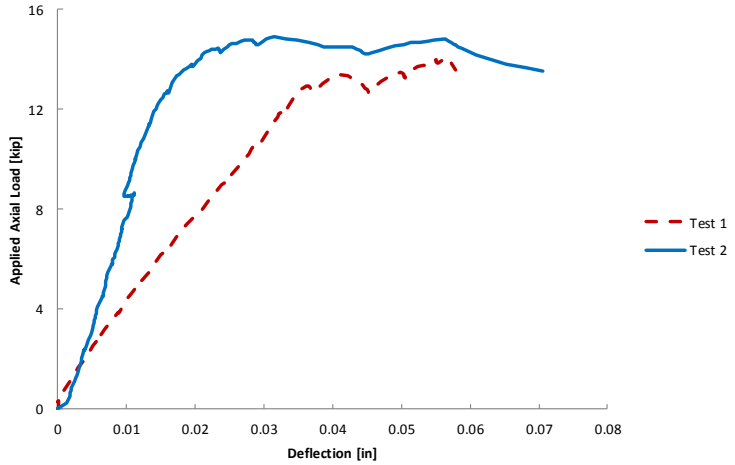

Fig. B–10: Results summary for informal pull-out tests.

B.5 TEST SETUP

Fig. B–11 and Fig. B–12 document the experimental program test setup. Schematic drawings, a photograph of the setup, and instrumentation locations and specifications are provided. As shown in Fig. B–12, the hydraulic loading ram reacts against a transfer beam, which passes loads into the columns, and then into the Ferguson lab strong floor. Shim plates were used at supports with more than one load cell to achieve balance between the load cells and neoprene pads were provided at all interface

locations between steel bearing plates and the specimen. Note that all plates (loading and bearing) were 12 in. by 36 in. by 1 in.

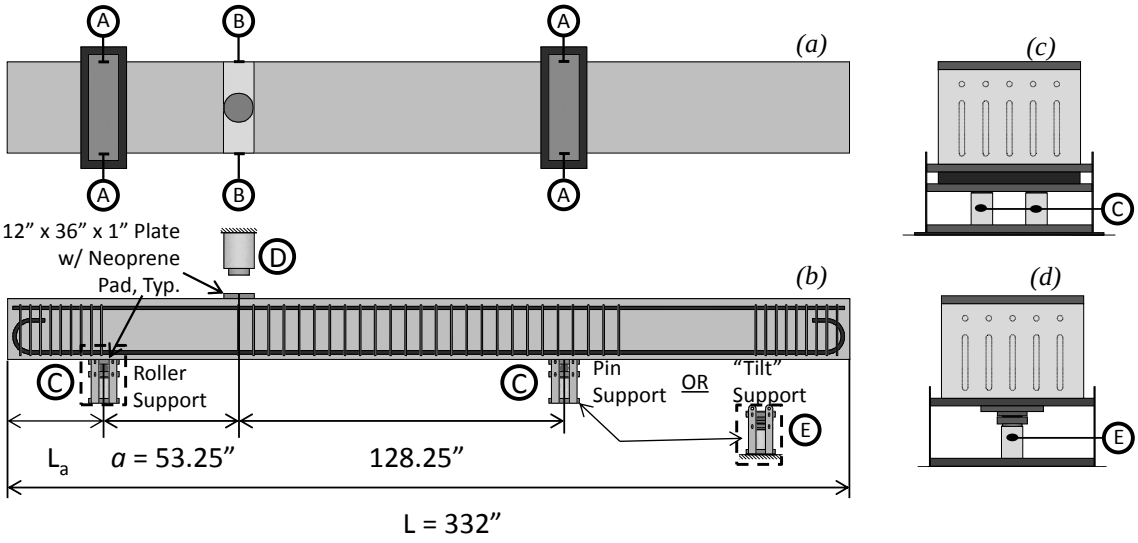

Location	Equipment		
	Manufacturer	Model	Capacity
A	Novotechnik	TR-0050	2 Inches
B	Novotechnick	TR-0100	4 Inches
C	Strainsense	SSTS504C	250 Tons
D	Force-Pak	R400-12	400 Tons
E	Strainsense	SSTS504C	250 Tons

Fig. B–11: Schematic view of program test setup with instrumentation summary table.

Fig. B–12: Shear test setup.

APPENDIX C

Materials and Material Testing

C.1 OVERVIEW

Appendix C provides a complete record of material testing conducted either at Ferguson Laboratory (concrete and grout compressive strengths) or by a 3rd party (rebar tension testing & concrete mix design). Results are provided as follows:

- Concrete mix design and average compressive strengths for concrete: Fig. C- 1 to Fig. C- 4.
- Reinforcing steel properties and determination of "yield" strength for B7 rod: Fig. C-5 to Fig. C-7.
- Summary of material properties for each test span: Table C–1.

C.2 NOTATION

f_c' = compressive strength of concrete

f_g' = compressive strength of grout

$f_{y,ga}$ = actual yield strength of grouted anchor transverse reinforcement

$f_{y,L}$ = actual yield strength of longitudinal reinforcement

$f_{y,ua}$ = actual yield strength of undercut anchor transverse reinforcement,

$f_{y,v}$ = actual yield strength of A615 transverse reinforcement

UT RESEARCH PROJECT

Date : **2/14/2014**
Mix Code : **4500727** Description : **4.5 SK NO FA, 3/4"LS, MRWR**

Revision Number : 4 Creation Date : 14 Feb 2014 Customer :
Plant : 973 PLANT Created By : cthomas2 Project :

Specifications

Consistence Class : 4.00 Air, % : 1.5
Strength Class : 3000 Max W/C : Max Agg Size : 1

Material Type	Material Code	Description	Supplier Source	Design Quantity	Specific Gravity	Volume ft3
Cement	CEMENT	CEMENT	ALAMO CEMENT CO-SANANTON	423 lb	3.15	2.15
Fine Aggregate	SAND	SAND	AUSTIN AGGREGATES-AUSTIN	1505 lb	2.62	9.20
Coarse Aggregate	57CLS	1" Limestone	COLORADO MATERIALS-SAN MA	1795 lb	2.57	11.19
Water	WATER	WATER	CITY-WATER	30.0 gal	1.00	4.01
Admixture	WREDUCER	WATER REDUCER	SIKA ADMIXTURES-DALLAS	7.0 /cwt	1.10	0.03
Admixture	WRRETARD	RETARDER/WATER REDUCER	SIKA ADMIXTURES-DALLAS	1.0 /cwt	1.20	0.00
			Yield	**3975 lb**	**27.00**	

Design Properties

Density : 147.2 lb/ft3 Grading Specification :
Cement Content : 423 lb Actual Dmax : 1 mm

Fig. C- 1: Concrete mix design (ready mix).

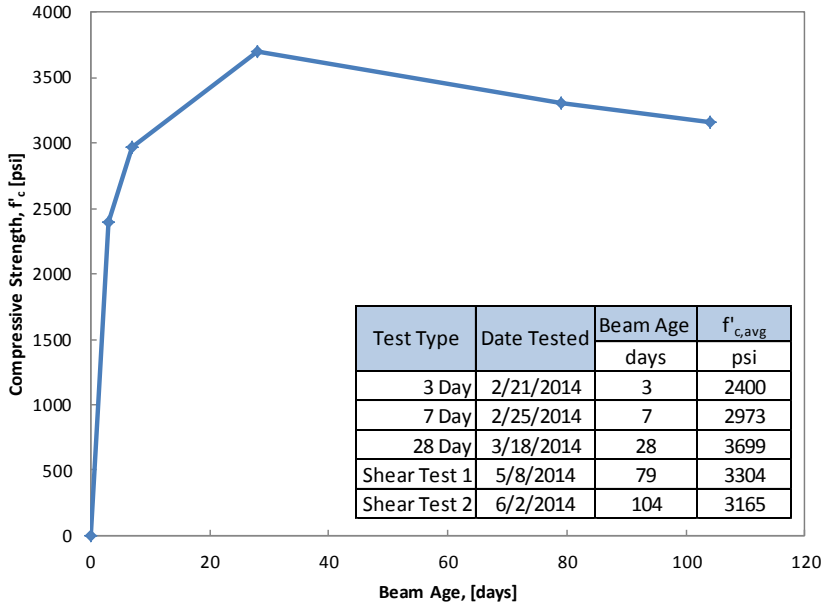

Test Type	Date Tested	Beam Age	$f'_{c,avg}$
		days	psi
3 Day	2/21/2014	3	2400
7 Day	2/25/2014	7	2973
28 Day	3/18/2014	28	3699
Shear Test 1	5/8/2014	79	3304
Shear Test 2	6/2/2014	104	3165

Fig. C- 2: Specimen SR1, concrete compressive strength history.

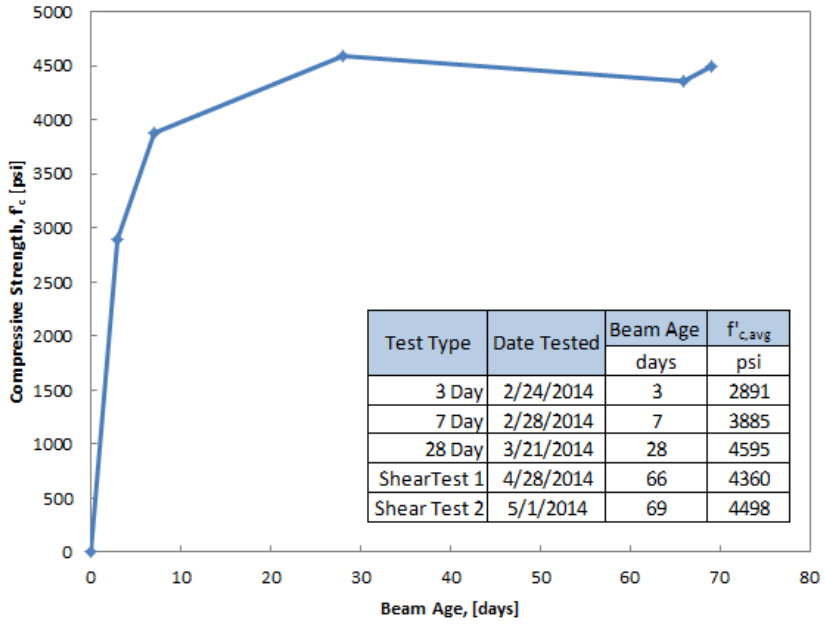

Test Type	Date Tested	Beam Age	$f'_{c,avg}$
		days	psi
3 Day	2/24/2014	3	2891
7 Day	2/28/2014	7	3885
28 Day	3/21/2014	28	4595
ShearTest 1	4/28/2014	66	4360
Shear Test 2	5/1/2014	69	4498

Fig. C- 3: Specimen SR2, concrete compressive strength history.

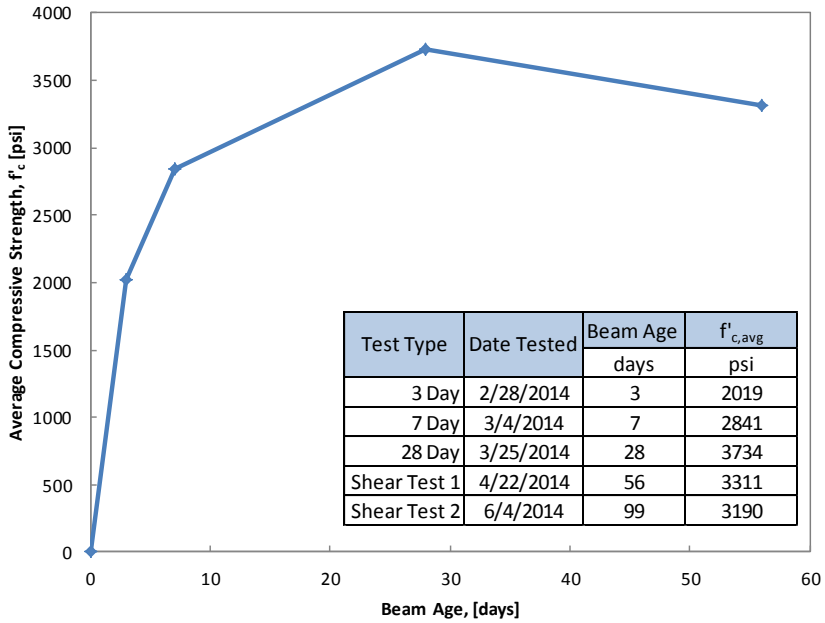

Test Type	Date Tested	Beam Age	$f'_{c,avg}$
		days	psi
3 Day	2/28/2014	3	2019
7 Day	3/4/2014	7	2841
28 Day	3/25/2014	28	3734
Shear Test 1	4/22/2014	56	3311
Shear Test 2	6/4/2014	99	3190

Fig. C- 4: Specimen SR3, concrete compressive strength history.

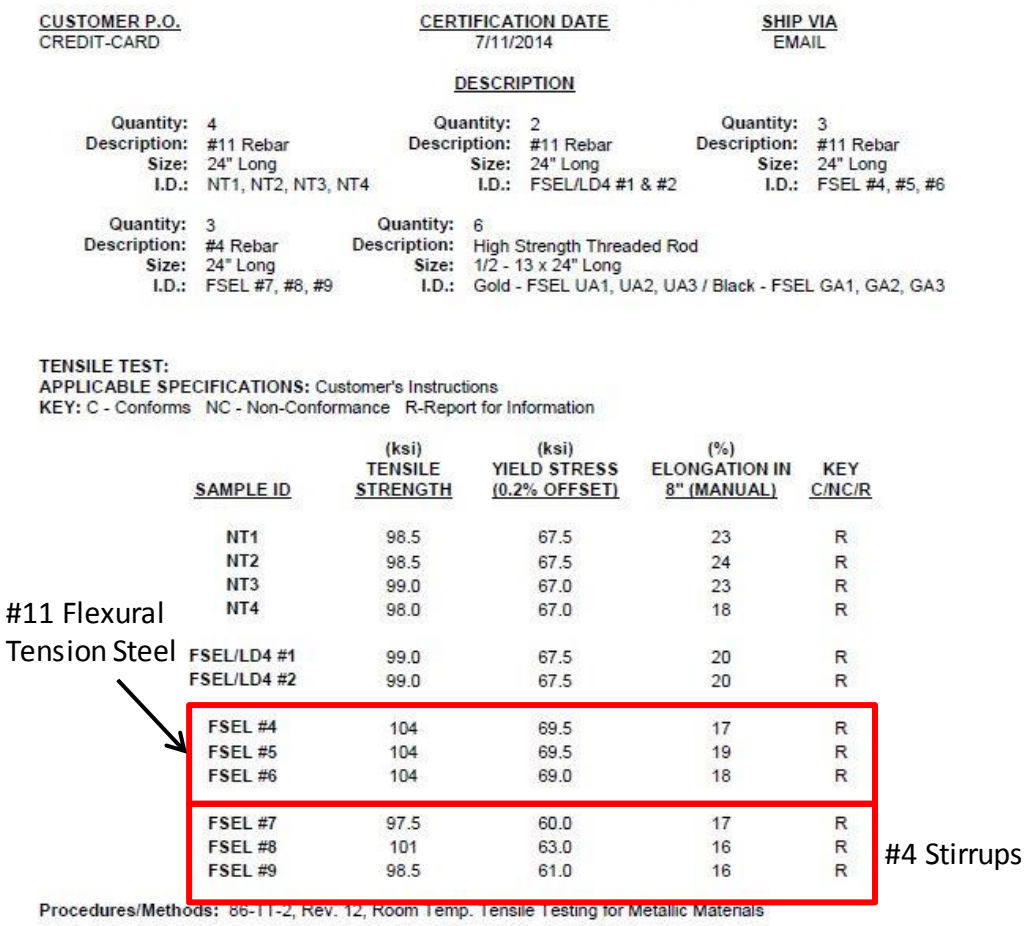

CUSTOMER P.O.
CREDIT-CARD

CERTIFICATION DATE
7/11/2014

SHIP VIA
EMAIL

DESCRIPTION

Quantity: 4
Description: #11 Rebar
Size: 24" Long
I.D.: NT1, NT2, NT3, NT4

Quantity: 2
Description: #11 Rebar
Size: 24" Long
I.D.: FSEL/LD4 #1 & #2

Quantity: 3
Description: #11 Rebar
Size: 24" Long
I.D.: FSEL #4, #5, #6

Quantity: 3
Description: #4 Rebar
Size: 24" Long
I.D.: FSEL #7, #8, #9

Quantity: 6
Description: High Strength Threaded Rod
Size: 1/2 - 13 x 24" Long
I.D.: Gold - FSEL UA1, UA2, UA3 / Black - FSEL GA1, GA2, GA3

TENSILE TEST:
APPLICABLE SPECIFICATIONS: Customer's Instructions
KEY: C - Conforms NC - Non-Conformance R-Report for Information

SAMPLE ID	(ksi) TENSILE STRENGTH	(ksi) YIELD STRESS (0.2% OFFSET)	(%) ELONGATION IN 8" (MANUAL)	KEY C/NC/R
NT1	98.5	67.5	23	R
NT2	98.5	67.5	24	R
NT3	99.0	67.0	23	R
NT4	98.0	67.0	18	R
FSEL/LD4 #1	99.0	67.5	20	R
FSEL/LD4 #2	99.0	67.5	20	R
FSEL #4	104	69.5	17	R
FSEL #5	104	69.5	19	R
FSEL #6	104	69.0	18	R
FSEL #7	97.5	60.0	17	R
FSEL #8	101	63.0	16	R
FSEL #9	98.5	61.0	16	R

Procedures/Methods: 86-11-2, Rev. 12, Room Temp. Tensile Testing for Metallic Materials

#11 Flexural Tension Steel

#4 Stirrups

Fig. C-5: Tension test results for #11 longitudinal bars and #4 shear reinforcement.

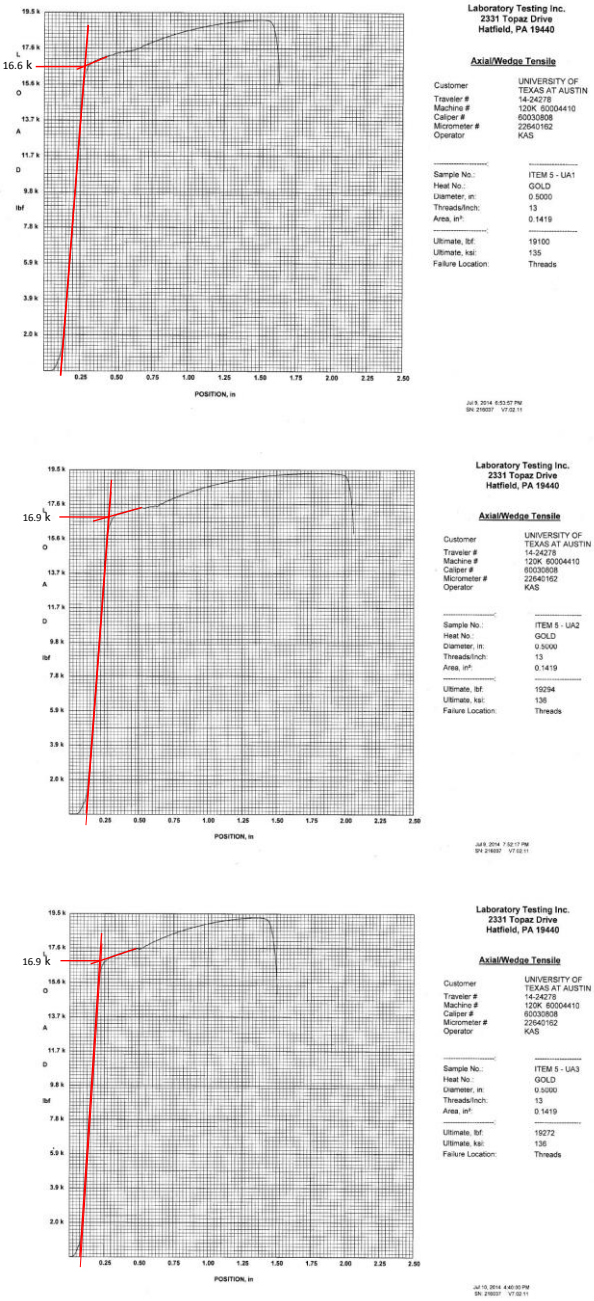

Fig. C-6: Determination of undercut anchor yield stress by intersection of linear portions of the load/deflection diagram before and after the proportional limit.

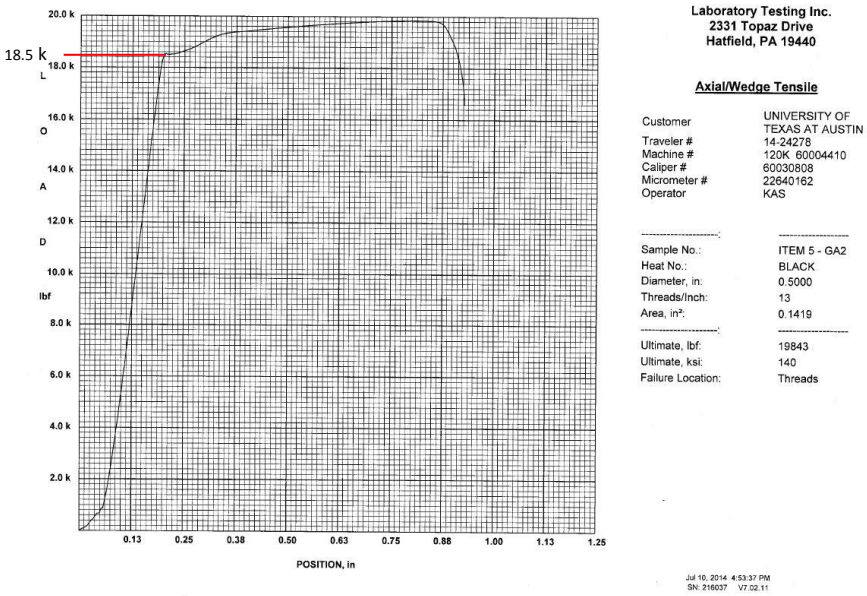

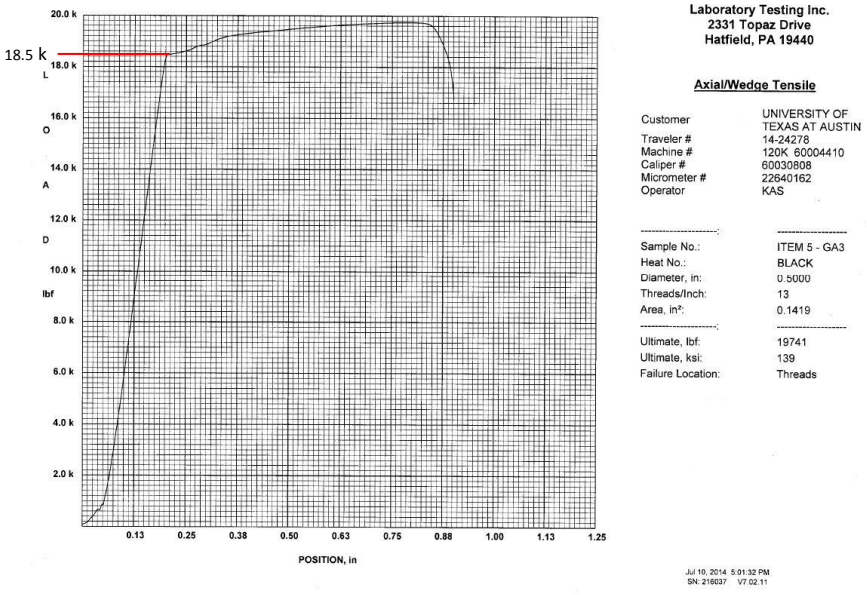

Fig. C-7: Determination of grouted anchor yield stress; taken as the maximum value of the linear portion of the load/deflection plot.

Table C–1: Summary of material properties for each test span.

Span ID	Transverse Reinforcement	f'c - 28 Day	f'_c - Test	f'_g - Test	$f_{y,L}$	$f_{y,v}$ **or** $f_{y,ua}$ **or** $f_{y,ga}$
		psi	psi	psi	ksi	ksi
LD1S-C	None	3714	3658	N/A	69.3	N/A
LD1N-C	None	3714	3658	N/A	69.3	N/A
SR2S-C	None	4595	4360	N/A	69.3	N/A
SR3N-RC	ACI Minimum, CIP	3734	3311	N/A	69.3	61.3
SR1S-UA	Undercut Anchors	3699	3165	N/A	69.3	118.3
SR2N-UA	Undercut Anchors	4595	4498	N/A	69.3	118.3
SR1N-GA	Grouted Anchors	3699	3304	8576	69.3	130.3
SR3S-GA	Grouted Anchors	3734	3190	9960	69.3	130.3

APPENDIX D

Experimental Methods

D.1 OVERVIEW

This section summarizes the parameters investigated by the experimental program; outlines installation procedures for undercut and grouted anchors; and describes shear testing procedures.

D.2 NOTATION

a = shear span, defined as the distance between centerlines of the load and the nearest support

a/d = span-to-depth ratio, defined as shear span divided by specimen depth

b_w = width of specimen (equivalent to effective shear width for rectangular sections)

d = specimen depth, defined as distance between extreme compression fiber and centroid of longitudinal tension steel

h = overall specimen height

S = distance between centerlines of pin and roller supports

s_v = spacing of transverse reinforcement

D.3 INVESTIGATED PARAMETERS

The goal of this project was to investigate the effectiveness of two shear strengthening techniques: 1) post-installing undercut anchors; 2) post-installing and grouting threaded rods. All other parameters were kept as consistent as possible (with

some variation in concrete compressive strength). Notably, span-to-depth ratio, specimen depth, longitudinal reinforcement ratio, and transverse reinforcement spacing and area are all kept constant. Table D–1 summarizes specimen nomenclature and purpose; Table D–2 lists properties kept constant for all tests.

Table D–1:Test matrix for parameters investigated

Specimen	Purpose	f'_c	Transverse Reinforcement Material	Nominal Reinforcement Yield Strength	Effective Reinforcemennt Area
		(psi)	-	ksi	in^2
SR2S-C	Unreinforced Control	4360	N/A	N/A	N/A
LD1N-C	Unreinforced Control	3658	N/A	N/A	N/A
LD1S-C	Unreinforced Control	3658	N/A	N/A	N/A
SR3N-RC	ACI Minimum Transverse Reinforcement	3311	ASTM A 615, #4 Rebar	60.0	0.20
SR1S-UA	Undercut Anchor Shear Strengthening	3165	ASTM A 193, Gr. B7 Threaded Rod	105.0	0.142
SR2N-UA	Undercut Anchor Shear Strengthening	4498	ASTM A 193, Gr. B7 Threaded Rod	105.0	0.142
SR1N-GA	Grouted Anchor Shear Strengthening	3304	ASTM A 193, Gr. B7 Threaded Rod	105.0	0.142
SR3S-GA	Grouted Anchor Shear Strengthening	3190	ASTM A 193, Gr. B7 Threaded Rod	105.0	0.142

Table D–2: Parameters held constant for all tests

a/d	d	ρ	a	s_v	b_w	h	S
-	(in)	-	(in)	(in)	(in)	(in)	(in)
2.50	21.295	0.01	53.2375	10.50	36.00	24.00	181.50

D.4 ANCHOR INSTALLATION PROCEDURE

This section describes installation techniques for both types of post-installed anchors. Procedures are applicable specifically to this program, but follow general best practices for undercut anchor installation and grouting. Additionally, photos of specialty equipment and installation are provided.

Installing undercut anchors

1) Diamond drill holes of the required depth and diameter in locations where post-installed shear reinforcement is desired. 0.75 inch diameter holes with a depth of 21 inches were used in this program.
2) Create undercut pocket using a specialized drilling tool (Fig. D–1 (b), (c), & (d)).
3) Thoroughly clean the hole of any dust and debris created by the above drilling operations.
4) "Set" the undercut anchor by placing the anchor and using a setting tool (Fig. D–1 (a)) to force the anchor's expansion sleeve into the undercut pocket, wedging it in place.
5) Place steel washer plate and torque a nut onto the anchor to the level specified by the anchor's manufacturer.

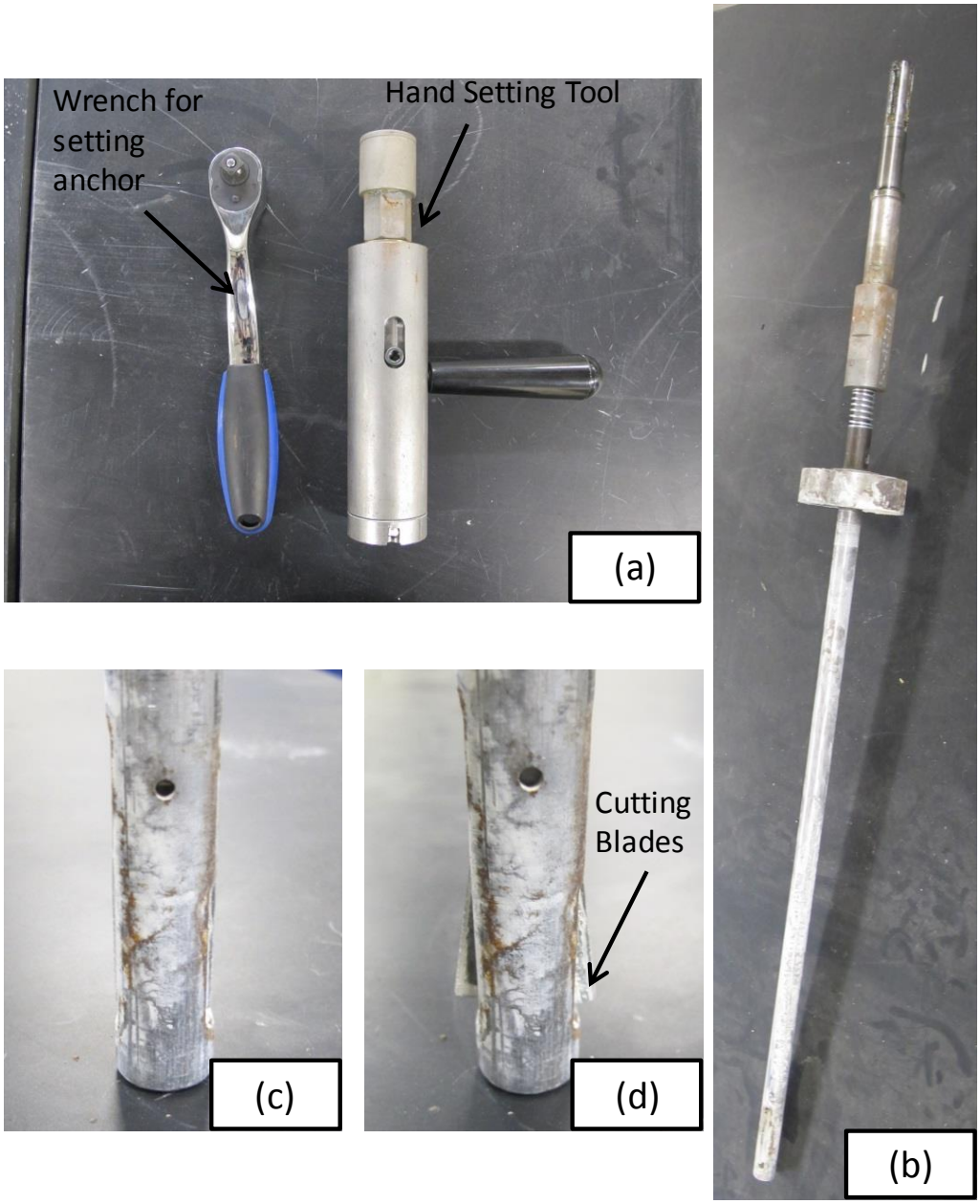

Fig. D–1: Undercut anchor tooling. (a) setting tools; (b) view of full undercut tool; (c) cutting end of undercut tool, blades not extended; (d) undercutting blades extended.

Installing grouted anchors

1) Diamond drill holes of the required depth and diameter in locations where post-installed shear reinforcement is desired. Note that hole diameter will depend on the bond stress that can be developed at the grout/concrete interface. For this program, 3 inch diameter holes with a depth of 21 inches were used.
2) After removing core debris, roughen the surface of the cored hole with a wire brush. Hole were roughened by attaching a wire bristle head to a long piece of threaded rod and then to an electric drill.
3) Thoroughly clean the hole of dust and debris to ensure sufficient bond between the grout and concrete.
4) Soak hole with water and keep damp for at least 24 hours prior to grout placement
5) Attach all required hardware/fixtures to the polycarbonate faceplates, then anchor faceplates over cored holes (Fig. D–2 (a)). Ensure that the threaded rods are reasonably centered in the cored holes.
6) Mix desired quantity of grout to either a "flowable" or "plastic" state (100-145% flow) as defined by ASTM C1437[32].
7) Inject grout via mortar gun or other means until grout begins to flow out of the air release fixture at the top of the faceplate. Slowly remove the vent tubing from the cored hole, then continue to inject grout until it flows from the air release fixture for a second time (Fig. D–2 (b)).
8) Seal injection fixture and cap air release fixture (Fig. D–2 (c)).
9) Allow grout to cure for at least 24 hours. Remove faceplates and grind down grout to be even with concrete if necessary.
10) Apply a layer of mortar, approximately ¼" thick onto plate washers and install by tightening a nut with a wrench until mortar is evenly distributed (Fig. D–2 (d)).

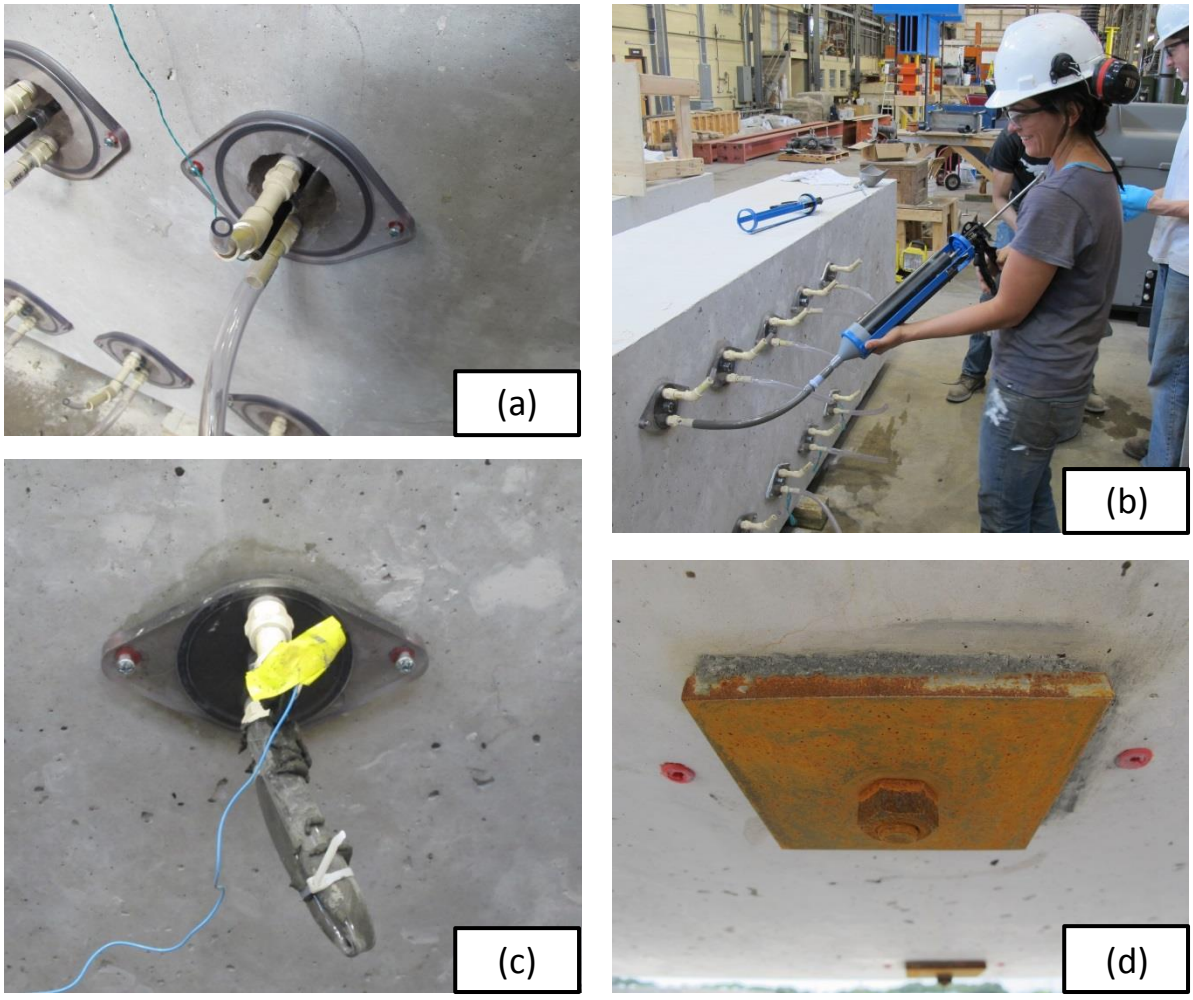

Fig. D–2: Grouting process. (a) faceplate fixture anchored to specimen; (b) grout injection; (c) seal fixtures after core hole is filled with grout; (d) mortared washer plate.

D.5 SHEAR TESTING

Shear tests were conducted as "three point" tests, utilizing the setup described in Appendix B.5. Specimen capacities were estimated using ACI 318 prior to shear testing and load was applied quasi-statically at a rate of approximately 200 pounds per second in load steps equal to roughly 10% of the specimen's nominal shear capacity.

After each load step, the specimen was allowed to settle, cracks were marked, and the specimen's condition was photographed. If present, the largest width of the critical shear crack was also recorded. Load stepping continued until it was deemed unsafe to stop and mark crack formations (typically around 70-80% of the nominal capacity). At this point, the specimen was loaded until failure, defined as whichever of the following occurred first: 1) Applied load dropping to 70% or less of the peak load; 2) Load stabilization with increasing deflections, indicative of flexural yielding.

The load progression for each specimen is presented in Fig. D–3 through Fig. D–10. Load in each photograph is expressed as a percentage of the failure load for that particular specimen. Note that for unreinforced spans, the failure load is taken as the load at first diagonal cracking, even if a higher peak load was achieved over the course of testing.

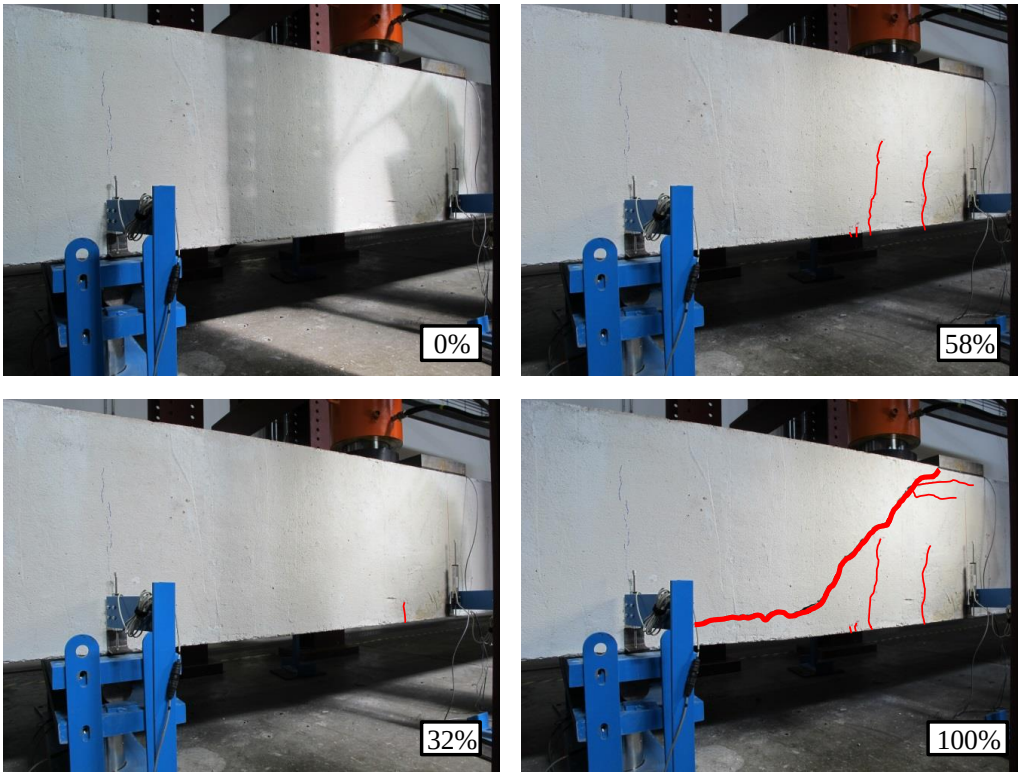

Fig. D–3: Load progression, SR2S-C.

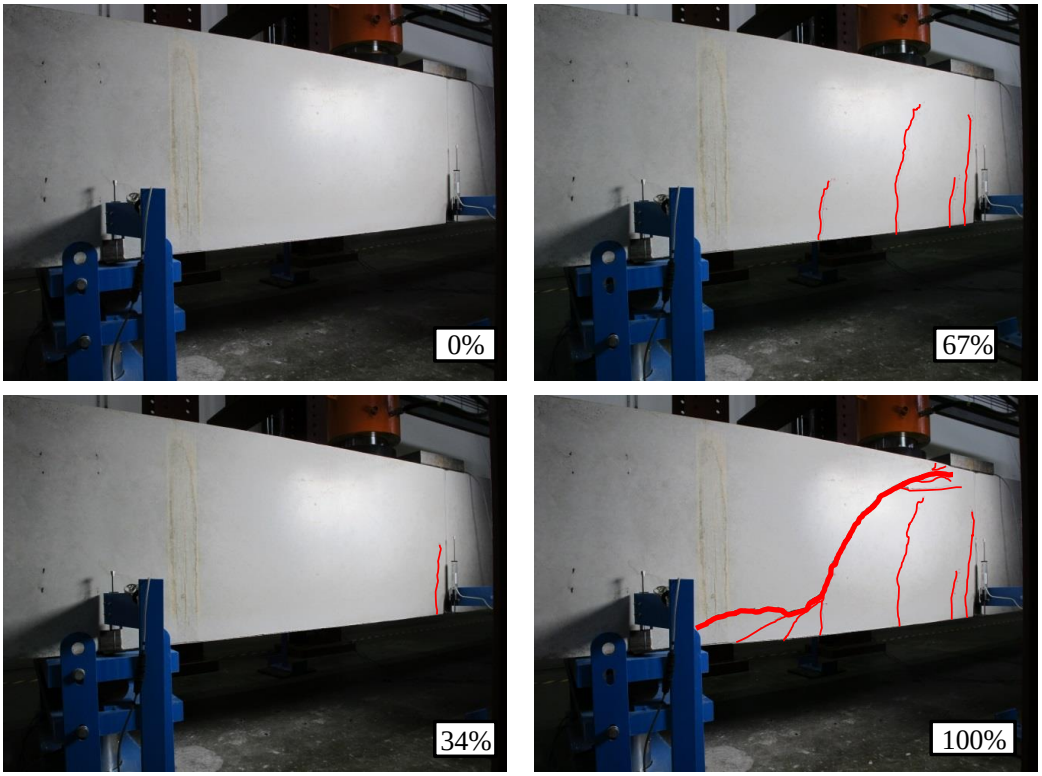

Fig. D–4: Load Progression, LD1N-C.

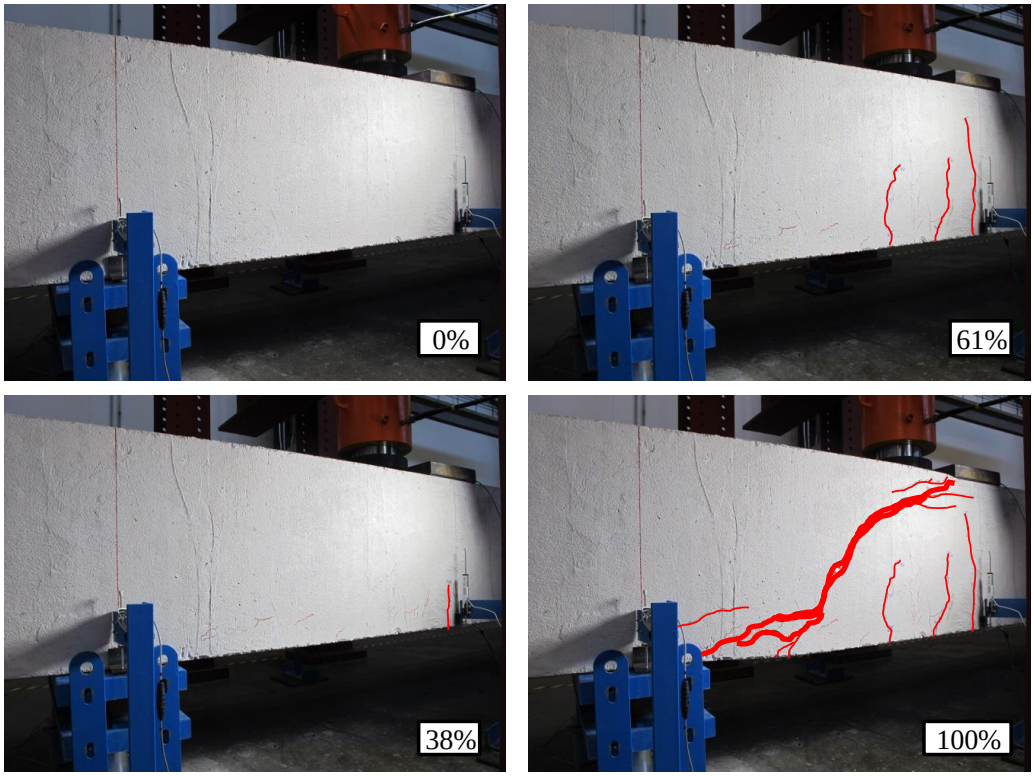

Fig. D–5: Load progression, LD1S-C.

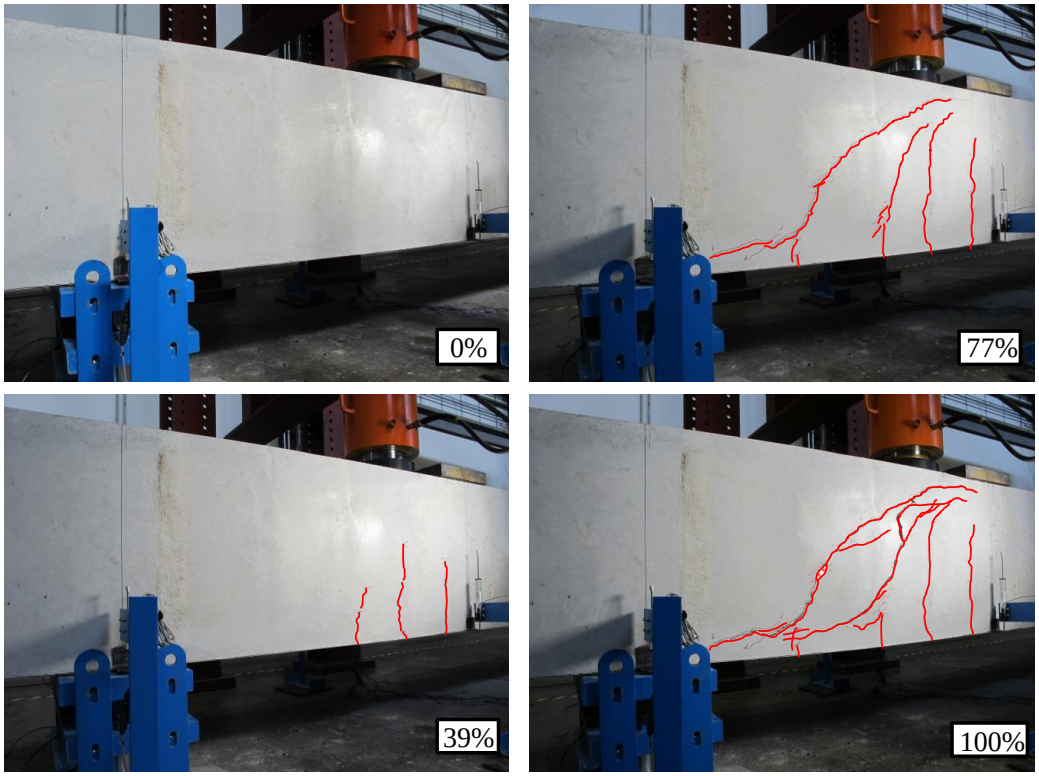

Fig. D–6: Load Progression, SR3N-RC.

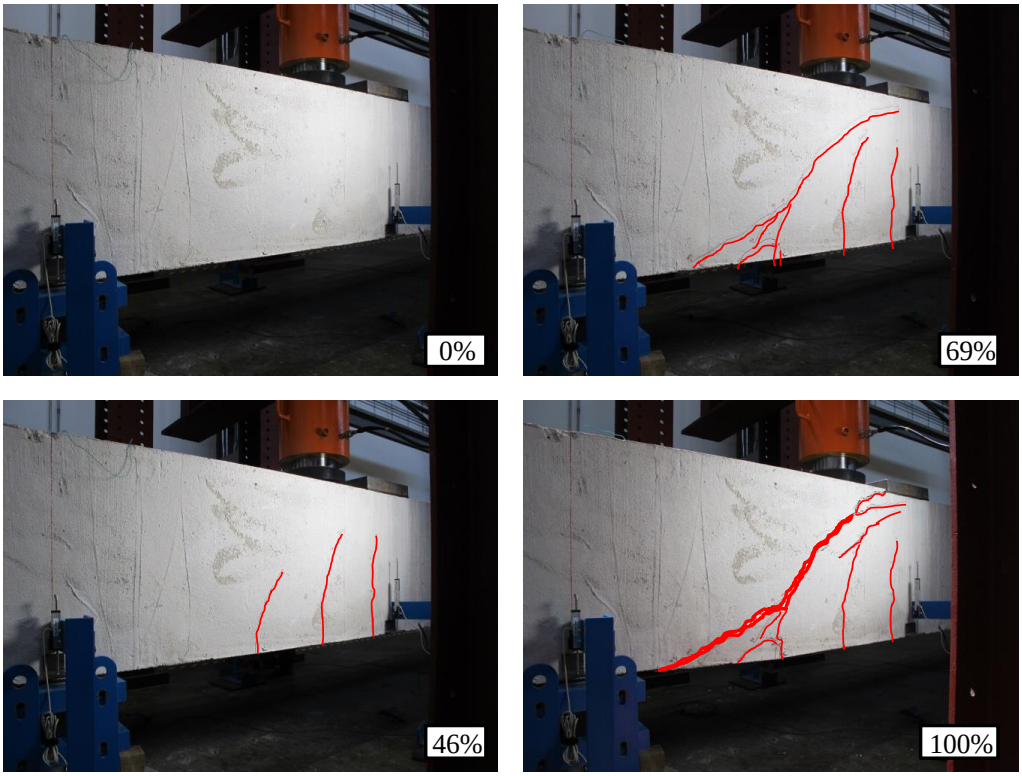

Fig. D–7: Load progression, SR1S-UA.

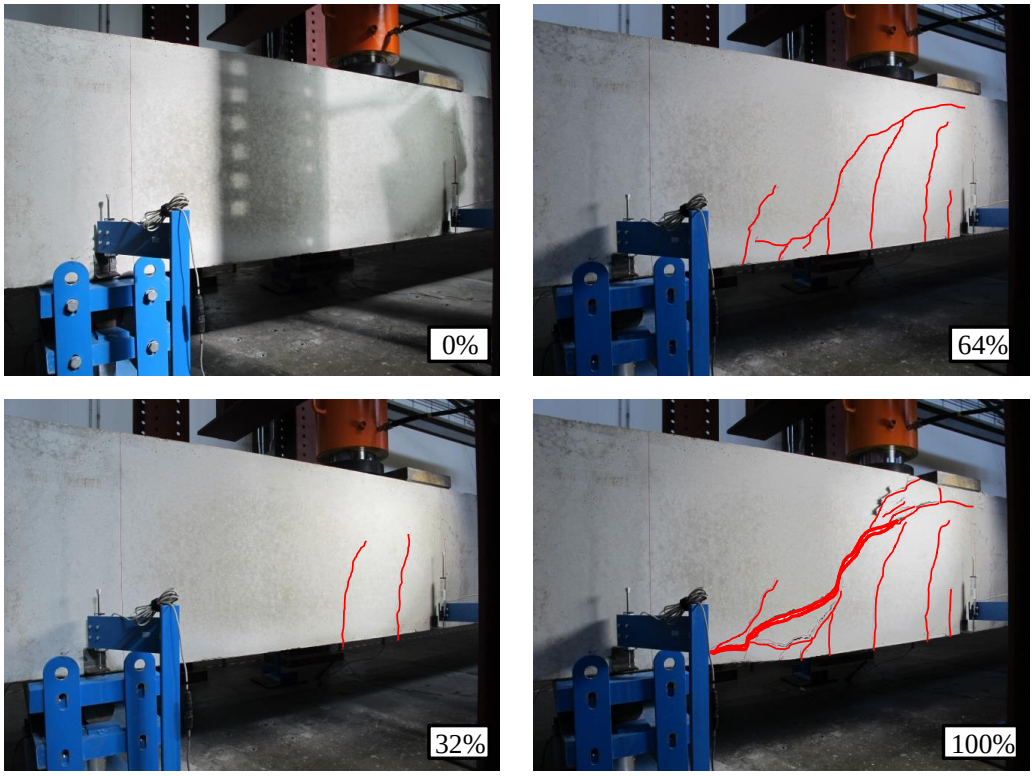

Fig. D–8: Load progression, SR2N-UA.

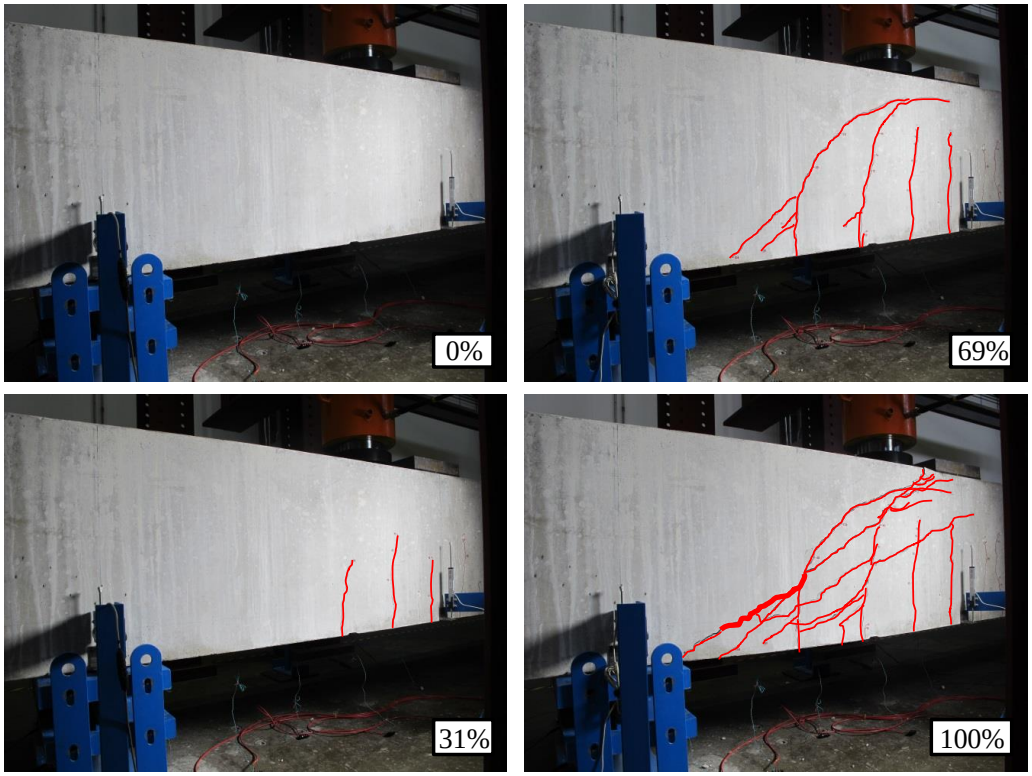

Fig. D–9: Load progression, SR1N-GA.

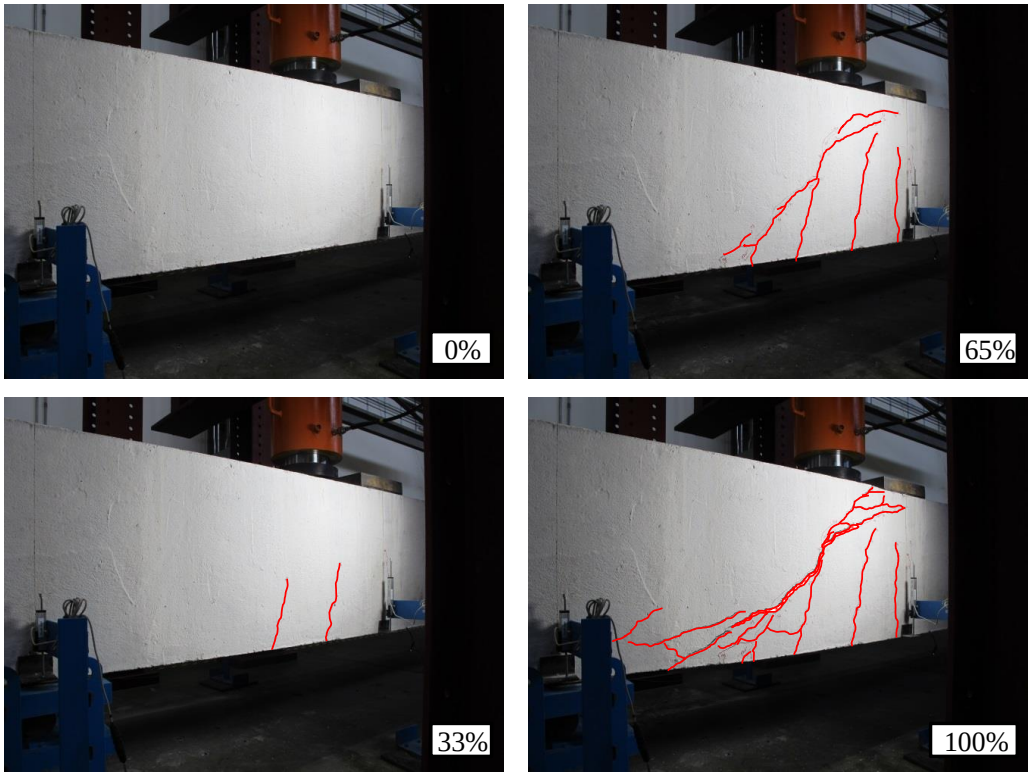

Fig. D–10: Load progression, SR3S-GA.

APPENDIX E

Experimental Results

E.1 OVERVIEW

This appendix presents experimental test results and strain. A shortened dataset, which replicates the actual load-deflection behavior of the full dataset, and test notes are also provided. Additionally, a short discussion on strain measurements and strain data collected during shear testing is presented.

E.2 NOTATION & EQUATIONS

a = shear span, defined as the distance between the point of applied load and the nearest support; a = 26.6 inches

BTG X= bolt gauge; BTG 1 is furthest plan-South and numbers ascend with BTG 5 furthest plan-North

L_AVG= calculated average longitudinal strain in tension bars

L_E = strain gauge attached to plan-East longitudinal tension bar

L_M = strain gauge attached to middle longitudinal tension bar

L_W = strain gauge attached to plan-West longitudinal tension bar

La = length of beam over-hanging the near support

$P_{applied}$ = total load applied through hydraulic ram

R_{near} = measured support reaction nearest point load

R_w = reaction due to self-weight at the near support

V_{test} = calculated shear force at a distance *a/2* away from the near support (considered the critical shear section)

w = beam self-weight per linear inch

Δ_{calc} = calculated deflection under point load accounting for rigid body motion of supports

δ_{far} = deflection at far support, taken as the average reading of linear potentiometers

δ_{near} = deflection at support nearest load taken, as the average reading of linear potentiometers

δ_p = deflection under load point, taken as the average reading of linear potentiometers

$$\boldsymbol{V_{test} = R_w + R_{near} - L_a w - \frac{a}{2} w} \qquad \textit{Equation E–1}$$

$$\boldsymbol{\Delta_{calc} = \delta_{far} + (1 - 0.29)(\delta_{near} - \delta_{far})} \qquad \textit{Equation E– 2}$$

E.3 RESULTS & SHORTENED DATASET

Each test contained thousands of data points and reporting the entirety of each test record was deemed impractical. Therefore, a shortened dataset, which maintains high fidelity to the actual load-deflection behavior, was constructed by selecting several important data points. Shortened data records and associated load-deflection plots for each test are presented in Table E–2 through Table E–9 and Fig. E–1, respectively. Table E–1 presents properties which remained constant for each span during shear testing. Fig. E–2 through Fig. E–9 are copies of the experimental test records taken during shear testing.

Table E–1: Constants for tested shear spans.

Specimen	L_a	w	R_w
	(in)	(lb/in)	(lb)
SR3N-RC	38.000	70.0	6512
SR2S-C	38.000	74.1	7407
SR2N-UA	35.250	73.6	7248
SR1N-GA	34.625	71.3	6867
SR1S-UA	34.750	72.1	6871
SR3S-GA	34.750	73.0	6969
LD1N-C	38.000	70.8	7541
LD1S-C	38.000	72.6	7503

Table E–2: SR2S-C shortened dataset (continued on next page).

Record No.	R_{Near} (lb)	$P_{applied}$ (lb)	δ_{near} (in)	δ_{far} (in)	δ_{P} (in)	Δ_{calc} (in)	V_{Test} (lb)
4898	0	0	0.0000	0.0000	0.0001	0.0001	2619
5860	21330	29991	0.0045	0.0012	0.0191	0.0226	23949
6316	20594	28975	0.0046	0.0013	0.0194	0.0230	23213
6362	23757	33420	0.0049	0.0013	0.0214	0.0253	26376
6454	28509	40110	0.0054	0.0017	0.0286	0.0329	31128
6788	27097	38123	0.0053	0.0017	0.0291	0.0334	29715
6866	31503	44320	0.0055	0.0018	0.0341	0.0385	34122
6960	35585	50031	0.0058	0.0023	0.0434	0.0481	38204
7507	33710	47432	0.0057	0.0023	0.0443	0.0490	36328
7566	38034	53511	0.0062	0.0025	0.0488	0.0539	40653
7668	42750	60121	0.0067	0.0029	0.0601	0.0657	45368
8439	40351	56764	0.0067	0.0029	0.0611	0.0667	42970
8484	44066	61974	0.0069	0.0031	0.0654	0.0712	46684
8529	47000	66110	0.0069	0.0031	0.0705	0.0763	49619
8592	49949	70231	0.0068	0.0033	0.0791	0.0849	52568
9187	47566	66912	0.0067	0.0033	0.0801	0.0858	50185
9286	53288	74933	0.0069	0.0035	0.0879	0.0938	55907
9350	56950	80077	0.0074	0.0036	0.0966	0.1029	59569
10005	54677	76911	0.0073	0.0037	0.0973	0.1035	57296
10068	60001	84358	0.0077	0.0039	0.1051	0.1117	62620
10137	64068	90062	0.0078	0.0041	0.1164	0.1231	66687
10775	61434	86403	0.0078	0.0040	0.1175	0.1241	64053
10811	65030	91429	0.0078	0.0040	0.1221	0.1287	67649
10848	68052	95674	0.0080	0.0041	0.1280	0.1348	70671
10964	75008	105439	0.0084	0.0045	0.1474	0.1546	77627
11060	80065	112545	0.0085	0.0048	0.1639	0.1713	82684
11097	82056	115384	0.0086	0.0048	0.1707	0.1782	84675
11129	83287	117176	0.0086	0.0049	0.1775	0.1851	85905
11140	82411	115993	0.0086	0.0049	0.1812	0.1887	85030
11169	82729	116481	0.0086	0.0051	0.1893	0.1969	85347
11178	79958	112568	0.0084	0.0049	0.1930	0.2004	82576
11194	77774	109573	0.0082	0.0049	0.1990	0.2062	80392
11220	78172	110097	0.0080	0.0049	0.2063	0.2134	80791
11235	76955	108363	0.0080	0.0049	0.2125	0.2195	79573
11273	78198	110063	0.0079	0.0049	0.2232	0.2302	80817
11314	80023	112603	0.0079	0.0051	0.2349	0.2419	82642
11343	81517	114657	0.0080	0.0051	0.2428	0.2499	84136
11388	82991	116654	0.0076	0.0051	0.2564	0.2632	85609
11398	82778	116352	0.0075	0.0051	0.2602	0.2670	85396
11442	84257	118318	0.0073	0.0052	0.2733	0.2800	86875

Record No.	R_{Near} (lb)	$P_{applied}$ (lb)	δ_{near} (in)	δ_{far} (in)	δ_{P} (in)	Δ_{calc} (in)	V_{Test} (lb)
11502	86816	121733	0.0072	0.0054	0.2911	0.2978	89435
11607	92074	128966	0.0073	0.0058	0.3198	0.3267	94693
11778	100025	139931	0.0075	0.0061	0.3671	0.3742	102644
11851	103004	144023	0.0077	0.0060	0.3872	0.3944	105623
11934	106211	148475	0.0073	0.0063	0.4110	0.4180	108829
11935	107108	149670	0.0078	0.0069	0.4134	0.4209	109727
11936	105002	147431	0.0079	0.0070	0.4139	0.4215	107621
12013	107758	150990	0.0077	0.0071	0.4366	0.4440	110376
12082	109671	153574	0.0073	0.0071	0.4567	0.4640	112290
12086	109035	153083	0.0071	0.0071	0.4595	0.4666	111654
12139	110266	154571	0.0074	0.0071	0.4758	0.4831	112885
12143	110007	154459	0.0073	0.0071	0.4774	0.4846	112626
12218	110811	155564	0.0072	0.0070	0.5015	0.5086	113429
12233	110833	155594	0.0071	0.0070	0.5060	0.5130	113452
12261	110311	154865	0.0069	0.0070	0.5158	0.5228	112930
12288	108554	152422	0.0066	0.0069	0.5259	0.5326	111173
12292	108047	150669	0.0057	0.0068	0.5292	0.5352	110665
12293	76548	107695	-0.0004	0.0053	0.5454	0.5467	79167
12294	73995	104493	-0.0009	0.0054	0.5462	0.5471	76614
12392	68383	96885	-0.0024	0.0052	0.5505	0.5503	71002
13298	65596	92948	-0.0032	0.0050	0.5517	0.5509	68215

Table E–3: LD1N-C shortened dataset (continued on next page).

Record No.	R_{Near} (lb)	$P_{applied}$ (lb)	δ_{near} (in)	δ_{far} (in)	δ_{P} (in)	Δ_{calc} (in)	V_{Test} (lb)
3333	29	7	0.0000	0.0000	-0.0002	-0.0002	2994
4948	15006	20438	0.0042	0.0013	0.0129	0.0163	17971
5052	20000	27261	0.0049	0.0018	0.0174	0.0214	22965
5122	21677	29602	0.0052	0.0020	0.0194	0.0237	24642
5417	20809	28490	0.0052	0.0021	0.0204	0.0247	23774
5520	24980	34224	0.0055	0.0022	0.0261	0.0307	27945
5648	29173	40068	0.0060	0.0026	0.0348	0.0398	32138
6836	26864	36992	0.0060	0.0026	0.0368	0.0418	29829
6893	29629	40745	0.0065	0.0028	0.0389	0.0443	32594
7023	34594	47627	0.0070	0.0029	0.0499	0.0557	37559
7057	36241	49901	0.0071	0.0028	0.0530	0.0588	39206
8120	33939	46832	0.0070	0.0029	0.0541	0.0599	36904
8162	37557	51777	0.0073	0.0030	0.0582	0.0642	40522
8265	43551	60144	0.0079	0.0034	0.0726	0.0791	46516
9407	40696	57281	0.0074	0.0034	0.0734	0.0796	43661
9440	43527	61284	0.0077	0.0035	0.0764	0.0829	46492
9473	46197	65038	0.0080	0.0034	0.0805	0.0871	49162
9537	49808	70086	0.0081	0.0037	0.0906	0.0974	52773
10391	47520	66847	0.0082	0.0038	0.0919	0.0988	50485
10472	52977	74530	0.0086	0.0040	0.0995	0.1067	55942
10510	55029	77400	0.0088	0.0042	0.1050	0.1124	57994
10547	56933	80057	0.0089	0.0043	0.1100	0.1175	59898
11641	54455	76561	0.0088	0.0044	0.1115	0.1190	57420
11666	56778	79857	0.0090	0.0044	0.1144	0.1221	59743
11706	60066	84472	0.0091	0.0045	0.1203	0.1281	63031
11761	64073	90094	0.0096	0.0049	0.1313	0.1396	67038
11850	70060	98506	0.0100	0.0052	0.1488	0.1574	73025
11945	76069	106933	0.0105	0.0056	0.1667	0.1758	79034
12062	82732	116279	0.0107	0.0060	0.1892	0.1985	85697
12083	83376	117226	0.0106	0.0061	0.1939	0.2032	86341
12110	84567	118918	0.0106	0.0062	0.1990	0.2083	87532
12152	84963	119491	0.0106	0.0063	0.2080	0.2173	87928
12167	82401	115868	0.0104	0.0062	0.2136	0.2227	85366
12169	80489	113212	0.0104	0.0062	0.2151	0.2243	83454
12174	75664	106558	0.0099	0.0060	0.2192	0.2279	78629
12186	73326	103350	0.0099	0.0060	0.2235	0.2323	76291
12217	71024	100134	0.0096	0.0059	0.2337	0.2422	73989
12228	70708	99685	0.0095	0.0059	0.2369	0.2453	73673
12257	69430	97817	0.0094	0.0058	0.2457	0.2541	72395
12264	68461	96427	0.0093	0.0057	0.2476	0.2559	71426

Record No.	R_{Near} (lb)	$P_{applied}$ (lb)	δ_{near} (in)	δ_{far} (in)	δ_{p} (in)	Δ_{calc} (in)	V_{Test} (lb)
12287	67515	95074	0.0092	0.0058	0.2548	0.2631	70480
12347	68039	95752	0.0088	0.0057	0.2721	0.2801	71004
12386	68754	96703	0.0086	0.0057	0.2828	0.2905	71719
12410	68909	96873	0.0086	0.0058	0.2893	0.2971	71874
12562	73088	102642	0.0084	0.0059	0.3294	0.3371	76053
12618	74435	104453	0.0086	0.0060	0.3435	0.3513	77400
12727	76951	107838	0.0086	0.0060	0.3726	0.3805	79916
12824	78392	109817	0.0083	0.0061	0.3993	0.4070	81357
12843	77766	108778	0.0079	0.0062	0.4067	0.4141	80731
12844	64860	90765	0.0046	0.0059	0.4131	0.4181	67825
12847	61329	86503	0.0041	0.0058	0.4147	0.4193	64294
12860	59747	84369	0.0036	0.0060	0.4191	0.4235	62712
12872	59379	83876	0.0034	0.0060	0.4240	0.4282	62344
12908	59062	83471	0.0027	0.0061	0.4360	0.4397	62027
12919	58878	83235	0.0019	0.0060	0.4396	0.4427	61843
12932	57781	81696	0.0014	0.0060	0.4455	0.4482	60746
12937	57104	80769	0.0010	0.0059	0.4474	0.4499	60069
13149	54075	76560	-0.0005	0.0058	0.4492	0.4506	57040

Table E–4: LD1S-C shortened dataset (continued on next page).

Record No.	R_{Near} (lb)	$P_{applied}$ (lb)	δ_{near} (in)	δ_{far} (in)	δ_P (in)	Δ_{calc} (in)	V_{Test} (lb)
2846	7	29	0.0002	0.0001	0.0001	0.0002	2821
4047	21374	30122	0.0066	0.0024	0.0211	0.0265	24188
4510	20542	28951	0.0067	0.0024	0.0214	0.0269	23356
4588	25074	35362	0.0074	0.0027	0.0257	0.0317	27888
4669	28465	40147	0.0078	0.0031	0.0318	0.0382	31279
5684	26604	37504	0.0077	0.0031	0.0332	0.0396	29418
5737	29590	41751	0.0082	0.0032	0.0363	0.0430	32404
5812	32011	45137	0.0087	0.0034	0.0431	0.0502	34825
5888	35564	50156	0.0094	0.0036	0.0513	0.0590	38378
6804	33247	46888	0.0094	0.0036	0.0518	0.0594	36061
6876	38087	53726	0.0102	0.0039	0.0588	0.0672	40901
6923	40014	56442	0.0104	0.0040	0.0639	0.0725	42828
6987	42633	60100	0.0106	0.0044	0.0729	0.0817	45447
7993	40381	56927	0.0106	0.0043	0.0738	0.0826	43195
8075	46258	65237	0.0114	0.0047	0.0823	0.0917	49072
8147	49707	70087	0.0122	0.0049	0.0913	0.1014	52521
8962	47361	66775	0.0122	0.0049	0.0921	0.1022	50175
9070	53701	75732	0.0131	0.0053	0.1024	0.1132	56515
9148	56804	80088	0.0134	0.0054	0.1120	0.1230	59618
10041	54532	76895	0.0134	0.0055	0.1130	0.1241	57346
10152	62217	87750	0.0139	0.0057	0.1273	0.1388	65032
10272	70056	98803	0.0146	0.0063	0.1499	0.1621	72870
10547	87040	122726	0.0167	0.0080	0.2004	0.2146	89855
10656	92486	130429	0.0176	0.0084	0.2200	0.2349	95301
10679	93169	131399	0.0180	0.0084	0.2245	0.2397	95983
10685	92896	131060	0.0182	0.0084	0.2259	0.2412	95710
10719	83559	118070	0.0190	0.0080	0.2398	0.2555	86373
10757	80072	113138	0.0187	0.0079	0.2510	0.2666	82886
10780	77389	109430	0.0181	0.0077	0.2584	0.2734	80203
10846	74596	105405	0.0172	0.0077	0.2763	0.2908	77410
10883	74067	104596	0.0168	0.0076	0.2864	0.3005	76882
10901	74244	104795	0.0167	0.0075	0.2906	0.3046	77058
10948	73818	104118	0.0163	0.0076	0.3036	0.3173	76632
10982	74083	104405	0.0159	0.0075	0.3127	0.3261	76897
11116	77232	108578	0.0151	0.0078	0.3440	0.3569	80046
11478	85011	119069	0.0135	0.0078	0.4280	0.4398	87826
11598	87078	121851	0.0131	0.0080	0.4636	0.4752	89893
11745	88734	124058	0.0116	0.0083	0.5110	0.5216	91548
11792	88970	124375	0.0112	0.0084	0.5289	0.5393	91784
11892	88264	123352	0.0104	0.0084	0.5685	0.5784	91078

Record No.	R_{Near} (lb)	$P_{applied}$ (lb)	δ_{near} (in)	δ_{far} (in)	δ_P (in)	Δ_{calc} (in)	V_{Test} (lb)
11976	87367	122093	0.0092	0.0084	0.6020	0.6109	90181
11977	87301	117482	0.0061	0.0074	0.6094	0.6158	90115
11978	67296	94516	0.0048	0.0076	0.6118	0.6175	70110
11986	64036	90203	0.0035	0.0076	0.6167	0.6214	66850
12005	62955	88754	0.0026	0.0075	0.6251	0.6291	65769
12032	62462	88113	0.0021	0.0075	0.6367	0.6404	65276
12312	61874	87628	-0.0027	0.0074	0.7745	0.7748	64688
12313	61859	87606	-0.0027	0.0075	0.7749	0.7751	64674
12670	58962	83544	-0.0033	0.0073	0.7770	0.7768	61776

Table E–5: SR3N-RC shortened dataset (continued on next 2 pages).

Record No.	R_{Near} (lb)	$P_{applied}$ (lb)	δ_{near} (in)	δ_{far} (in)	δ_{P} (in)	Δ_{calc} (in)	V_{Test} (lb)
1959	0	7	0.0000	0.0000	0.0000	0.0000	1987
1988	4190	5937	0.0014	0.0002	0.0047	0.0058	6178
2058	11632	16416	0.0035	0.0008	0.0118	0.0145	13619
2099	14117	19941	0.0039	0.0008	0.0144	0.0174	16104
3243	13381	18939	0.0040	0.0009	0.0145	0.0176	15369
3302	18087	25577	0.0045	0.0013	0.0181	0.0216	20075
3368	23036	32611	0.0050	0.0017	0.0235	0.0275	25023
3393	24668	34922	0.0051	0.0018	0.0257	0.0298	26656
3417	26043	36865	0.0053	0.0019	0.0276	0.0319	28031
3445	27477	38888	0.0056	0.0020	0.0305	0.0350	29465
3466	28286	40029	0.0058	0.0021	0.0328	0.0375	30273
4901	25764	36474	0.0059	0.0021	0.0338	0.0386	27751
4960	28058	39689	0.0062	0.0023	0.0361	0.0412	30045
4993	30396	43008	0.0064	0.0024	0.0391	0.0443	32384
5020	31683	44818	0.0065	0.0025	0.0421	0.0475	33670
5044	32713	46261	0.0066	0.0026	0.0455	0.0509	34700
5065	33691	47629	0.0066	0.0027	0.0477	0.0532	35678
5099	35198	49800	0.0069	0.0029	0.0525	0.0582	37185
5134	36992	52309	0.0070	0.0029	0.0574	0.0632	38980
5187	39816	56305	0.0072	0.0031	0.0648	0.0708	41803
5236	42478	60043	0.0074	0.0034	0.0722	0.0785	44465
6950	39581	55988	0.0073	0.0035	0.0733	0.0795	41568
7005	42022	59417	0.0074	0.0036	0.0759	0.0822	44009
7033	44500	62920	0.0076	0.0038	0.0798	0.0863	46487
7106	49059	69336	0.0080	0.0041	0.0908	0.0976	51046
7241	56633	80035	0.0088	0.0045	0.1115	0.1190	58620
8155	54074	76414	0.0087	0.0044	0.1125	0.1199	56061
8193	56684	80086	0.0089	0.0046	0.1159	0.1236	58672
8222	59023	83405	0.0092	0.0047	0.1203	0.1282	61010
8280	63030	89048	0.0094	0.0048	0.1290	0.1371	65017
8413	70809	100011	0.0098	0.0053	0.1520	0.1605	72796
9691	67992	96036	0.0098	0.0053	0.1523	0.1607	69979
9722	71087	100392	0.0101	0.0054	0.1572	0.1660	73074
9769	75058	105991	0.0103	0.0055	0.1648	0.1736	77045
9815	78028	110178	0.0102	0.0056	0.1726	0.1815	80015
9905	82476	116484	0.0105	0.0058	0.1891	0.1983	84463
9927	83174	117454	0.0108	0.0060	0.1945	0.2039	85161
9936	78147	110462	0.0106	0.0059	0.2000	0.2092	80134
9946	77817	109999	0.0106	0.0059	0.2028	0.2120	79804
9955	78126	110455	0.0106	0.0060	0.2046	0.2138	80114

Record No.	R_{Near} (lb)	$P_{applied}$ (lb)	δ_{near} (in)	δ_{far} (in)	δ_P (in)	Δ_{calc} (in)	V_{Test} (lb)
10000	81053	114554	0.0108	0.0060	0.2134	0.2228	83040
10062	84987	120050	0.0111	0.0064	0.2261	0.2359	86974
11532	81751	115517	0.0111	0.0065	0.2278	0.2376	83738
11577	85030	120115	0.0112	0.0065	0.2333	0.2432	87017
11604	87376	123412	0.0113	0.0066	0.2386	0.2485	89363
11640	90037	127149	0.0114	0.0067	0.2458	0.2558	92025
11690	93169	131549	0.0116	0.0068	0.2560	0.2662	95156
11802	99175	140009	0.0115	0.0071	0.2789	0.2891	101162
13328	95564	134903	0.0114	0.0071	0.2805	0.2906	97552
13374	99020	139803	0.0114	0.0073	0.2866	0.2967	101007
13443	104019	146843	0.0115	0.0075	0.2994	0.3097	106006
13522	108606	153296	0.0116	0.0077	0.3146	0.3251	110593
13612	113414	160042	0.0118	0.0081	0.3328	0.3436	115401
14147	110605	156062	0.0117	0.0081	0.3345	0.3451	112592
14174	113090	159579	0.0117	0.0082	0.3390	0.3497	115077
14228	117046	165119	0.0118	0.0084	0.3498	0.3606	119033
14278	120039	169328	0.0119	0.0085	0.3598	0.3707	122026
14335	123076	173581	0.0122	0.0087	0.3715	0.3827	125063
14430	127766	180128	0.0126	0.0089	0.3917	0.4032	129753
15028	124316	175262	0.0123	0.0089	0.3937	0.4050	126303
15059	127043	179103	0.0125	0.0090	0.3997	0.4111	129031
15072	128029	180486	0.0125	0.0089	0.4018	0.4132	130016
15117	131015	184652	0.0125	0.0091	0.4107	0.4222	133002
15192	135257	190589	0.0125	0.0092	0.4266	0.4381	137244
15310	140961	198563	0.0123	0.0095	0.4534	0.4649	142949
15422	146668	206554	0.0120	0.0098	0.4824	0.4938	148655
15424	146705	206591	0.0120	0.0098	0.4833	0.4946	148692
15432	142978	201619	0.0116	0.0097	0.4879	0.4989	144965
15442	141147	199191	0.0113	0.0097	0.4921	0.5029	143134
15452	140669	198565	0.0112	0.0097	0.4956	0.5064	142656
15457	140610	198492	0.0112	0.0097	0.4976	0.5083	142597
15461	140639	198543	0.0112	0.0097	0.4991	0.5098	142627
15509	141293	199610	0.0110	0.0098	0.5155	0.5261	143280
15514	141270	199587	0.0109	0.0097	0.5173	0.5278	143257
15531	139959	197827	0.0106	0.0097	0.5246	0.5349	141946
15535	139268	196833	0.0104	0.0098	0.5267	0.5369	141255
15536	137997	194876	0.0101	0.0097	0.5283	0.5382	139984
15544	130379	184694	0.0092	0.0096	0.5357	0.5450	132366
15555	127487	180726	0.0087	0.0095	0.5419	0.5508	129474
15568	126469	179341	0.0085	0.0095	0.5478	0.5566	128456

Record No.	R_{Near} (lb)	$P_{applied}$ (lb)	δ_{near} (in)	δ_{far} (in)	δ_P (in)	Δ_{calc} (in)	V_{Test} (lb)
15579	126011	178729	0.0084	0.0095	0.5524	0.5612	127998
15585	125856	178522	0.0084	0.0095	0.5549	0.5636	127843
15592	125722	178338	0.0083	0.0095	0.5576	0.5663	127709
15600	125618	178226	0.0082	0.0094	0.5610	0.5696	127605
15646	124033	176107	0.0076	0.0093	0.5804	0.5886	126020
15722	119261	169669	0.0065	0.0094	0.6176	0.6249	121248
15727	117620	167352	0.0065	0.0092	0.6212	0.6284	119608
15732	115977	165120	0.0064	0.0090	0.6245	0.6317	117964
15742	115047	163896	0.0063	0.0089	0.6299	0.6369	117034
15754	114759	163520	0.0063	0.0090	0.6362	0.6433	116746
15808	114002	162669	0.0059	0.0092	0.6634	0.6702	115989
15846	113049	161503	0.0057	0.0092	0.6845	0.6912	115036
15883	111530	159498	0.0054	0.0092	0.7060	0.7125	113517
15910	110051	157547	0.0052	0.0091	0.7218	0.7281	112038
15925	108896	155972	0.0051	0.0091	0.7311	0.7374	110883
15926	108800	155825	0.0050	0.0091	0.7316	0.7377	110788
15927	108668	155663	0.0050	0.0091	0.7321	0.7384	110655
15936	104902	150081	0.0048	0.0089	0.7406	0.7466	106889
15937	102494	146308	0.0044	0.0086	0.7439	0.7496	104481

Table E–6: SR1S-AB shortened dataset (continued on next 2 pages).

Record No.	R_{Near} (lb)	$P_{applied}$ (lb)	δ_{near} (in)	δ_{far} (in)	δ_P (in)	Δ_{calc} (in)	V_{Test} (lb)
1546	103	118	0.0002	-0.0002	0.0002	0.0003	2549
1599	3384	4879	0.0013	-0.0001	0.0037	0.0046	5830
1640	7342	10507	0.0028	0.0002	0.0081	0.0102	9788
1710	10681	15209	0.0036	0.0006	0.0116	0.0143	13127
1910	10320	14708	0.0038	0.0006	0.0118	0.0146	12766
1941	11953	17004	0.0041	0.0006	0.0130	0.0161	14399
1972	13512	19233	0.0047	0.0008	0.0147	0.0183	15958
2003	15248	21646	0.0052	0.0010	0.0166	0.0206	17694
2034	16895	24000	0.0054	0.0010	0.0176	0.0217	19341
2072	19079	27090	0.0058	0.0013	0.0203	0.0248	21525
2109	21345	30283	0.0063	0.0015	0.0225	0.0274	23791
2373	20719	29415	0.0063	0.0015	0.0225	0.0274	23165
2424	22021	31254	0.0066	0.0017	0.0236	0.0288	24467
2463	24830	35234	0.0070	0.0017	0.0263	0.0317	27276
2513	28154	39890	0.0075	0.0020	0.0298	0.0357	30600
2559	30368	43002	0.0080	0.0021	0.0342	0.0405	32814
2593	31882	45150	0.0084	0.0022	0.0376	0.0443	34328
3043	30617	43362	0.0086	0.0023	0.0380	0.0447	33063
3091	33978	48107	0.0089	0.0025	0.0410	0.0480	36424
3140	36780	52079	0.0095	0.0027	0.0455	0.0530	39226
3214	38213	54109	0.0099	0.0027	0.0568	0.0646	40659
3294	42589	60296	0.0102	0.0029	0.0687	0.0768	45035
3666	40669	57567	0.0102	0.0029	0.0697	0.0777	43115
3697	42839	60664	0.0102	0.0028	0.0730	0.0811	45285
3738	45736	64761	0.0105	0.0031	0.0784	0.0868	48182
3802	49228	69659	0.0110	0.0034	0.0884	0.0971	51674
3865	53168	75204	0.0115	0.0036	0.0984	0.1076	55614
4376	51315	72622	0.0116	0.0037	0.0991	0.1084	53761
4398	53168	75249	0.0118	0.0037	0.1018	0.1112	55614
4430	55948	79184	0.0121	0.0039	0.1066	0.1162	58394
4486	59874	84694	0.0123	0.0040	0.1150	0.1249	62320
4545	63874	90328	0.0126	0.0042	0.1246	0.1347	66320
4953	61676	87209	0.0126	0.0042	0.1257	0.1358	64122
4980	63683	90071	0.0128	0.0042	0.1281	0.1383	66129
5011	66294	93764	0.0130	0.0044	0.1330	0.1435	68740
5085	70294	99391	0.0131	0.0047	0.1445	0.1551	72740
5150	74464	105277	0.0134	0.0048	0.1563	0.1672	76910
5590	72566	102583	0.0135	0.0049	0.1570	0.1679	75012
5610	74330	105099	0.0136	0.0050	0.1594	0.1705	76776
5661	78765	111359	0.0139	0.0052	0.1681	0.1794	81211

Record No.	R_{Near} (lb)	$P_{applied}$ (lb)	δ_{near} (in)	δ_{far} (in)	δ_P (in)	Δ_{calc} (in)	V_{Test} (lb)
5709	81934	115795	0.0141	0.0053	0.1762	0.1876	84380
5759	85110	120267	0.0145	0.0055	0.1850	0.1968	87556
6444	82780	116988	0.0147	0.0055	0.1860	0.1980	85226
6467	84927	120033	0.0148	0.0055	0.1886	0.2007	87373
6503	88001	124388	0.0150	0.0057	0.1949	0.2072	90447
6547	90567	127970	0.0150	0.0059	0.2027	0.2151	93013
6588	92723	131031	0.0150	0.0060	0.2123	0.2247	95169
6636	95715	135247	0.0153	0.0060	0.2236	0.2362	98161
7869	91322	129055	0.0154	0.0060	0.2257	0.2383	93768
7899	91373	129107	0.0153	0.0060	0.2256	0.2382	93819
8057	91219	128908	0.0153	0.0059	0.2257	0.2382	93665
8078	93653	132380	0.0155	0.0062	0.2297	0.2425	96099
8103	96255	136065	0.0158	0.0062	0.2354	0.2483	98701
8151	99990	141301	0.0160	0.0065	0.2468	0.2601	102436
8198	103283	145935	0.0162	0.0067	0.2585	0.2719	105729
8243	106371	150230	0.0164	0.0068	0.2696	0.2832	108817
9194	102577	144846	0.0163	0.0068	0.2717	0.2852	105023
9221	105151	148517	0.0164	0.0068	0.2764	0.2899	107597
9262	109003	153922	0.0167	0.0071	0.2855	0.2994	111449
9304	112157	158350	0.0174	0.0074	0.2956	0.3100	114603
9344	114847	162086	0.0178	0.0075	0.3051	0.3199	117293
9380	117104	165248	0.0179	0.0076	0.3142	0.3291	119550
11072	112073	158074	0.0181	0.0076	0.3175	0.3325	114519
11109	116065	163753	0.0184	0.0077	0.3257	0.3410	118511
11154	119998	169261	0.0186	0.0079	0.3356	0.3511	122444
11187	122586	172872	0.0187	0.0080	0.3432	0.3588	125032
11226	125372	176748	0.0190	0.0083	0.3525	0.3684	127818
11265	127841	180182	0.0191	0.0084	0.3616	0.3776	130287
11304	130164	183410	0.0193	0.0086	0.3707	0.3868	132610
11343	132479	186638	0.0192	0.0089	0.3804	0.3966	134925
11382	134765	189815	0.0195	0.0092	0.3899	0.4063	137211
11421	137000	192963	0.0197	0.0093	0.4003	0.4170	139446
11450	138109	194572	0.0197	0.0092	0.4094	0.4261	140555
11472	138489	195159	0.0199	0.0094	0.4177	0.4345	140935
11488	138627	195400	0.0199	0.0095	0.4239	0.4408	141073
11499	135643	191341	0.0197	0.0096	0.4308	0.4475	138089
11510	134353	189595	0.0197	0.0096	0.4359	0.4526	136799
11521	133851	188916	0.0195	0.0095	0.4415	0.4581	136297
11552	129630	183134	0.0192	0.0090	0.4580	0.4742	132076
11613	127140	179849	0.0188	0.0089	0.4876	0.5035	129586

Record No.	R_{Near} (lb)	$P_{applied}$ (lb)	δ_{near} (in)	δ_{far} (in)	δ_P (in)	Δ_{calc} (in)	V_{Test} (lb)
11644	125807	178089	0.0187	0.0088	0.5032	0.5190	128253
11675	120719	171190	0.0181	0.0087	0.5211	0.5364	123165
11706	120079	170410	0.0181	0.0087	0.5368	0.5522	122526
11738	120035	170462	0.0179	0.0086	0.5523	0.5675	122481
11799	120322	171087	0.0178	0.0085	0.5817	0.5968	122768
11830	120490	171403	0.0178	0.0085	0.5968	0.6118	122936
11861	120519	171520	0.0177	0.0084	0.6113	0.6263	122965
11922	120276	171350	0.0175	0.0083	0.6384	0.6531	122722
11983	115794	165308	0.0164	0.0081	0.6690	0.6829	118240
12022	107289	153512	0.0159	0.0077	0.6922	0.7057	109735
12032	105562	151108	0.0159	0.0075	0.6988	0.7122	108008
12038	98650	141044	0.0155	0.0073	0.7074	0.7205	101096

Table E–7: SR2N-UA shortened dataset (continued on next 2 pages).

Record No.	R_{Near} (lb)	$P_{applied}$ (lb)	δ_{near} (in)	δ_{far} (in)	δ_{P} (in)	Δ_{calc} (in)	V_{Test} (lb)
3785	-15	-16	0.0004	0.0001	0.0003	0.0005	2677
4119	10618	15032	0.0036	0.0009	0.0106	0.0134	13309
4970	10095	14303	0.0039	0.0010	0.0108	0.0138	12787
4975	10139	14362	0.0038	0.0010	0.0107	0.0137	12831
5292	10036	14222	0.0038	0.0010	0.0108	0.0138	12728
5556	21218	30115	0.0061	0.0020	0.0217	0.0266	23910
6646	20225	28701	0.0062	0.0021	0.0219	0.0270	22917
6673	21519	30533	0.0064	0.0023	0.0229	0.0281	24211
6701	23395	33198	0.0067	0.0023	0.0243	0.0297	26087
6743	25793	36613	0.0069	0.0025	0.0274	0.0330	28485
6785	27985	39719	0.0073	0.0028	0.0303	0.0362	30677
6827	29934	42472	0.0074	0.0030	0.0332	0.0393	32626
6872	31802	45099	0.0076	0.0031	0.0367	0.0430	34494
8449	29411	41815	0.0075	0.0032	0.0377	0.0439	32103
8489	31235	44391	0.0076	0.0033	0.0392	0.0456	33927
8531	33809	47983	0.0079	0.0034	0.0420	0.0486	36501
8573	35405	50220	0.0079	0.0034	0.0464	0.0530	38097
8615	36824	52236	0.0082	0.0035	0.0517	0.0585	39516
8657	38898	55165	0.0083	0.0036	0.0576	0.0645	41590
8719	42369	60016	0.0081	0.0037	0.0664	0.0732	45061
9590	39654	56201	0.0078	0.0037	0.0671	0.0737	42346
9621	41427	58696	0.0079	0.0037	0.0688	0.0755	44118
9652	44324	62781	0.0081	0.0039	0.0733	0.0801	47016
9683	46472	65806	0.0082	0.0040	0.0769	0.0839	49164
9714	48170	68175	0.0083	0.0039	0.0813	0.0883	50862
9745	49825	70523	0.0087	0.0040	0.0857	0.0930	52517
9776	51671	73114	0.0090	0.0040	0.0904	0.0979	54363
9801	53120	75152	0.0097	0.0041	0.0940	0.1020	55812
11225	50281	71126	0.0100	0.0042	0.0946	0.1029	52973
11256	53237	75299	0.0100	0.0042	0.0985	0.1068	55929
11287	55693	78750	0.0102	0.0043	0.1017	0.1101	58385
11318	57731	81643	0.0103	0.0045	0.1061	0.1147	60422
11349	59452	84057	0.0104	0.0046	0.1099	0.1186	62143
11380	61180	86485	0.0105	0.0047	0.1139	0.1227	63872
11411	62938	88980	0.0107	0.0048	0.1182	0.1271	65629
11423	63680	90011	0.0106	0.0048	0.1200	0.1289	66372
12531	61048	86295	0.0106	0.0049	0.1209	0.1298	63740
12562	61990	87635	0.0106	0.0048	0.1221	0.1310	64682
12593	65020	91911	0.0107	0.0051	0.1266	0.1357	67712
12624	67550	95473	0.0108	0.0051	0.1309	0.1401	70242

Record No.	R_{Near}	$P_{applied}$	δ_{near}	δ_{far}	δ_P	Δ_{calc}	V_{Test}
	(lb)	(lb)	(in)	(in)	(in)	(in)	(lb)
12655	69543	98284	0.0111	0.0053	0.1356	0.1449	72235
12686	71190	100602	0.0111	0.0052	0.1400	0.1494	73882
12717	72786	102869	0.0113	0.0054	0.1448	0.1544	75477
12746	74411	105157	0.0115	0.0055	0.1495	0.1592	77103
13889	71726	101367	0.0115	0.0055	0.1488	0.1586	74418
13930	74477	105231	0.0116	0.0055	0.1528	0.1626	77168
13971	77771	109897	0.0117	0.0056	0.1585	0.1684	80463
14012	80485	113702	0.0116	0.0057	0.1640	0.1738	83177
14053	82882	117087	0.0117	0.0059	0.1706	0.1806	85574
14091	85081	120170	0.0116	0.0060	0.1768	0.1867	87772
15419	82281	116213	0.0116	0.0061	0.1779	0.1879	84972
15460	85980	121453	0.0117	0.0062	0.1836	0.1936	88672
15501	89040	125767	0.0117	0.0063	0.1891	0.1992	91731
15542	91827	129675	0.0117	0.0063	0.1956	0.2057	94519
15583	94261	133133	0.0118	0.0065	0.2022	0.2125	96953
15609	95783	135245	0.0121	0.0065	0.2058	0.2163	98475
16685	93195	131596	0.0121	0.0066	0.2070	0.2175	95887
16726	96379	136070	0.0123	0.0067	0.2125	0.2232	99071
16767	99446	140405	0.0125	0.0069	0.2185	0.2293	102138
16808	102063	144069	0.0129	0.0071	0.2245	0.2357	104755
16849	104445	147461	0.0131	0.0071	0.2310	0.2424	107137
16888	106356	150132	0.0134	0.0073	0.2379	0.2495	109048
16939	104921	148144	0.0132	0.0074	0.2388	0.2503	107612
16990	104376	147393	0.0131	0.0072	0.2391	0.2505	107068
17041	104009	146871	0.0131	0.0072	0.2393	0.2507	106701
17092	103730	146481	0.0132	0.0073	0.2396	0.2510	106421
17143	103502	146157	0.0132	0.0073	0.2398	0.2512	106193
17194	103311	145878	0.0132	0.0073	0.2398	0.2512	106002
17395	102701	145040	0.0131	0.0072	0.2399	0.2513	105393
17496	102071	144158	0.0132	0.0072	0.2402	0.2516	104763
17647	100503	142021	0.0132	0.0072	0.2411	0.2525	103195
17798	100040	141381	0.0133	0.0072	0.2415	0.2530	102732
18218	99504	140609	0.0132	0.0071	0.2419	0.2533	102196
18264	103726	146570	0.0133	0.0073	0.2488	0.2604	106418
18299	106285	150132	0.0134	0.0074	0.2549	0.2666	108977
19119	103953	146871	0.0133	0.0074	0.2563	0.2679	106644
19165	107880	152354	0.0134	0.0076	0.2635	0.2752	110572
19211	110653	156254	0.0134	0.0077	0.2712	0.2830	113344
19257	113145	159735	0.0134	0.0077	0.2795	0.2912	115837
19303	115520	163061	0.0134	0.0078	0.2877	0.2995	118212

Record No.	R_{Near}	$P_{applied}$	δ_{near}	δ_{far}	δ_P	Δ_{calc}	V_{Test}
	(lb)	(lb)	(in)	(in)	(in)	(in)	(lb)
19333	117094	165239	0.0134	0.0080	0.2933	0.3051	119785
20411	113842	160639	0.0145	0.0080	0.2949	0.3075	116534
20457	117328	165555	0.0147	0.0081	0.3016	0.3143	120020
20503	120352	169839	0.0150	0.0082	0.3088	0.3218	123043
20569	124294	175381	0.0151	0.0083	0.3195	0.3326	126985
20633	127676	180112	0.0151	0.0085	0.3303	0.3434	130368
21749	124034	174960	0.0150	0.0085	0.3321	0.3452	126726
21800	128087	180687	0.0150	0.0085	0.3402	0.3533	130779
21851	131581	185588	0.0150	0.0087	0.3489	0.3620	134273
21902	134831	190143	0.0150	0.0087	0.3578	0.3710	137523
21953	137964	194537	0.0147	0.0087	0.3681	0.3811	140656
22004	141354	199269	0.0146	0.0089	0.3792	0.3922	144046
22055	144619	203787	0.0144	0.0091	0.3925	0.4053	147311
22106	148111	208651	0.0143	0.0094	0.4060	0.4189	150803
22157	151582	213478	0.0137	0.0095	0.4194	0.4319	154274
22208	155001	218232	0.0134	0.0097	0.4321	0.4444	157693
22309	162067	227997	0.0150	0.0100	0.4592	0.4727	164759
22410	168979	237585	0.0151	0.0105	0.4848	0.4985	171671
22511	175582	246732	0.0148	0.0109	0.5098	0.5234	178274
22612	182067	255702	0.0148	0.0111	0.5349	0.5486	184759
22713	188515	264620	0.0146	0.0114	0.5603	0.5739	191207
22814	195021	273634	0.0144	0.0114	0.5884	0.6020	197713
22845	196918	276275	0.0144	0.0115	0.5974	0.6109	199609
22876	198608	278666	0.0144	0.0115	0.6066	0.6202	201299
22907	199531	279995	0.0142	0.0115	0.6162	0.6296	202223
22919	199728	280317	0.0142	0.0116	0.6203	0.6338	202420
22929	199771	280397	0.0141	0.0115	0.6240	0.6373	202463
22940	199681	280315	0.0141	0.0116	0.6279	0.6412	202373
22951	199422	280012	0.0139	0.0115	0.6321	0.6453	202114
22967	197160	276976	0.0138	0.0114	0.6390	0.6521	199852
22978	194222	272977	0.0138	0.0115	0.6451	0.6582	196914
22983	183726	256387	0.0127	0.0106	0.6581	0.6702	186418
22987	162064	228330	0.0116	0.0103	0.6688	0.6800	164756
22992	151059	213039	0.0110	0.0100	0.6786	0.6893	153751
22997	139576	197217	0.0107	0.0100	0.6885	0.6990	142268

Table E–8: SR1N-GA shortened dataset (continued on next page).

Record No.	R_{Near} (lb)	$P_{applied}$ (lb)	δ_{near} (in)	δ_{far} (in)	δ_{P} (in)	Δ_{calc} (in)	V_{Test} (lb)
8019	-7	0	-0.0002	-0.0005	-0.0001	-0.0004	2493
9051	19657	27695	0.0050	0.0010	0.0184	0.0222	22158
9575	26938	37970	0.0065	0.0013	0.0277	0.0326	29439
9674	32035	45154	0.0072	0.0015	0.0378	0.0433	34536
10457	29887	42166	0.0071	0.0016	0.0387	0.0442	32388
10490	32049	45168	0.0073	0.0016	0.0408	0.0464	34550
10673	42662	60109	0.0084	0.0021	0.0670	0.0736	45163
11501	40168	56620	0.0084	0.0021	0.0677	0.0743	42669
11568	46544	65606	0.0090	0.0024	0.0765	0.0835	49045
11682	53436	75277	0.0098	0.0028	0.0957	0.1035	55937
12574	50663	71420	0.0097	0.0027	0.0965	0.1042	53164
12625	54943	77418	0.0103	0.0028	0.1024	0.1106	57444
12745	64078	90224	0.0117	0.0034	0.1261	0.1353	66579
13805	61467	86567	0.0116	0.0034	0.1267	0.1359	63968
13846	65519	92270	0.0118	0.0036	0.1324	0.1418	68020
14004	74698	105142	0.0126	0.0040	0.1552	0.1653	77198
15002	71962	101322	0.0127	0.0042	0.1565	0.1667	74463
15049	75823	106717	0.0129	0.0043	0.1623	0.1727	78324
15200	85379	120128	0.0141	0.0048	0.1879	0.1993	87880
15982	82645	116317	0.0140	0.0048	0.1893	0.2005	85146
16064	89515	125952	0.0146	0.0050	0.2015	0.2133	92016
16194	96146	135266	0.0146	0.0056	0.2277	0.2396	98647
17175	92820	130619	0.0146	0.0055	0.2294	0.2413	95321
17302	102513	144182	0.0158	0.0060	0.2502	0.2632	105014
17376	106724	150126	0.0162	0.0061	0.2653	0.2785	109225
18436	103613	145732	0.0142	0.0060	0.2666	0.2784	106114
18502	107820	151628	0.0145	0.0062	0.2744	0.2864	110321
18659	117507	165176	0.0149	0.0065	0.3012	0.3137	120007
19414	114492	160946	0.0150	0.0065	0.3030	0.3155	116993
19472	118994	167262	0.0149	0.0066	0.3114	0.3239	121495
19815	141517	198754	0.0163	0.0076	0.3820	0.3958	144018
19847	143314	201288	0.0168	0.0077	0.3894	0.4035	145815
20262	169937	238337	0.0180	0.0090	0.5040	0.5194	172438
20272	169774	238128	0.0179	0.0090	0.5079	0.5232	172275
20282	170150	238673	0.0177	0.0090	0.5110	0.5262	172651
20293	170680	239416	0.0178	0.0091	0.5147	0.5300	173181
20301	170997	239843	0.0179	0.0092	0.5174	0.5327	173498
20311	171284	240241	0.0178	0.0092	0.5210	0.5363	173785
20341	168182	236010	0.0174	0.0092	0.5332	0.5482	170683
20371	153728	216236	0.0168	0.0089	0.5538	0.5683	156229

Record No.	R_{Near} (lb)	$P_{applied}$ (lb)	δ_{near} (in)	δ_{far} (in)	δ_P (in)	Δ_{calc} (in)	V_{Test} (lb)
20401	149681	210766	0.0165	0.0088	0.5688	0.5831	152182
20431	148916	209780	0.0164	0.0087	0.5811	0.5952	151417
20461	147404	207736	0.0163	0.0087	0.5942	0.6083	149905
20491	145957	205847	0.0163	0.0087	0.6072	0.6213	148458
20521	141868	200256	0.0160	0.0086	0.6223	0.6361	144369
20551	132290	187128	0.0152	0.0081	0.6413	0.6544	134790
20587	120311	170510	0.0139	0.0078	0.6645	0.6766	122812

Table E–9: SR3S-GA shortened dataset (continued on next 2 pages).

Record No.	R_{Near} (lb)	$P_{applied}$ (lb)	δ_{near} (in)	δ_{far} (in)	δ_P (in)	Δ_{calc} (in)	V_{Test} (lb)
3029	22	59	0.0002	0.0001	-0.0001	0.0000	2513
3234	10509	15155	0.0039	0.0024	0.0130	0.0164	13000
3376	10223	14751	0.0039	0.0024	0.0129	0.0164	12714
3392	10833	15634	0.0040	0.0024	0.0134	0.0169	13324
3408	11737	16943	0.0043	0.0026	0.0145	0.0182	14228
3439	13554	19525	0.0047	0.0029	0.0166	0.0208	16045
3470	15532	22365	0.0054	0.0033	0.0191	0.0239	18023
3501	17620	25359	0.0057	0.0036	0.0213	0.0264	20111
3517	18708	26933	0.0059	0.0037	0.0223	0.0276	21199
3533	19833	28514	0.0061	0.0039	0.0235	0.0289	22324
3552	21069	30287	0.0062	0.0041	0.0254	0.0310	23560
3811	20517	29493	0.0062	0.0041	0.0255	0.0311	23008
4056	20333	29235	0.0063	0.0042	0.0255	0.0312	22825
4072	21150	30405	0.0063	0.0043	0.0261	0.0319	23641
4088	22429	32237	0.0064	0.0044	0.0274	0.0333	24920
4104	23613	33921	0.0067	0.0047	0.0285	0.0346	26104
4135	25157	36128	0.0068	0.0048	0.0321	0.0383	27648
4166	26775	38416	0.0070	0.0048	0.0359	0.0422	29266
4221	28709	41123	0.0073	0.0051	0.0442	0.0508	31200
4274	31539	45117	0.0078	0.0054	0.0514	0.0585	34030
4640	30171	43181	0.0078	0.0054	0.0518	0.0589	32662
4656	30553	43740	0.0077	0.0053	0.0521	0.0591	33045
4672	32053	45874	0.0080	0.0055	0.0539	0.0612	34545
4693	33568	48022	0.0082	0.0056	0.0560	0.0635	36059
4724	34759	49721	0.0083	0.0057	0.0607	0.0682	37250
4755	36274	51854	0.0083	0.0057	0.0648	0.0724	38765
4801	39105	55848	0.0085	0.0058	0.0716	0.0794	41596
4864	42237	60277	0.0088	0.0063	0.0819	0.0900	44728
5321	40722	58114	0.0087	0.0062	0.0825	0.0904	43214
5337	42362	60460	0.0089	0.0063	0.0846	0.0928	44853
5353	43847	62572	0.0091	0.0065	0.0865	0.0949	46339
5384	46222	65926	0.0093	0.0068	0.0916	0.1002	48714
5415	48267	68817	0.0096	0.0071	0.0956	0.1045	50758
5455	49855	71083	0.0096	0.0072	0.1030	0.1119	52346
5505	52745	75143	0.0097	0.0073	0.1110	0.1200	55236
5879	51061	72753	0.0098	0.0073	0.1117	0.1207	53552
5895	52613	74982	0.0098	0.0073	0.1137	0.1227	55104
5911	53988	76939	0.0100	0.0076	0.1161	0.1254	56479
5942	56326	80212	0.0102	0.0078	0.1208	0.1303	58817
5973	58238	82919	0.0105	0.0081	0.1258	0.1356	60729

Record No.	R_{Near} (lb)	$P_{applied}$ (lb)	δ_{near} (in)	δ_{far} (in)	δ_P (in)	Δ_{calc} (in)	V_{Test} (lb)
6019	60775	86494	0.0107	0.0083	0.1333	0.1433	63266
6058	63503	90334	0.0110	0.0086	0.1405	0.1508	65994
6383	61863	87994	0.0110	0.0086	0.1415	0.1518	64354
6399	63547	90400	0.0111	0.0085	0.1438	0.1541	66038
6415	65032	92504	0.0112	0.0086	0.1464	0.1568	67523
6446	67532	96035	0.0114	0.0088	0.1515	0.1622	70023
6492	70694	100493	0.0116	0.0089	0.1596	0.1704	73185
6544	73981	105119	0.0117	0.0090	0.1685	0.1795	76472
7041	71488	101588	0.0117	0.0092	0.1696	0.1806	73980
7057	72937	103678	0.0118	0.0092	0.1717	0.1827	75428
7088	75437	107223	0.0119	0.0094	0.1763	0.1874	77928
7119	77071	109512	0.0119	0.0098	0.1816	0.1929	79562
7133	77359	109918	0.0120	0.0101	0.1838	0.1952	79850
7136	77271	109815	0.0119	0.0101	0.1846	0.1960	79762
7167	77180	109703	0.0121	0.0099	0.1917	0.2032	79672
7198	79283	112689	0.0122	0.0100	0.1971	0.2087	81774
7229	81283	115513	0.0124	0.0101	0.2033	0.2150	83774
7284	84569	120147	0.0127	0.0102	0.2133	0.2252	87060
7785	82252	116866	0.0126	0.0103	0.2145	0.2264	84744
7801	83877	119198	0.0128	0.0103	0.2172	0.2292	86368
7817	85304	121213	0.0128	0.0103	0.2196	0.2316	87795
7848	85966	122133	0.0128	0.0103	0.2216	0.2337	88457
7894	86804	123346	0.0128	0.0104	0.2236	0.2357	89295
7940	89811	127569	0.0132	0.0108	0.2321	0.2446	92302
7988	92311	131107	0.0135	0.0110	0.2417	0.2545	94802
8038	95230	135196	0.0139	0.0112	0.2518	0.2649	97721
8659	92833	131783	0.0137	0.0111	0.2527	0.2657	95324
8675	94215	133792	0.0137	0.0111	0.2550	0.2680	96706
8706	96943	137653	0.0140	0.0114	0.2606	0.2739	99434
8752	100289	142354	0.0142	0.0116	0.2697	0.2832	102780
8798	103215	146488	0.0143	0.0118	0.2782	0.2917	105707
8843	105811	150129	0.0142	0.0119	0.2862	0.2998	108302
9386	103231	146445	0.0143	0.0120	0.2876	0.3012	105722
9402	104503	148291	0.0143	0.0120	0.2899	0.3036	106994
9418	105848	150204	0.0143	0.0119	0.2927	0.3063	108339
9449	108069	153337	0.0143	0.0120	0.2975	0.3111	110560
9495	110869	157257	0.0146	0.0123	0.3062	0.3201	113361
9541	113355	160773	0.0148	0.0125	0.3144	0.3285	115846
9587	115701	164083	0.0150	0.0128	0.3222	0.3366	118192
9663	120106	170285	0.0155	0.0131	0.3371	0.3519	122597

Record No.	R_{Near} (lb)	$P_{applied}$ (lb)	δ_{near} (in)	δ_{far} (in)	δ_P (in)	Δ_{calc} (in)	V_{Test} (lb)
9739	124723	176795	0.0161	0.0135	0.3535	0.3688	127214
9815	129628	183703	0.0162	0.0136	0.3716	0.3870	132119
9891	134576	190675	0.0165	0.0140	0.3905	0.4062	137067
9967	139451	197523	0.0166	0.0143	0.4101	0.4261	141942
10082	147288	208563	0.0168	0.0144	0.4423	0.4583	149779
10183	154073	218095	0.0172	0.0150	0.4734	0.4900	156564
10246	158411	224155	0.0173	0.0152	0.4939	0.5106	160902
10308	162161	229408	0.0173	0.0156	0.5151	0.5319	164653
10319	157052	222450	0.0169	0.0155	0.5218	0.5383	159543
10333	155793	220750	0.0167	0.0151	0.5277	0.5440	158285
10341	155705	220654	0.0167	0.0150	0.5310	0.5472	158196
10354	155903	220962	0.0167	0.0150	0.5360	0.5522	158394
10365	156174	221366	0.0166	0.0149	0.5397	0.5558	158665
10378	156541	221917	0.0167	0.0149	0.5446	0.5607	159032
10391	156914	222459	0.0167	0.0148	0.5494	0.5655	159405
10415	157648	223539	0.0168	0.0148	0.5587	0.5749	160139
10431	158096	224186	0.0167	0.0147	0.5645	0.5806	160587
10443	158279	224472	0.0168	0.0147	0.5687	0.5849	160771
10452	158147	224318	0.0168	0.0147	0.5727	0.5888	160638
10462	157324	223193	0.0168	0.0147	0.5771	0.5933	159815
10472	156860	222575	0.0167	0.0147	0.5814	0.5975	159351
10488	157065	222890	0.0169	0.0148	0.5875	0.6037	159557
10504	157432	223441	0.0169	0.0148	0.5940	0.6103	159923
10518	157689	223837	0.0169	0.0147	0.5995	0.6157	160180
10526	157821	224043	0.0169	0.0147	0.6026	0.6188	160312
10542	157731	223939	0.0169	0.0146	0.6093	0.6255	160222
10558	157664	223886	0.0169	0.0147	0.6159	0.6321	160155
10574	157252	223349	0.0169	0.0147	0.6226	0.6389	159743
10590	156236	221965	0.0169	0.0145	0.6296	0.6458	158727
10606	154611	219743	0.0168	0.0145	0.6372	0.6533	157102
10637	153257	217955	0.0169	0.0145	0.6509	0.6671	155748
10668	151373	215415	0.0170	0.0145	0.6650	0.6813	153864
10679	150247	213885	0.0171	0.0146	0.6704	0.6868	152738
10691	148445	211383	0.0172	0.0146	0.6762	0.6927	150936
10698	124558	177777	0.0152	0.0204	0.6947	0.7114	127049
10706	120983	172840	0.0152	0.0206	0.7011	0.7179	123475
10716	118483	169412	0.0151	0.0206	0.7070	0.7237	120974
10729	115540	165336	0.0151	0.0204	0.7156	0.7323	118032

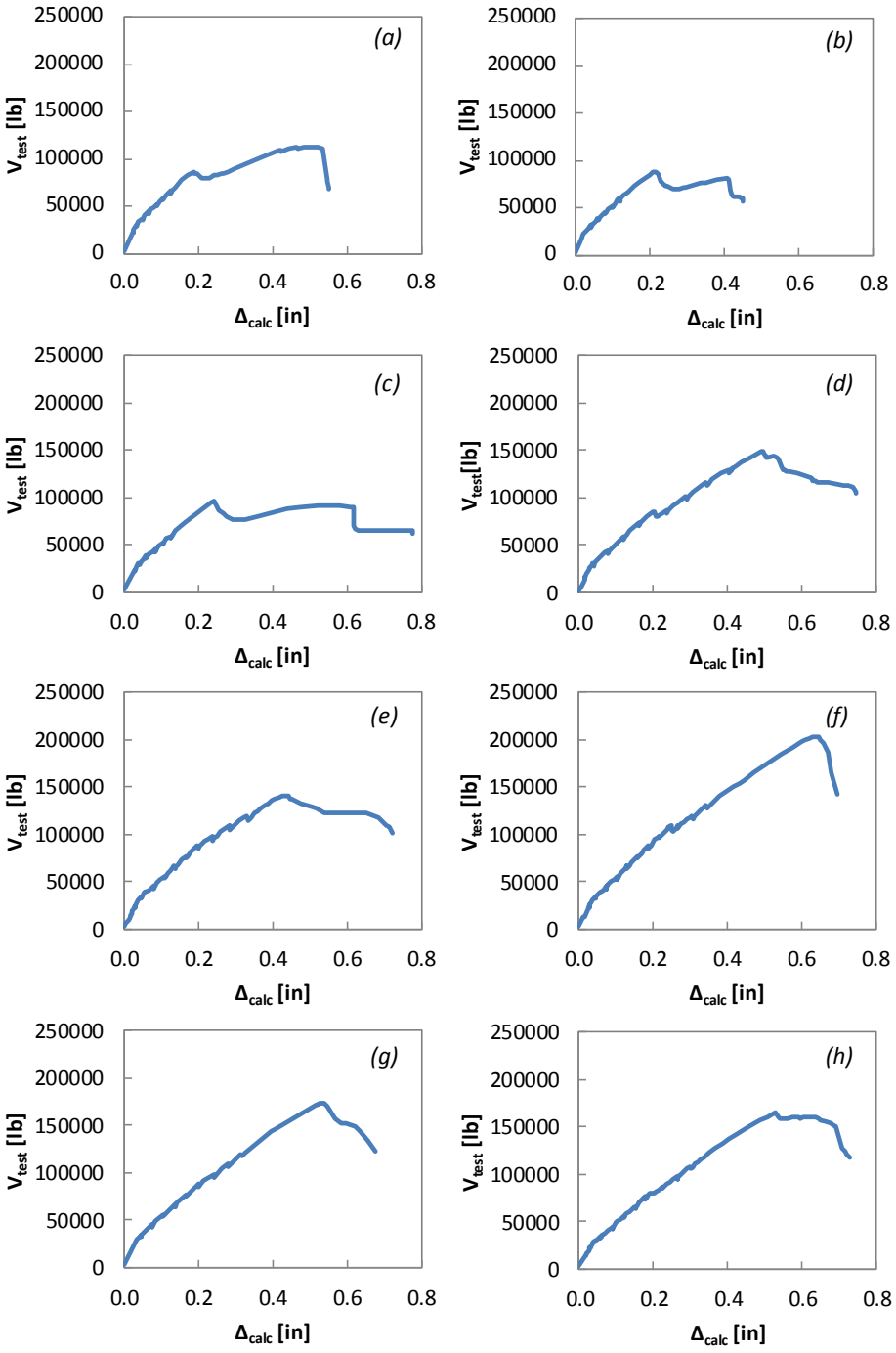

Fig. E–1: Load-deflection plots produced from shortened datasets. (a) SR2S-C; (b) LD1N-C; (c) LD1S-C; (d) SR3N-RC; (e) SR1S-UA; (f) SR2N-UA; (g) SR1N-GA; (h) SR3S-GA.

FSEL | STRUCTURAL TEST RECORD
STR_0326-0063_ | REVISION

8. ACTUAL STRUCTURAL RESPONSE

Time	Target Load	Actual Load	Comments and Observations
	0 k	k	
	10	10.105	
	20	20.062	
	30	29.991	Slight initial cracking.
	40	40.110	
	50	50.038	First cracking. Load rate dropped to ~100 lb/sec @ 45 kips
	60	60.121	
	70	70.231	
	80	80.077	
	Failure	90.065	
			Shear crack first seen @ 116 kips Reached up to 155 kip.

MPR PROJECT 0326-0063 Form Rev. 0 | Page 6

Fig. E–2: SR2S-C structural test record.

FSEL STRUCTURAL TEST RECORD
STR_0326-0063_ | REVISION

8. ACTUAL STRUCTURAL RESPONSE

	Time	Target Load	Actual Load	Comments and Observations
1	4/24/14 9:47Am	0 k	0 k	
2	9:51	10	10.2	No Observations; LP W Slipping?
3	9:54	20	20.2	No Observations; LP W Slipping
4	10:04	30	30.0	No Observations
5	10:09	40	40.1	Flexural Cracks Beneath Load.
6	10:20	50	49.9	Additional Flexural Cracks; Extension
7	10:30	60	60.1	"
8	10:41	70	70.1	"
9	10:50	80	80.1	WLP Bracket Lost; Limited Add. Cracking
10		Failure		

MPR PROJECT 0326-0063 Form Rev. 0 | Page 6

Fig. E–3: LD1N-C structural test record.

FSEL | **STRUCTURAL TEST RECORD**
STR_0326-0063_ | REVISION

8. ACTUAL STRUCTURAL RESPONSE

Time	Target Load	Actual Load	Comments and Observations
	0 k	0 k	
4:02	10	10.1	No cracks → L-pot (SE) slipping
4:08	20	20.1	" "
4:11	30	30.1	" "
4:16	40	40.1	First Flexural Crack Forms (1), "
4:26	50	50.1	More Flexural Cracks Form (4 total), "
4:36	60	60.1	More Flexural Cracks Form (7 total), "
4:45	70	70.1	More Flexural Cracks Form (8 total), "
4:53	80	80.1	Flexural Cracks grow (8 total), L-pot (SE) falls off
5:22	125	131.4	Large Shear Crack

Fig. E–4: LD1S-C structural test record.

FSEL STRUCTURAL TEST RECORD
STR_0326-0063_ | REVISION

8. ACTUAL STRUCTURAL RESPONSE

	Time	Target Load	Actual Load	Comments and Observations
1	10:19	20 k	19.9 k	No cracks.
2	10:30	40	40.0	
3		60	60.0	Flexural cracking initiated - middepth
4	11:01	80	80.0	Extension of flexural cracks.
5	11:11	100	100.0	Flexure - Shear Cracking.
6	11:25	120	120.1	Diagonal Cracking @~117.5^k w_c=
7	11:39	140	140.0	Extension of Existing Cracks.
8	11:54	160	160.0	Minor Spalling along Diag Crack.
9	12:01	100	100.1	
10	~12:10	Failure	106.6^k	

w_c [mm]

E	W
~~0.0~~ 0.5	0.9
1.1	1.5
1.5	1.6
2.0	2.5

MPR PROJECT 0326-0063 Form Rev. 0 | Page 6

Fig. E–5: SR3N-RC structural test record.

FSEL | STRUCTURAL TEST RECORD
STR_0326-0063_ | REVISION

8. ACTUAL STRUCTURAL RESPONSE

Time	Target Load	Actual Load	Comments and Observations
2:08 P	15 k	15.1 k	No cracking found
2:12 P	30	30.3	No cracking found
2:16 P	45	45.1	one flex. crack close to loading point west (smooth) side, no cracks on east side
2:21 P	60	60.3	around 51-52 kips → flex. cracking (load rate ↓↓) flex. cracks observed on both sides of test region, right to the south of loading pt.
2:26 P	75	75.2	New flexural cracks flex Extension of existing ^ cracks
2:32 P	90	90.3	No new flex. cracks just extension of existing cracks.
2:37 P	105	105.3	New flex-shear crack, both sides, middle of the test region, ⊕ extension of existing cracks.
2:42 P	120	120.3	Extension of existing cracks
2:49 P	135	135.2	~128 diagonal cracking (load rate ↓↓) ~0.4 mm crack width (W)/~0.5 mm (E) → diag. cracking on both sides
3:03 P	150	150.2	Diag. crack extended near support on E side, ~1.1mm wide West side → ≈ 1mm wide / extended towards load pt.
3:12 P	165	165.2	E side → crack extending under load plate, extended close to support, ~1.5mm W → ≈ 1.5 mm, no noticeable growth on dig. crack length
3:30 P	Failure	~195	

123 K
Expanded Cracking load

MPR PROJECT 0326-0063 Form Rev. 0 | Page 6

Fig. E–6: SR1S-UA structural test record.

FSEL STRUCTURAL TEST RECORD
STR_0326-0063_ | REVISION

8. ACTUAL STRUCTURAL RESPONSE

	Time	Target Load	Actual Load	Comments and Observations
1		~~20~~ 15 k	15.05 k	
2		~~40~~ 30	30.1	
3		~~60~~ 45	45.1	Few first flexural cracks
4		~~80~~ 60	60.0	Cracked @ ~47.5k ; More flex cracks
5		~~100~~ 75	75.2	Flex Cracks extended to [redacted]
6		~~120~~ 90	90.0	Cracks extend wider Comp Block
7		~~140~~ 105	105.2	More Flex Cracking
8		120	Low	
9	11:03 am	135	135.2	
10	11:14 am	150	150.0	First Diagonal Cracking ~15ft (½mm)
11	~11:35 am	165	165.2	Start Primary Crack Fully Formed ~0.9mm
12	11:45 am	180	180.1	Crack Widening ~1.3mm @ ~ 1ft ~1mm avg
13	~12:11 pm	Failure	200.4	Jt Broke

MPR PROJECT 0326-0063 Form Rev. 0 | Page 6

Fig. E–7: SR2N-UA structural test record.

FSEL | STRUCTURAL TEST RECORD
STR_0326-0063_ | REVISION

8. ACTUAL STRUCTURAL RESPONSE

Time	Target Load	Actual Load	Comments and Observations
~10:30AM	15 k	15.04 k	✓
10:37	30	30.51	✓
10:41	45	45.15	First Cracking (Flex Crack ~145 P)
10:50	60	60.11	Continued Flex Cracking
10:59	75	75.28	✓
11:07	90	90.22	✓
11:17	105	105.14	Some Flex Cracks turning diagonal
11:27	120	120.13	Flex Shear Cracking
11:36	135	135.27	Diagonal Crack forms (~130k) ~0.4mm
11:47	150	150.13	0.5 mm
11:57	165	165.18	0.8 mm
12:14	Failure	240.24	One Plate Bent in, Small spalling crushing on top surface, bottom of beam spalling Badly

MPR PROJECT 0326-0063 Form Rev. 0 | Page 6

Fig. E–8: SR1N-GA structural test record.

FSEL | **STRUCTURAL TEST RECORD**
STR_0326-0063_ | REVISION

8. ACTUAL STRUCTURAL RESPONSE

Time	Target Load	Actual Load	Comments and Observations
2:35 P	15 k	15.2 k	
2:38 P	30	30.3 k	
2:44 P	45	45.1 k	~ 35.5 CRACK (flex) to right of load
2:49 P	60	60.3 k	
2:54 P	75	75.1 k	
2:59 P	90	90.3 k	
3:03 P	105	105.1 k	
3:09 P	120	120.1 k	~ 109.9 CRACK (Shear) w/ 0.35mm w.idth
3:15 P	135	135.2 k	Shear crack extending toward support and multiple cracks forming, 0.2mm width
3:22 P	150	150.1 k	1mm width crack splitting + debonding
3:38 P	FAILURE	229.4 Peak	~ 229.4 CRACK ~ 224

Fig. E–9: SR3S-GA structural test record.

E.4 STRAIN DATA COLLECTION

Strain gauges were attached to three out of the five tension bars located in each test span. Readings from tension bar gauges confirm that longitudinal steel did not yield at any point during shear testing (Fig. E–10). Additionally, attempts to strain gauge shear reinforcement for each test were also made. Unfortunately, only data from the undercut anchor retrofit tests appears to be reliable.

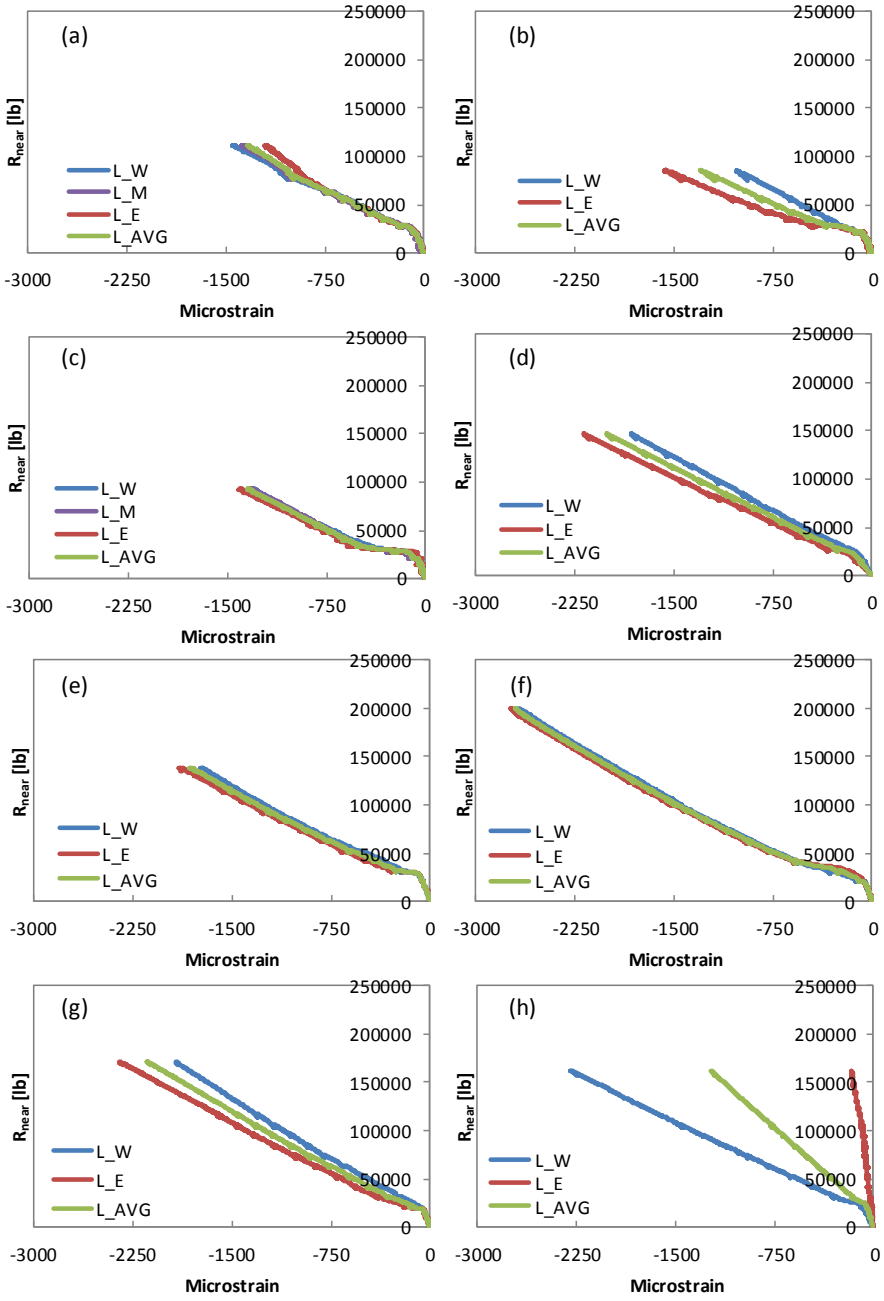

Fig. E–10: Longitudinal strain data.(a) SR2S-C; (b) LD1N-C; (c) LD1S-C; (d) SR3N-RC; (e) SR1S-UA; (f) SR2N-UA; (g) SR1N-GA; (h) SR3S-GA.

Several factors contributed to obtaining faulty data from transverse strain gauges. First, issues typically associated with strain gauging, namely water-tightness and

adequate bond to rebar. Surface gauges were attached to #4 rebar, and may not have been adequately bonded or sealed. In addition, gauges should be placed at the likely locations for crack formation. If the gauge does not intersect a crack, it will pick up a strain that does not correspond to the maximum strain in the bar.

Second, bolt gauges were used to measure the strain in both undercut and grouted anchors. Gauges are installed by drilling a small (2mm diameter) hole in one end of the anchor and embedding a strain gauge. These gauges worked well in undercut anchors because they are anchored in two discrete points. The anchor must develop all of the force at the tension face of the beam and at the location of the undercut. As long as the gauge is placed past either of these points, it should pick up a reliable strain reading. Grouted anchors, however, act as bonded reinforcement and stresses along their length are not constant. As such, the strain reading would be highly dependent on where the gauge was placed, and reliable readings simply could not be obtained. Data from gauges attached to transverse reinforcement providing readable results are presented in Fig. E–11.

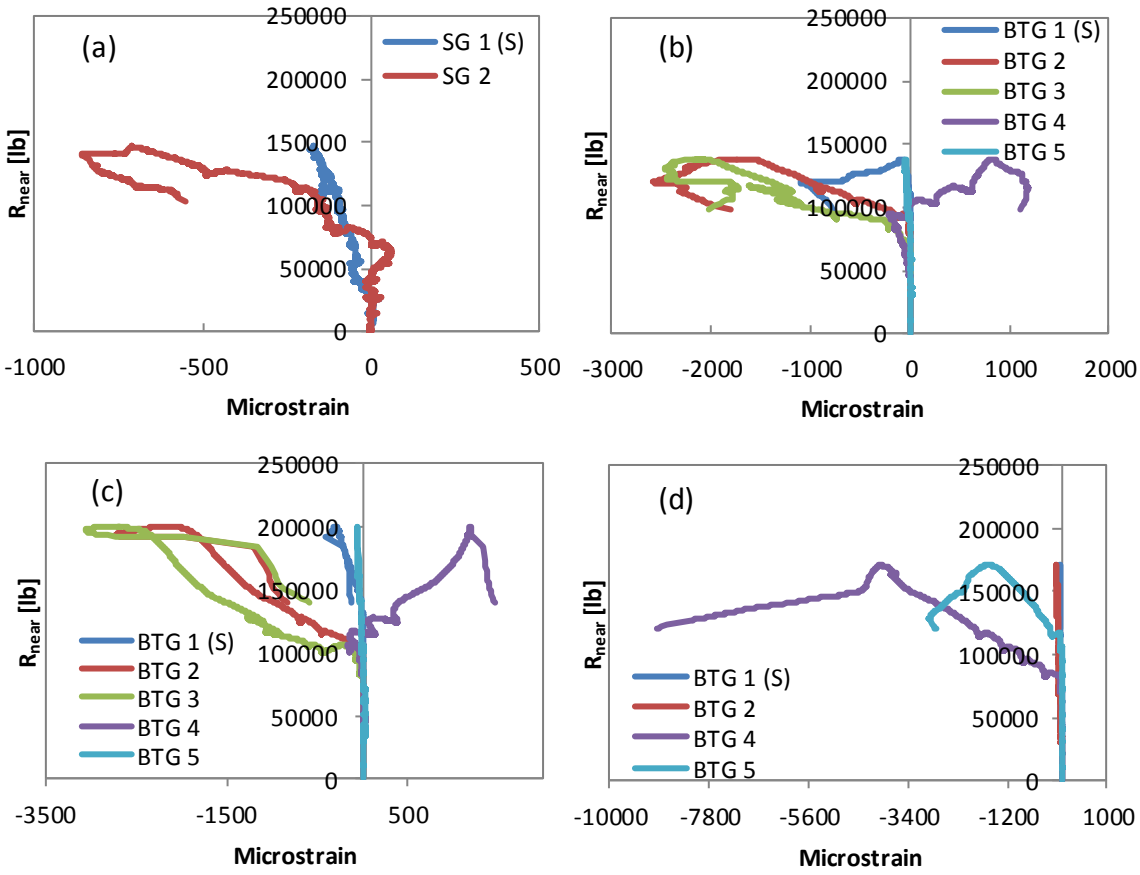

Fig. E–11: Usable strain gauge data. (a) SR3N-RC; (b) SR1S-UA; (c) SR2N-UA; (d) SR1N-GA.

APPENDIX F

Post-Test Analysis

F.1 OVERVIEW

This appendix discusses the details of post-test analysis. The major objective of this research was to evaluate the efficacy of utilizing undercut and grouted anchors as shear strengthening reinforcement. Ideally, those methods could be easily implemented using current design codes. As such, results are compared against three code provisions: ACI 318 simple equations, ACI 318 general equations, and AASHTO shear provisions. In addition, the above code expressions limit the yield stress of transverse reinforcement; theoretical capacities are therefore calculated with actual material strength values and code-limited material strengths. The following sections discuss calculation methods and assumptions. Additionally, alternate presentations of the comparison between experimental and analytical results are provided.

F.2 CALCULATION METHODS AND ASSUMPTIONS

As mentioned, three different code provisions were used to calculate the design shear strength of each span. Calculated values were compared against experimental results. What follows is a brief explanation of the assumptions relevant to calculations for each set of provisions. However, the author suggests referencing ACI 318 and AASHTO directly for a complete explanation of assumptions and limitations of particular procedures.

ACI 318, Simple Provisions

The ACI 318 model uses a truss analogy in calculating the concrete and steel contributions to sectional shear strength. The model fixes the truss angle at 45 degrees,

and calculates the steel contribution, acting as vertical (or diagonal) tension ties, accordingly. The model assumes that transverse reinforcement will yield prior to section failure. In addition, the simple provisions ignore the effects of longitudinal steel, member depth, and shear span, opting instead for a conservative, empirically derived value for the concrete contribution (Equation 2). The yield stress of transverse reinforcement is limited to 60 ksi as a means of controlling crack widths.

ACI 318, General Provisions

Assumptions for these provisions are the same as stated above, except that the concrete contribution is replaced by Equation 5. This equation accounts for factors which may have considerable effects on transversely *unreinforced* specimens, including longitudinal reinforcement ratio and member depth.

AASHTO Provisions

AASHTO's shear provisions are based on simplifications made to the modified compression field theory. The entire member is treated as one "element", where equilibrium, compatibility, and constitutive relationships are all considered in terms of average stresses and strains; cracked concrete is treated as a separate material with its own properties[30]. As the MCFT is based on fundamental principles, it is often considered the most "rational" model for determining shear capacities.

Like the ACI models, transverse reinforcement is assumed to yield prior to section failure. The AASHTO adaptation also limits transverse reinforcement yield stress to the minimum of the following values: 1) actual material yield stress; 2) material stress at 0.0035; 3) yield stress of 75.0 ksi. For completeness, calculations using all three values are provided.

Summary

Table F–1 through Table F–7 presents a summary of the output from the above. Additionally, the values of important calculated parameters are provided. The tables encompass calculations for each of the three sets of code provisions using actual material properties and properties limited by clauses in the codes. The critical section for shear was always assumed to be at the middle of the shear span (i.e. *a/2* away from the centerline of the load point).

Table F–1: ACI 318 simple provisions, calculations summary (actual material properties).

Specimen	Purpose	f'_c	$f_{y,v}$	w	$R_{w,mesured}$	V_u	$V_{c,calc}$	$V_{s,calc}$	$V_{n,calc}$	$V_u/V_{n,calc}$
		(psi)	ksi	(lb/in)	(lb)	(lb)	(lb)	(lb)	(lb)	-
SR3-N	Av, min	3311	61.3	70.0	6512	148692	88225	49729	137954	1.08
SR2-S	Control	4360	N/A	74.1	7407	85905	101240	0	101240	0.85
SR2-N	Undercut	4498	118.3	73.6	7248	202463	102830	68012	170842	1.19
SR1-N	Grout	3304	130.3	71.3	6867	173785	88131	74911	163042	1.07
SR1-S	Undercut	3165	118.3	72.1	6871	141073	86258	68012	154269	0.91
SR3-S	Grout	3190	130.3	73.0	6969	164653	86598	74911	161508	1.02
LD1N-C	Control	3658	N/A	70.8	7541	87899	92733	0	92733	0.95
LD1S-C	Control	3658	N/A	72.6	7503	95983	92733	0	92733	1.04
									Mean=	1.01
									Standard Deviation=	0.11

Table F–2: ACI 318 general provisions, calculations summary (actual material properties).

Specimen	Purpose	f'_c	$f_{y,v}$	w	$R_{w,mesured}$	V_u	$V_{c,calc}$	$V_{s,calc}$	$V_{n,calc}$	$V_u/V_{n,calc}$
		(psi)	ksi	(lb/in)	(lb)	(lb)	(lb)	(lb)	(lb)	-
SR3-N	Av, min	3311	61.3	70.0	6512	148692	99839	49729	149568	0.99
SR2-S	Control	4360	N/A	74.1	7407	85905	112350	0	112350	0.76
SR2-N	Undercut	4498	118.3	73.6	7248	202463	113637	68012	181649	1.11
SR1-N	Grout	3304	130.3	71.3	6867	173785	99688	74911	174599	1.00
SR1-S	Undercut	3165	118.3	72.1	6871	141073	97927	68012	165939	0.85
SR3-S	Grout	3190	130.3	73.0	6969	164653	98234	74911	173145	0.95
LD1N-C	Control	3658	N/A	70.8	7541	87899	104314	0	104314	0.84
LD1S-C	Control	3658	N/A	72.6	7503	95983	104314	0	104314	0.92
									Mean=	0.93
									Standard Deviation=	0.11

Table F–3: AASHTO provisions, calculations summary (actual material properties).

Specimen	Purpose	f'_c	$f_{y,v}$	w	$R_{w,mesured}$	V_u	β	ε_s	θ	$V_{c,calc}$	$V_{s,calc}$	$V_{n,calc}$	$V_u/V_{n,calc}$
		(psi)	ksi	(lb/in)	(lb)	(lb)	-	in/in	deg	(lb)	(lb)	(lb)	-
SR3-N	Av, min	3311	61.3	70.0	6512	148692	2.10	0.00156	34.45	83139	65246	148384	1.00
SR2-S	Control	4360	N/A	74.1	7407	85905	2.43	0.00116	33.05	110659	0	110659	0.78
SR2-N	Undercut	4498	118.3	73.6	7248	202463	1.91	0.00183	35.42	88450	86083	174534	1.16
SR1-N	Grout	3304	130.3	71.3	6867	173785	1.93	0.00180	35.31	76528	95182	171710	1.01
SR1-S	Undercut	3165	118.3	72.1	6871	141073	1.98	0.00172	35.03	76853	87314	164167	0.86
SR3-S	Grout	3190	130.3	73.0	6969	164653	1.94	0.00179	35.28	75440	95307	170748	0.96
LD1N-C	Control	3658	N/A	70.8	7541	87899	2.50	0.00109	32.82	104209	0	104209	0.84
LD1S-C	Control	3658	N/A	72.6	7503	95983	2.50	0.00109	32.82	104209	0	104209	0.92
												Mean=	0.94
												Standard Deviation=	0.12

Table F–4: ACI 318 simple provisions, calculations summary (stress-limited material properties).

Specimen	Purpose	f'_c	$f_{y,v}$	w	$R_{w,mesured}$	V_u	$V_{c,calc}$	$V_{s,calc}$	$V_{n,calc}$	$V_u/V_{n,calc}$
		(psi)	ksi	(lb/in)	(lb)	(lb)	(lb)	(lb)	(lb)	-
SR3-N	Av, min	3311	60	70.0	6512	148692	88225	49729	136899	1.09
SR2-S	Control	4360	N/A	74.1	7407	85905	101240	0	101240	0.85
SR2-N	Undercut	4498	60	73.6	7248	202463	102830	68012	137325	1.47
SR1-N	Grout	3304	60	71.3	6867	173785	88131	74911	122626	1.42
SR1-S	Undercut	3165	60	72.1	6871	141073	86258	68012	120752	1.17
SR3-S	Grout	3190	60	73.0	6969	164653	86598	74911	121092	1.36
LD1N-C	Control	3658	N/A	70.8	7541	87899	92733	0	92733	0.95
LD1S-C	Control	3658	N/A	72.6	7503	95983	92733	0	92733	1.04
									Mean=	1.17
									Standard Deviation=	0.23

Table F–5: ACI 318 general provisions, calculations summary (stress-limited material properties).

Specimen	Purpose	f'_c	$f_{y,v}$	w	$R_{w,mesured}$	V_u	$V_{c,calc}$	$V_{s,calc}$	$V_{n,calc}$	$V_u/V_{n,calc}$
		(psi)	ksi	(lb/in)	(lb)	(lb)	(lb)	(lb)	(lb)	-
SR3-N	Av, min	3311	60	70.0	6512	148692	99842	48674	148517	1.00
SR2-S	Control	4360	N/A	74.1	7407	85905	112350	0	112350	0.76
SR2-N	Undercut	4498	60	73.6	7248	202463	113718	34495	148213	1.37
SR1-N	Grout	3304	60	71.3	6867	173785	99800	34495	134295	1.29
SR1-S	Undercut	3165	60	72.1	6871	141073	98027	34495	132521	1.06
SR3-S	Grout	3190	60	73.0	6969	164653	98349	34495	132843	1.24
LD1N-C	Control	3658	N/A	70.8	7541	87899	104314	0	104314	0.84
LD1S-C	Control	3658	N/A	72.6	7503	95983	104314	0	104314	0.92
									Mean=	1.06
									Standard Deviation=	0.22

Table F–6: AASHTO provisions, calculations summary (stress-limited material properties).

Specimen	Purpose	f'_c	$f_{y,v}$	w	$R_{w,mesured}$	V_u	β	ε_s	θ	$V_{c,calc}$	$V_{s,calc}$	$V_{n,calc}$	$V_u/V_{n,calc}$
		(psi)	ksi	(lb/in)	(lb)	(lb)	-	in/in	deg	(lb)	(lb)	(lb)	-
SR3-N	Av, min	3311	61.33	70.0	6512	148692	2.10	0.00156	34.45	83139	65246	148384	1.00
SR2-S	Control	4360	N/A	74.1	7407	85905	2.43	0.00116	33.05	110659	0	110659	0.78
SR2-N	Undercut	4498	75	73.6	7248	202463	2.07	0.00159	34.58	95656	56294	151950	1.33
SR1-N	Grout	3304	75	71.3	6867	173785	2.15	0.00149	34.22	85010	57069	142078	1.22
SR1-S	Undercut	3165	75	72.1	6871	141073	2.16	0.00148	34.17	83608	57171	140780	1.00
SR3-S	Grout	3190	75	73.0	6969	164653	2.15	0.00148	34.18	83863	57153	141016	1.17
LD1N-C	Control	3658	N/A	70.8	7541	87899	2.50	0.00109	32.82	104209	0	104209	0.84
LD1S-C	Control	3658	N/A	72.6	7503	95983	2.50	0.00109	32.82	104209	0	104209	0.92
												Mean=	1.03
												Standard Deviation=	0.19

Table F–7: AASHTO provisions, calculations summary (strain-limited material properties).

Specimen	Purpose	f'_c	$f_{y,v}$	w	$R_{w,mesured}$	V_u	β	ε_s	θ	$V_{c,calc}$	$V_{s,calc}$	$V_{n,calc}$	$V_u/V_{n,calc}$
		(psi)	ksi	(lb/in)	(lb)	(lb)	-	in/in	deg	(lb)	(lb)	(lb)	-
SR3-N	Av, min	3311	61.33	70.0	6512	148692	2.10	0.00156	34.45	83139	65246	148384	1.00
SR2-S	Control	4360	N/A	74.1	7407	85905	2.43	0.00116	33.05	110659	0	110659	0.78
SR2-N	Undercut	4498	101.5	73.6	7248	202463	1.97	0.00174	35.09	91093	74743	165836	1.22
SR1-N	Grout	3304	101.5	71.3	6867	173785	2.04	0.00164	34.75	80686	75718	156404	1.11
SR1-S	Undercut	3165	101.5	72.1	6871	141073	2.04	0.00163	34.70	79319	75847	155167	0.91
SR3-S	Grout	3190	101.5	73.0	6969	164653	2.04	0.00163	34.71	79568	75824	155392	1.06
LD1N-C	Control	3658	N/A	70.8	7541	87899	2.50	0.00109	32.82	104209	0	104209	0.84
LD1S-C	Control	3658	N/A	72.6	7503	95983	2.50	0.00109	32.82	104209	0	104209	0.92
												Mean=	0.98
												Standard Deviation=	0.15

F.3 COMPARISON BETWEEN ANALYTICAL AND EXPERIMENTAL RESULTS

The primary conclusions of this project are contained within the main body of this report. However, this section expounds on a few additional details. Notably, looking at the results as a whole (combined reinforced and unreinforced sections) can be misleading. Better insights can be made by separating the reinforced and unreinforced specimens (Table F–8 through Table F–14; Fig. F–1 & Fig. F–2). While each set of provisions produce comparable results, the AASHTO provisions, on average, offer the best predictions. Unsurprisingly, enforcing strain limits for transverse reinforcement provides much more conservative results.

Table F–8: ACI 318 simple provisions, calculations summary (reinforced specimens only; actual material properties).

Specimen	Purpose	f'_c	$f_{y,v}$	w	$R_{w,mesured}$	V_u	$V_{c,calc}$	$V_{s,calc}$	$V_{n,calc}$	$V_u/V_{n,calc}$
		(psi)	ksi	(lb/in)	(lb)	(lb)	(lb)	(lb)	(lb)	-
SR3-N	Av, min	3311	61.33	70.0	6512	148692	88225	49729	137954	1.08
SR2-N	Undercut	4498	118.39	73.6	7248	202463	102830	68012	170842	1.19
SR1-N	Grout	3304	130.37	71.3	6867	173785	88131	74911	163042	1.07
SR1-S	Undercut	3165	118.39	72.1	6871	141073	86258	68012	154269	0.91
SR3-S	Grout	3190	130.37	73.0	6969	164653	86598	74911	161508	1.02
									Mean=	1.05
									Standard Deviation=	0.10

Table F–9: ACI 318 general provisions, calculations summary (reinforced specimens only; actual material properties).

Specimen	Purpose	f'_c	$f_{y,v}$	w	$R_{w,mesured}$	V_u	$V_{c,calc}$	$V_{s,calc}$	$V_{n,calc}$	$V_u/V_{n,calc}$
		(psi)	ksi	(lb/in)	(lb)	(lb)	(lb)	(lb)	(lb)	-
SR3-N	Av, min	3311	61.33	70.0	6512	148692	99839	49729	149568	0.99
SR2-N	Undercut	4498	118.39	73.6	7248	202463	113637	68012	181649	1.11
SR1-N	Grout	3304	130.37	71.3	6867	173785	99688	74911	174599	1.00
SR1-S	Undercut	3165	118.39	72.1	6871	141073	97927	68012	165939	0.85
SR3-S	Grout	3190	130.37	73.0	6969	164653	98234	74911	173145	0.95
									Mean=	0.98
									Standard Deviation=	0.10

Table F–10: AASHTO provisions, calculations summary (reinforced specimens only; actual material properties).

Specimen	Purpose	f'_c	$f_{y,v}$	w	$R_{w,mesured}$	V_u	β	ε_s	θ	$V_{c,calc}$	$V_{s,calc}$	$V_{n,calc}$	$V_u/V_{n,calc}$
		(psi)	ksi	(lb/in)	(lb)	(lb)	-	in/in	deg	(lb)	(lb)	(lb)	-
SR3-N	Av, min	3311	61.33	70.0	6512	148692	2.10	0.00156	34.45	83139	65246	148384	1.00
SR2-N	Undercut	4498	118.39	73.6	7248	202463	1.91	0.00183	35.42	88450	86083	174534	1.16
SR1-N	Grout	3304	130.37	71.3	6867	173785	1.93	0.00180	35.31	76528	95182	171710	1.01
SR1-S	Undercut	3165	118.39	72.1	6871	141073	1.98	0.00172	35.03	76853	87314	164167	0.86
SR3-S	Grout	3190	130.37	73.0	6969	164653	1.94	0.00179	35.28	75440	95307	170748	0.96
												Mean=	1.00
												Standard Deviation=	0.11

Table F–11: ACI 318 simple provisions, calculations summary (reinforced specimens only; stress-limited material properties).

Specimen	Purpose	f'_c	$f_{y,v}$	w	$R_{w,mesured}$	V_u	$V_{c,calc}$	$V_{s,calc}$	$V_{n,calc}$	$V_u/V_{n,calc}$
		(psi)	ksi	(lb/in)	(lb)	(lb)	(lb)	(lb)	(lb)	-
SR3-N	Av, min	3311	60	70.0	6512	148692	88225	49729	136899	1.09
SR2-N	Undercut	4498	60	73.6	7248	202463	102830	68012	137325	1.47
SR1-N	Grout	3304	60	71.3	6867	173785	88131	74911	122626	1.42
SR1-S	Undercut	3165	60	72.1	6871	141073	86258	68012	120752	1.17
SR3-S	Grout	3190	60	73.0	6969	164653	86598	74911	121092	1.36
									Mean=	1.30
									Standard Deviation=	0.17

Table F–12: ACI 318 general provisions, calculations summary (reinforced specimens only; stress-limited material properties).

Specimen	Purpose	f'_c	$f_{y,v}$	w	$R_{w,mesured}$	V_u	$V_{c,calc}$	$V_{s,calc}$	$V_{n,calc}$	$V_u/V_{n,calc}$
		(psi)	ksi	(lb/in)	(lb)	(lb)	(lb)	(lb)	(lb)	-
SR3-N	Av, min	3311	60	70.0	6512	148692	99842	48674	148517	1.00
SR2-N	Undercut	4498	60	73.6	7248	202463	113718	34495	148213	1.37
SR1-N	Grout	3304	60	71.3	6867	173785	99800	34495	134295	1.29
SR1-S	Undercut	3165	60	72.1	6871	141073	98027	34495	132521	1.06
SR3-S	Grout	3190	60	73.0	6969	164653	98349	34495	132843	1.24
									Mean=	1.19
									Standard Deviation=	0.15

Table F–13: AASHTO general provisions, calculations summary (reinforced specimens only; stress-limited material properties).

Specimen	Purpose	f'_c	$f_{y,v}$	w	$R_{w,mesured}$	V_u	β	ε_s	θ	$V_{c,calc}$	$V_{s,calc}$	$V_{n,calc}$	$V_u/V_{n,calc}$
		(psi)	ksi	(lb/in)	(lb)	(lb)	-	in/in	deg	(lb)	(lb)	(lb)	-
SR3-N	Av, min	3311	61.33	70.0	6512	148692	2.10	0.00156	34.45	83139	65246	148384	1.00
SR2-N	Undercut	4498	75.00	73.6	7248	202463	2.07	0.00159	34.58	95656	56294	151950	1.33
SR1-N	Grout	3304	75.00	71.3	6867	173785	2.15	0.00149	34.22	85010	57069	142078	1.22
SR1-S	Undercut	3165	75.00	72.1	6871	141073	2.16	0.00148	34.17	83608	57171	140780	1.00
SR3-S	Grout	3190	75.00	73.0	6969	164653	2.15	0.00148	34.18	83863	57153	141016	1.17
												Mean=	1.15
												Standard Deviation=	0.14

Table F–14: AASHTO general provisions, calculations summary (reinforced specimens only; strain-limited material properties).

Specimen	Purpose	f'_c	$f_{y,v}$	w	$R_{w,mesured}$	V_u	β	ε_s	θ	$V_{c,calc}$	$V_{s,calc}$	$V_{n,calc}$	$V_u/V_{n,calc}$
		(psi)	ksi	(lb/in)	(lb)	(lb)	-	in/in	deg	(lb)	(lb)	(lb)	-
SR3-N	Av, min	3311	61.33	70.0	6512	148692	2.10	0.00156	34.45	83139	65246	148384	1.00
SR2-N	Undercut	4498	101.5	73.6	7248	202463	1.97	0.00174	35.09	91093	74743	165836	1.22
SR1-N	Grout	3304	101.5	71.3	6867	173785	2.04	0.00164	34.75	80686	75718	156404	1.11
SR1-S	Undercut	3165	101.5	72.1	6871	141073	2.04	0.00163	34.70	79319	75847	155167	0.91
SR3-S	Grout	3190	101.5	73.0	6969	164653	2.04	0.00163	34.71	79568	75824	155392	1.06
												Mean=	1.06
												Standard Deviation=	0.12

Notably, none of the shear provisions explicitly account for the anchorage conditions of the reinforcement (bonded or un-bonded), given that deformed rebar is the current standard. Undoubtedly, anchorage conditions affect the load path and overall behavior of the section; those effects bear further investigation. The author hesitates to make a firm conclusion on the suitability of investigated shear provisions for the design of retrofits. However, these results indicate good agreement between analytical and experimental values, and should offer conservative designs once load and resistance factors are applied.

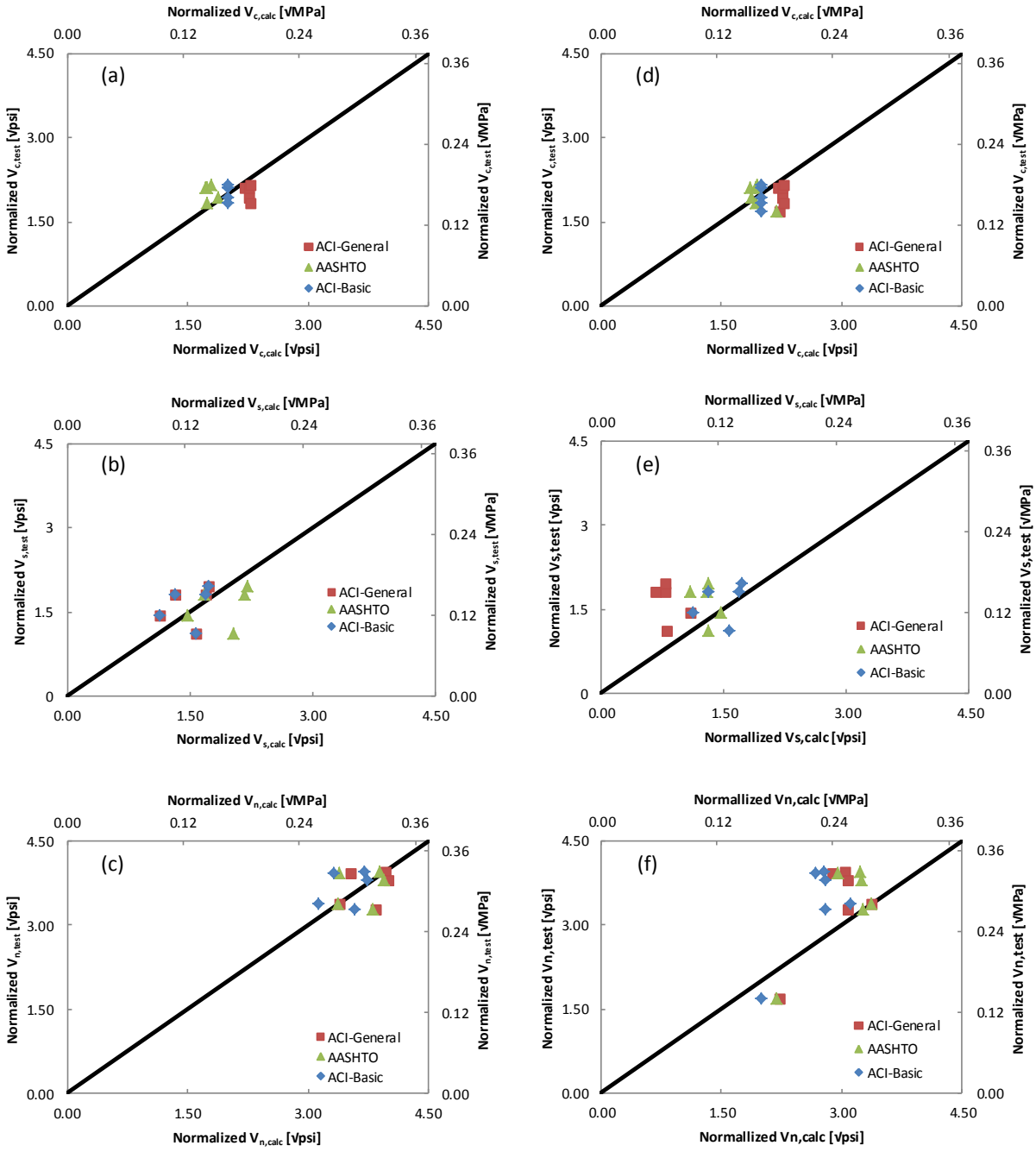

Fig. F–1: Comparison between experimental and analytical results. (a), (b), & (c) use actual material properties; (d), (e), & (f) use stress-limited material properties.

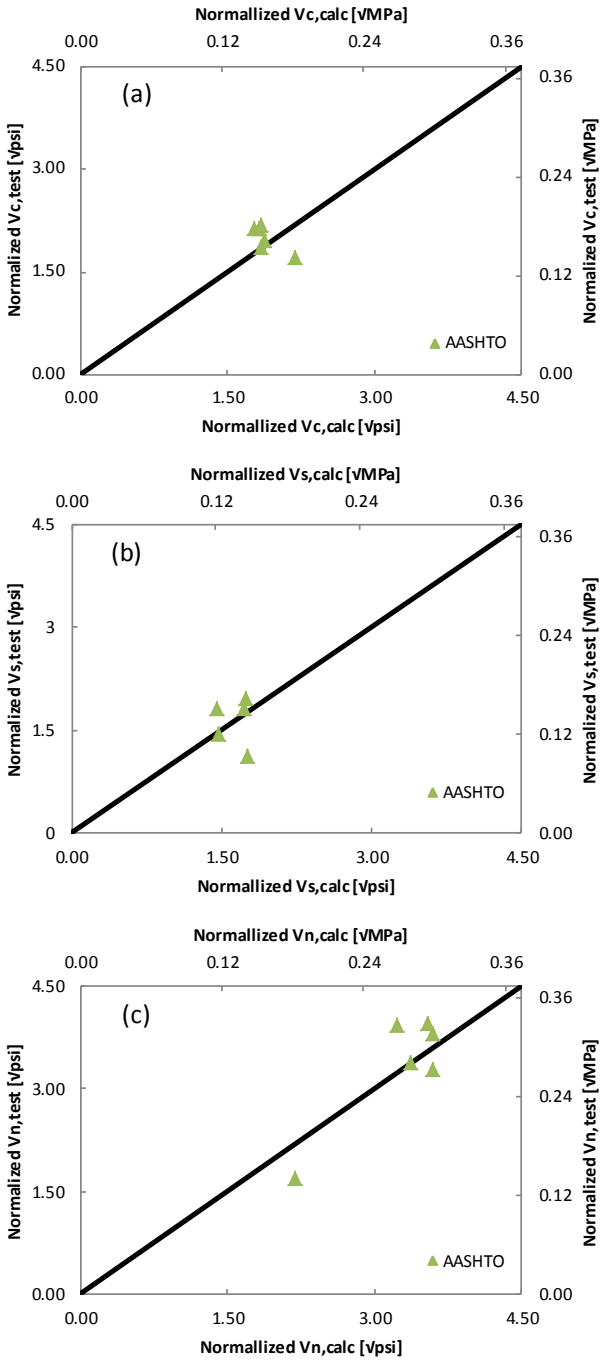

Fig. F–2: Comparison between experimental and analytical results (AASHTO strain-limited material properties).

REFERENCES

[1] *Increasing Shear Capacity within Existing Reinforced Concrete Structures*. Rep. no. ACI 364.2T-08. American Concrete Institute, 2008.

[2] Kunz J., Fernandez Ruiz M., and Muttoni A., *Enhanced Safety with Post-installed Shear Reinforcement*, fib Symposium, Tel-Aviv 2013, Tel-Aviv, Israel, 2013, 4p..

[3] Kunz, Jakob. "Strengthening with Post-installed Shear Reinforcement." *Conservation of Structures*, 2013, pp. 154-58.

[4] Ruiz, Miguel F., Aurelio Muttoni, and Jakob Kunz. "Strengthening of Flat Slabs Against Punching Shear Using Post-Installed Shear Reinforcement", *ACI Structural Journal*, Vol. 107, No. 4, July-August 2010, pp. 434-42.

[5] Heymsfield, Ernest, and Stephan A. Durham. "Retrofitting Short-Span Precast Channel Beam Bridges Constructed without Shear Reinforcement." *Journal of Bridge Engineering*, V. 16, No. 3, 2011, pp. 445-452.

[6] Barros, J. A. O., and G. M. Dalfré. "Assessment of the Effectiveness of the Embedded Through-Section Technique for the Shear Strengthening of Reinforced Concrete Beams." *Strain*, V.49, No. 1, 2013, pp. 75-93.

[7] Chaallal, O., A. Mofidi, B. Benmokrane, and K. Neale. "Embedded Through-Section FRP Rod Method for Shear Strengthening of RC Beams: Performance and Comparison with Existing Techniques." *Journal of Composites for Construction*, V. 15, No. 3, 2011, pp. 374-383.

[8] Randl, Norbert. *Research on Post-Installed Reinforcement for Structural Retrofitting*. Proc. of 18th Congress of IABSE, Seoul, 2012, Seoul. 5p..

[9] *Building Code Requirements for Structural Concrete (ACI 318-11) and Commentary*. Farmington Hills, MI: American Concrete Institute, 2011.

[10] *AASHTO LRFD Bridge Design Specifications*. 6th ed. Washington, DC: American Association of State and Highway Transportation Officials, 2012.

[11] Cook, R. A., D. M. Collins, R. E. Klingner, and D. Polyzois. "Load-Deflection Behavior of Cast-in-Place and Retrofit Concrete Anchors." *ACI Structural Journal*, v. 89, No. 6, November-December, 1992, pp. 639-49.

[12] Zamora, Noel A., Ronald A. Cook, Robert C. Konz, and Gary R. Consolazio. "Behavior and Design of Single, Headed and Unheaded, Grouted Anchors under Tensile Load." *ACI Structural Journal*, V. 100, No. 2, March-April 2003, pp. 222-30.

[13] Fuchs, Werner, Rolf Eligehausen, and John E. Breen. "Concrete Capacity Design Approach for Fastening to Concrete." *ACI Structural Journal*, V. 92, No. 1, January-February 1995, pp. 73-94.

[14] *Code Requirements for Nuclear Safety-related Concrete Structures: (ACI 349-06) and Commentary, an ACI Standard*. Farmington Hills, MI: American Concrete Institute, 2006.

[15] Bissonnette, Benoit, Alexander M. Vaysburd, and Kurt F. Von Fay. *Best Practices for Preparing Concrete Surfaces Prior to Repairs and Overlays*. Rep. no. MERL 12-17. Denver, Colorado: U.S. Department of the Interior, Bureau of Reclamation, 2012.

[16] Cook, Ronald A., Jennifer L. Burtz, and Marcus H. Ansley. *DESIGN GUIDELINES AND SPECIFICATIONS FOR ENGINEERED GROUTS*. Rep. no. BC354 RPWO # 48. Gainesville: Florida Department of Transportation, 2003.

[17] Hognestad, Eivind, Edward Cohen, C. A. Willson, Et Al. "Shear and Diagonal Tension." Rep. no. 326.59-1. *Journal of the American Concrete Institute*, V. 59, No. 1 January 1962.

[18] Wight, James K.., and James G.. MacGregor. *Reinforced Concrete Mechanics and Design*. 6th ed. Boston: Pearson, 2012.

[19] Reineck, Karl-Heinz, Evan Bentz, Birol Fitik, Daniel A. Kuchma, and Oguzhan Bayrak. "ACI-DAfStb Databases for Shear Tests on Slender Reinforced Concrete Beams with Stirrups." *ACI Structural Journal*, V. 111, No. 1, January-February 2013, pp. 1-10.

[20] Reineck, Karl-Heinz, Evan C. Bentz, Birol Fitik, Daniel A. Kuchma, and Oguzhan Bayrak. "ACI-DAfStb Database of Shear Tests on Slender Reinforced Concrete Beams without Stirrups." *ACI Structural Journal*, V. 110, No. 5, September-October 2013, pp. 867-75.

[21] Joint ACI-ASCE Committee 445. "Recent Approaches to Shear Design of Structural Concrete." *Journal of Structural Engineering*, V. 124, No. 12, 1998, pp. 1-56.

[22] Kani, G.N. J. "Basic Facts Concerning Shear Failure." *Journal of the American Concrete Institute*, V. 63, No. 6, June 1966, pp. 675-692.

[23] Kani, G.N.J. "How Safe are Our Large Reinforced Concrete Beams?" Journal of the American Concrete Institute, V. 64, No. 3, March 1967, pp. 128-141.

[24] Bazant, Zdenek P., and Hsu-Huei Sun. "Size Effect in Diagonal Shear Failure: Influence of Aggregate Size and Stirrups." *ACI Materials Journal*, V. 84, No. 4, July-August 1987, pp. 259-272.

[25] Bazant, Zdenek P., and Jin-Keun Kim. "Size Effects in Shear Failure of Longitudinally Reinforced Beams." *ACI Journal*, V. 81, No. 5, September-October 1984, pp. 456-68.

[26] Bazant, Zdenek P., and Mohammad T. Kazemi. "Size Effect on Diagonal Shear Failure of Beams without Stirrups." *ACI Structural Journal*, V. 88, No. 3, May-June 1991, pp. 268-76.

[27] Collins, Michael P., and Denis Mitchell. *Prestressed Concrete Structures*. Englewood Cliffs, NJ: Prentice Hall, 1991.

[28] Walraven, Joost C. "Fundamental Analysis of Aggregate Interlock." *ASCE Journal Structural Division*, V. 107, No. 11, November 1981, pp. 2245-270.

[29] Bentz, Evan C., and Michael P. Collins. "Development of the 2004 Canadian Standards Association (CSA) A23.3 Shear Provisions for Reinforced Concrete." *Canadian Journal of Civil Engineering*, V. 33, No. 5, 2006, pp. 521-34.

[30] Vecchio, Frank J., and Michael P. Collins. "The Modified Compression-Field Theory for Reinforced Concrete Elements Subjected to Shear." *ACI Journal*, V. 83, No. 2, March-April 1986, pp. 219-31.

[31] Bentz, Evan C., Frank J. Vecchio, and Michael P. Collins. "Simplified Modified Compression Field Theory for Calculating Shear Strength of Reinforced Concrete Elements." *ACI Structural Journal*, V. 103, No. 4, July-August 2006, pp. 614-24.

[32] *ASTM C1437 Standard Test Method for Flow of Hydraulic Cement Mortar*. West Conshohocken: American Society for Testing and Materials, 2013.